Wisconsin Highway Research Program

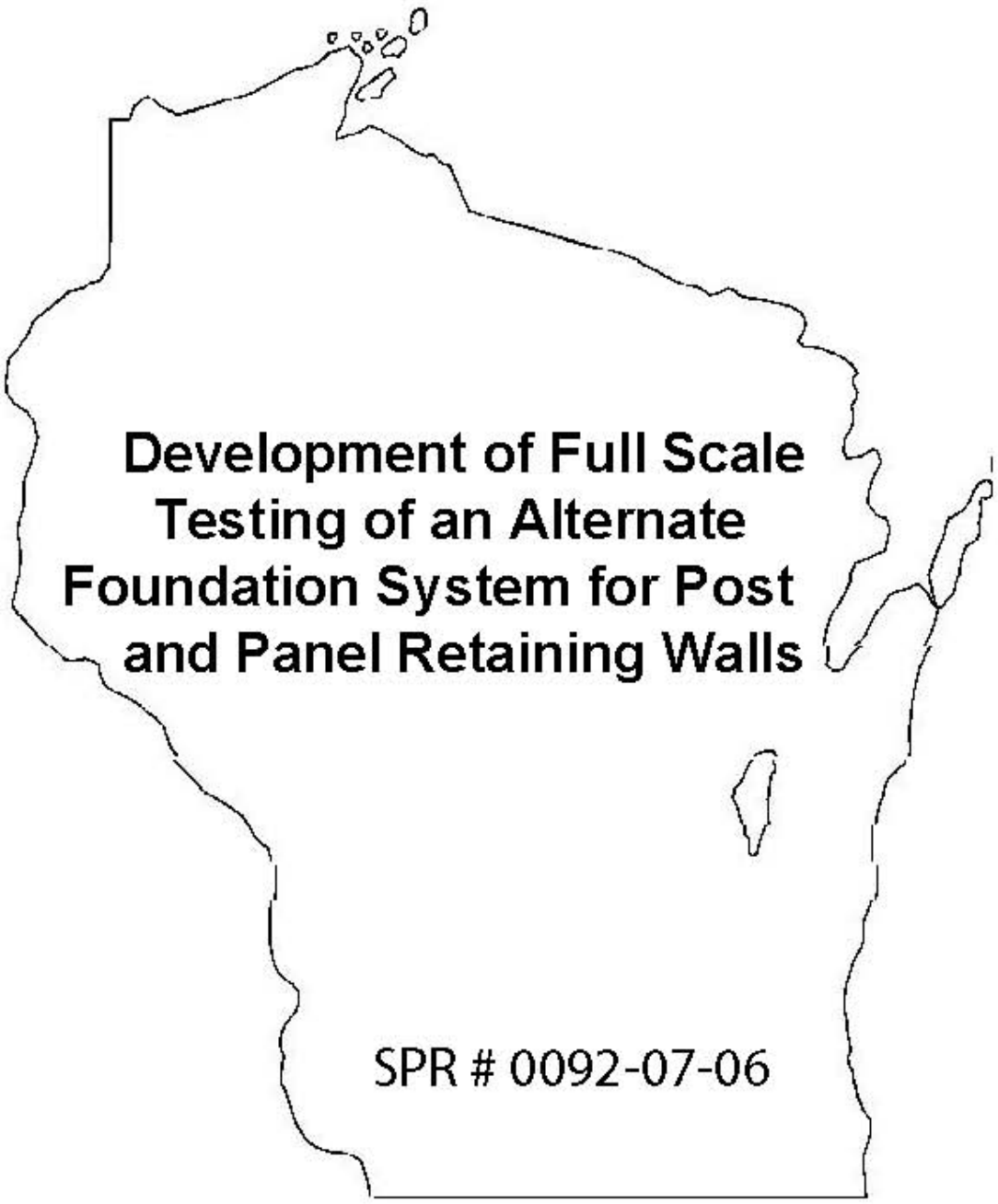

Development of Full Scale Testing of an Alternate Foundation System for Post and Panel Retaining Walls

SPR # 0092-07-06

Sam Helwany, Ph.D., P.E., Ritu Panda, M.S., and Hani Titi, Ph.D., P.E.

University of Wisconsin-Milwaukee
Department of Civil Engineering and Mechanics
January 2011

WHRP 11-01

Technical Report Documentation Page

1. Report No. WHRP 11-01	2. Government Accession	3. Recipient's Catalog No
4. Title and Subtitle Development of Full Scale Testing of an Alternate Foundation System for Post and Panel Retaining Walls		5. Report Date March 2009 6. Performing Organization Code Wisconsin Highway Research Program
7. Authors Sam Helwany		8. Performing Organization Report
9. Performing Organization Name and Address Department of Civil Engineering and Mechanics University of Wisconsin-Milwaukee		10. Work Unit No. (TRAIS) 11. Contract or Grant No. WisDOT SPR# 0092-07-06
12. Sponsoring Agency Name and Address Wisconsin Department of Transportation Division of Business Services Research Coordination Section 4802 Sheboygan Ave. Rm 104 Madison, WI 53707		13. Type of Report and Period Covered Final Report, 2006-2010 14. Sponsoring Agency Code
15. Supplementary Notes		

16. Abstract

The alternate post system offers benefits such as ease of construction, reduced construction time, and lower wall costs. While this system seems feasible, there are concerns regarding its performance, in particular the amount of bending in the post and the defection of the wall due to active earth pressures exerted by the retained soil. Other concerns include the potential damage to the plate during driving, control and accuracy of post alignment, and long term issues such as corrosion and soil creep. The objective of this research project is to assess the feasibility of the alternate post system. If the system is deemed feasible, the research team will develop design criteria for the alternate post system based on exposed wall heights, applied soil loads, post dimensions, and parameters of the retained soil and the foundation soil.

17. Key Words	18. Distribution Statement No restriction. This document is available to the public through the National Technical Information Service 5285 Port Royal Road Springfield VA 22161

19. Security Classif.(of this report) Unclassified	19. Security Classif. (of this page) Unclassified	20. No. of Pages	21. Price

Form DOT F 1700.7 (8-72) Reproduction of completed page authorized

DISCLAIMER

This research was funded through the Wisconsin Highway Research Program by the Wisconsin Department of Transportation and the Federal Highway Administration under Project 0092-07-06. The contents of this report reflect the views of the authors who are responsible for the facts and accuracy of the data presented herein. The contents do not necessarily reflect the official views of the Wisconsin Department of Transportation or the Federal Highway Administration at the time of publication.

This document is disseminated under the sponsorship of the Department of Transportation in the interest of information exchange. The United States Government assumes no liability for its contents or use thereof. This report does not constitute a standard, specification or regulation.

The United States Government does not endorse products or manufacturers. Trade and manufacturers' names appear in this report only because they are considered essential to the object of the document.

EXECUTIVE SUMMARY

The “post and panel” wall is a retaining wall type that has gained a reasonable amount of usage because it offers advantages under certain conditions. The procedure for the design of a post and panel wall involves selecting a post spacing, determining the soil and surcharge loads acting on that post, and then determining the optimum length and diameter of the post necessary to develop passive soil pressures sufficient to resist those loads acting on the post. A post and panel wall may be designed either as a cantilever system or as a tieback system. This type of wall may be used for either conventional “bottom up” construction or to retain existing facilities by “top down” construction.

Typical post design consists of a steel “H” section set in a column of concrete. The column of concrete extends from the final ground surface to the computed base elevation of the post. The steel “H” section extends from the bottom of the concrete to the design elevation of the top of the wall. Installing wall panels between the exposed sections of the posts completes construction. The panels are held in place by the flanges of the “H” sections. The concrete column is usually in the range of 0.6 to 1.2 m (2 to 4 ft) in diameter.

Several contractors offering an alternate post design have approached WisDOT. They have proposed eliminating the concrete column and replacing it with a steel plate of the same width and length as the concrete column. This plate would be welded to the “H” section and then the composite unit would be driven into the ground to the required plan base elevation. The remainder of the construction would proceed without change.

The alternate post system offers benefits such as ease of construction, reduced construction time, and lower wall costs. The objective of this research project is to assess the feasibility of the alternative system. A design criteria for the alternative system is developed based on exposed wall heights, applied soil loads, post dimensions, and parameters of the retained soil and the foundation soil. Full-scale testing of the alternative system and the conventional pile with concrete pier system are included as part of this project. The performance of the two systems is compared under otherwise identical in-situ and loading conditions.

TABLE OF CONTENTS

LIST OF FIGURES

LIST OF TABLES

ACKNOWLEDGMENTS

The authors wish to acknowledge WisDOT for supporting the Research Project titled: Development of Full Scale Testing of an Alternate Foundation System for Post and Panel Retaining Walls. We appreciate the continuing help and support from WisDOT personnel especially Mr. Robert Arndorfer, and Mr. Jeffery Horsfall, and all the Geotechnical TOC members. Our appreciation should also be given to the drilling crews of WisDOT for their field exploration work. Finally, we thank Edward Gillen, Inc. of Milwaukee for performing the field tests associated with this project.

CHAPTER 1

1.1 INTRODUCTION

The "post and panel" wall is a retaining wall type that has gained a reasonable amount of usage because it offers advantages under certain conditions. The procedure for the design of a post and panel wall involves selecting a post spacing, determining the soil and surcharge loads acting on that post, and then determining the optimum length and diameter of the post necessary to develop passive soil pressures sufficient to resist those loads acting on the post. A post and panel wall may be designed either as a cantilever system or as a tieback system. This type of wall may be used for either conventional "bottom up" construction or to retain existing facilities by "top down" construction.

Typical post design consists of a steel "H" section set in a column of concrete as shown in Figure 1. The column of concrete extends from the final ground surface to the computed base elevation of the post. The steel "H" section extends from the bottom of the concrete to the design elevation of the top of the wall. Installing wall panels between the exposed sections of the posts completes construction. The panels are held in place by the flanges of the "H" sections. The concrete column is usually in the range of 0.6 to 1.2 m (2 to 4 ft) in diameter.

Several contractors offering an alternate post design have approached WisDOT. They have proposed eliminating the concrete column and replacing it with a steel plate of the same width and length as the concrete column (Figure 2). This plate would be welded to the "H" section and then the composite unit would be driven into the ground to the required plan base elevation. The remainder of the construction would proceed without change.

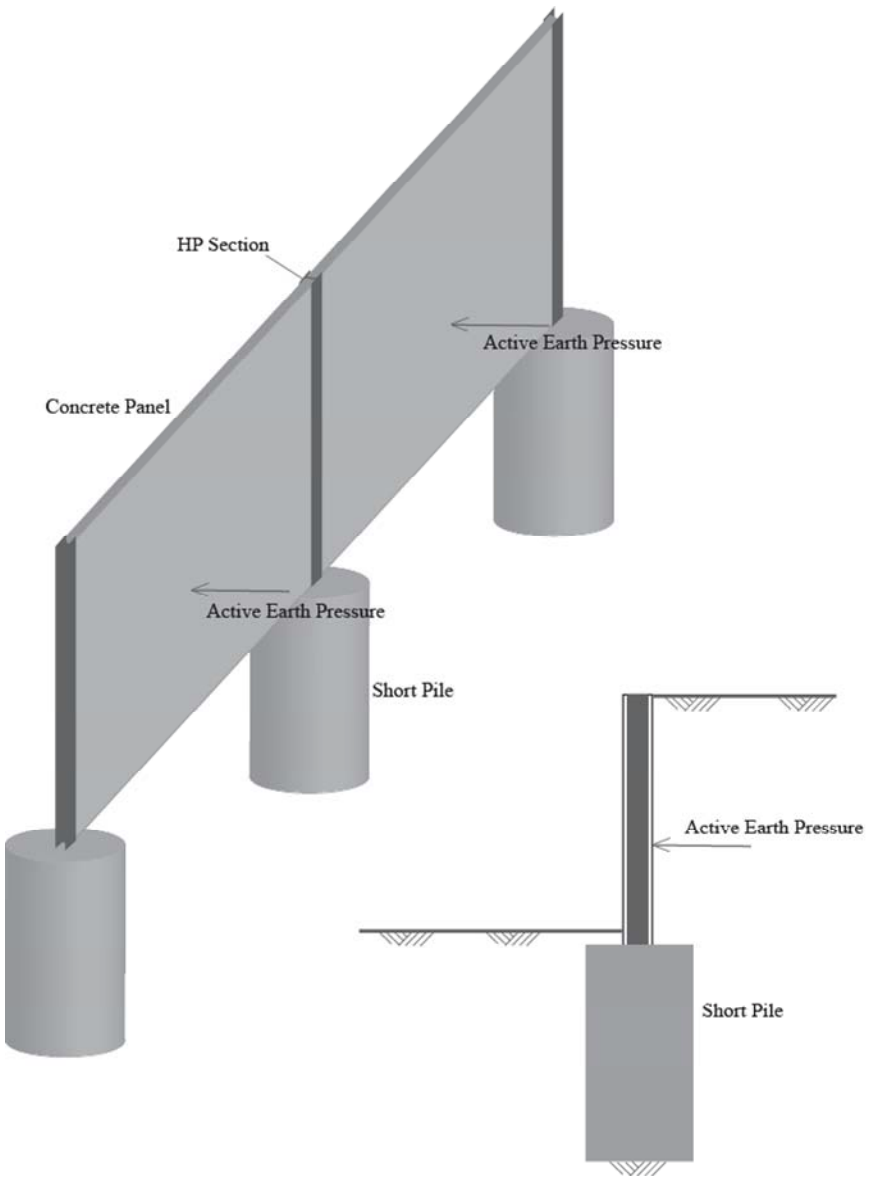

Figure 1 Post-and-Panel (Pile with Concrete Pier)

1.2 PROBLEM STATEMENT

The alternate post system (termed: "the pile with plate system" henceforth) offers benefits such as ease of construction, reduced construction time, and lower wall costs. While this system seems feasible, there are concerns regarding its performance, in particular the amount of bending in the post and the defection of the wall due to active earth pressures exerted by the retained soil. Other concerns include the potential damage

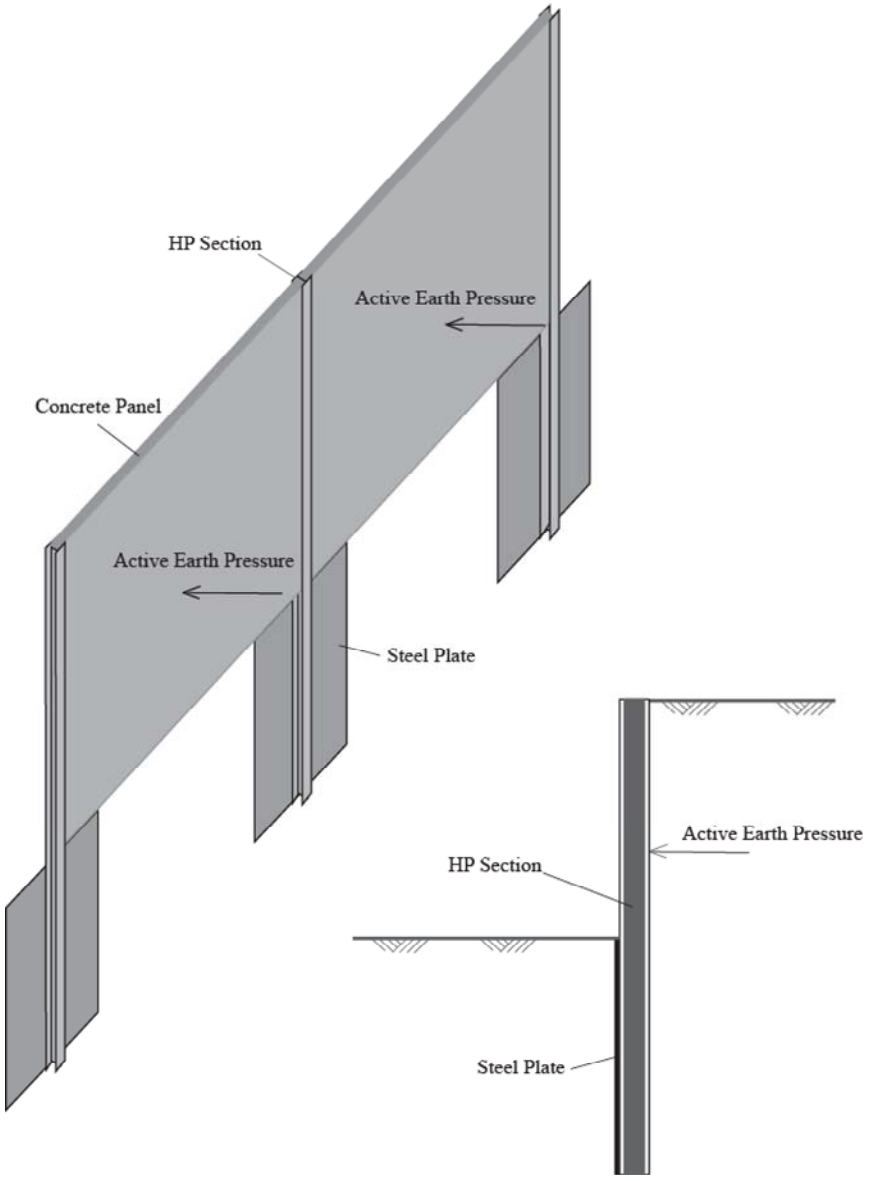

Figure 2 Alternative System (Pile with Plate)

to the plate during driving, control and accuracy of post alignment, and long term issues such as corrosion and soil creep.

1.3 OBJECTIVE

The objective of this research project is to assess the feasibility of the pile with plate system. If the system is deemed feasible, the research team will develop design criteria

for the pile with plate system based on exposed wall heights, applied soil loads, post dimensions, and parameters of the retained soil and the foundation soil. Full-scale testing of the pile with plate system and the conventional pile with concrete pier system will also be included as part of this project. The performance of the two systems will be compared under otherwise identical in-situ and loading conditions.

CHAPTER 2

2.1 CURRENT STATE OF KNOWLEDGE--LATERALLY LOADED PILES

Fully- and partially-embedded piles and drilled shafts can be subjected to lateral loads, as well as axial loads, in various applications including sign posts, power poles, marine pilings, and "post and panel" retaining walls.

Piles and drilled shafts resist lateral loads via shear, bending, and earth passive resistance. Thus, their resistance to lateral loads depends on (a) pile stiffness and strength: pile configuration, in particular, the pile length-to-diameter ratio plays an important role in determining pile stiffness, hence its ability to resist shear and bending moments (b) soil type, stiffness, and strength, and (c) end conditions: fixed end (due to pile group cap) versus free end.

Several analytical approaches are available for the design of laterally loaded piles and drilled shafts. These approaches can be divided into three categories: elastic approach, ultimate load approach, and numerical approach.

The elastic approach is used to estimate the response of piles subjected to working loads assuming that the soil and the pile behave as elastic materials. Ultimate loads cannot be calculated using this "elastic" approach. Matlock and Reese (1960) proposed a method for calculating moments and displacements along a pile embedded in a cohesionless soil and subjected to lateral loads and moments at the ground surface. They used a simple Winkler's model that substitutes the elastic soil that surrounds the pile with a series of independent elastic springs. Using the theory of beams on an elastic foundation they were able to obtain useful equations that allow the calculation of lateral deflections, slopes, bending moments, and shear forces at any point along the axis of a laterally loaded pile. A similar elastic solution by Davisson and Gill (1963) is also available for laterally loaded piles embedded in cohesive soils. Note that this approach requires the coefficient of subgrade reaction at various depths be known. Best results can be obtained if this coefficient is measured in the field, but that is rarely done.

Several methods that use the ultimate load approach are available for the design of laterally loaded piles and drilled shafts (example: Broms' method, 1964; and Meyerhof's method, 1995). These methods provide solutions in the form of graphs and tables that are easy to use by students and engineers.

The ultimate load approach embodied in Broms' method is suitable for short and long piles, for restrained- and free-headed piles, and for cohesive and cohesionless soils. A short pile will rotate as one unit when it is subjected to lateral loads as shown in Figure 3. The soil in contact with the short pile is assumed to fail in shear when the ultimate lateral load is reached. On the other hand, a long pile is assumed to fail due to the bending moments caused by the ultimate lateral load, i.e., the shaft of the pile will fail at the point of maximum bending moment forming a "plastic hinge" as shown in the same figure.

Broms' method presents the solution for short piles embedded in cohesive soils with a set of curves shown in Figure 4a. The curves relate the pile's embedment length-to-diameter ratio, L/D, to the normalized ultimate lateral force, Q_u/c_uD^2, for various e/D ratios. In the figure, the term "restrained-headed" pile indicates that the head of the pile is connected to a rigid cap that prevents the head of the pile from rotation.

In general, piles having a length-to-diameter ratio (L/D) greater than 20 are long piles. Figure 4b can be used for long piles embedded in cohesive soils. The curves in this figure relate the normalized ultimate lateral force, Q_u/c_uD^2, to the normalized yield moment of the pile, M_{yield}/c_uD^3, for various e/D ratios. These curves are used only when L/D>20 and when the moment generated by the ultimate lateral load is greater than the yield moment of the pile.

For short piles embedded in cohesionless soils, Broms' method provides the curves given in Figure 5a that relate the pile's embedment length-to-diameter ratio, L/D, to the normalized ultimate lateral force, $Q_u/K_pD^3\gamma$, for various e/D ratios. Note that K_p is the

passive lateral earth pressure coefficient, and γ is the unit weight of the soil around the pile.

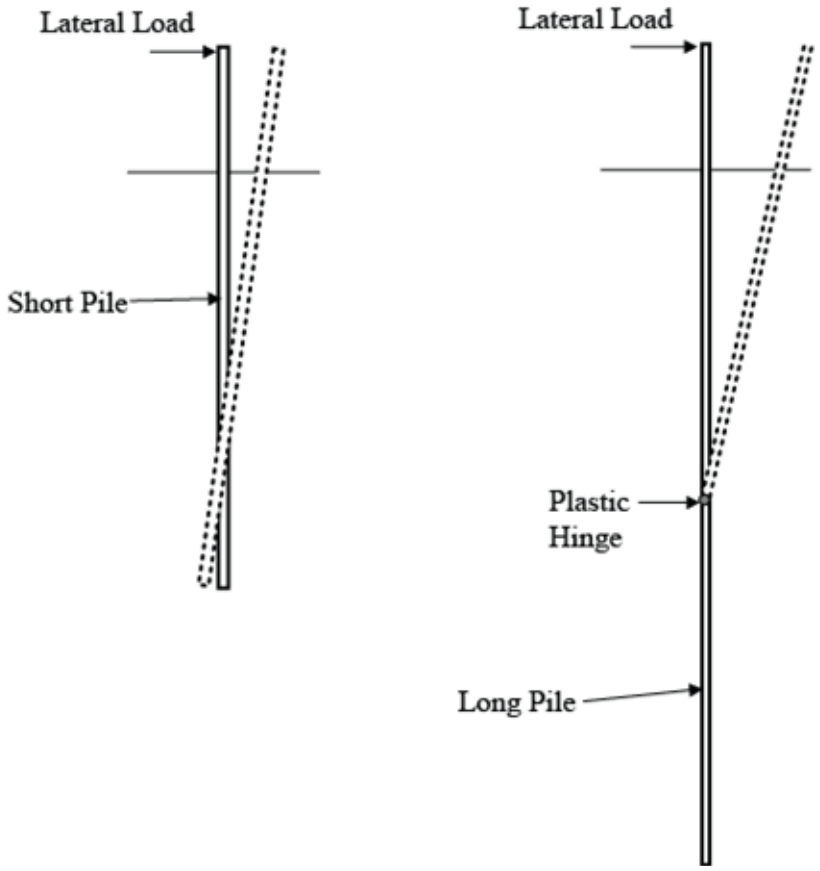

Figure 3: Long and Short Piles

Figure 5b can be used for long piles embedded in cohesionless soils. The curves in this figure relate the normalized ultimate lateral force, $Q_u/K_pD^3\gamma$, to the normalized yield moment of the pile, $M_{yield}/K_pD^4\gamma$, for various e/D ratios. These curves are used only when L/D>20 and when the moment generated by the ultimate lateral load is greater than the yield moment of the pile.

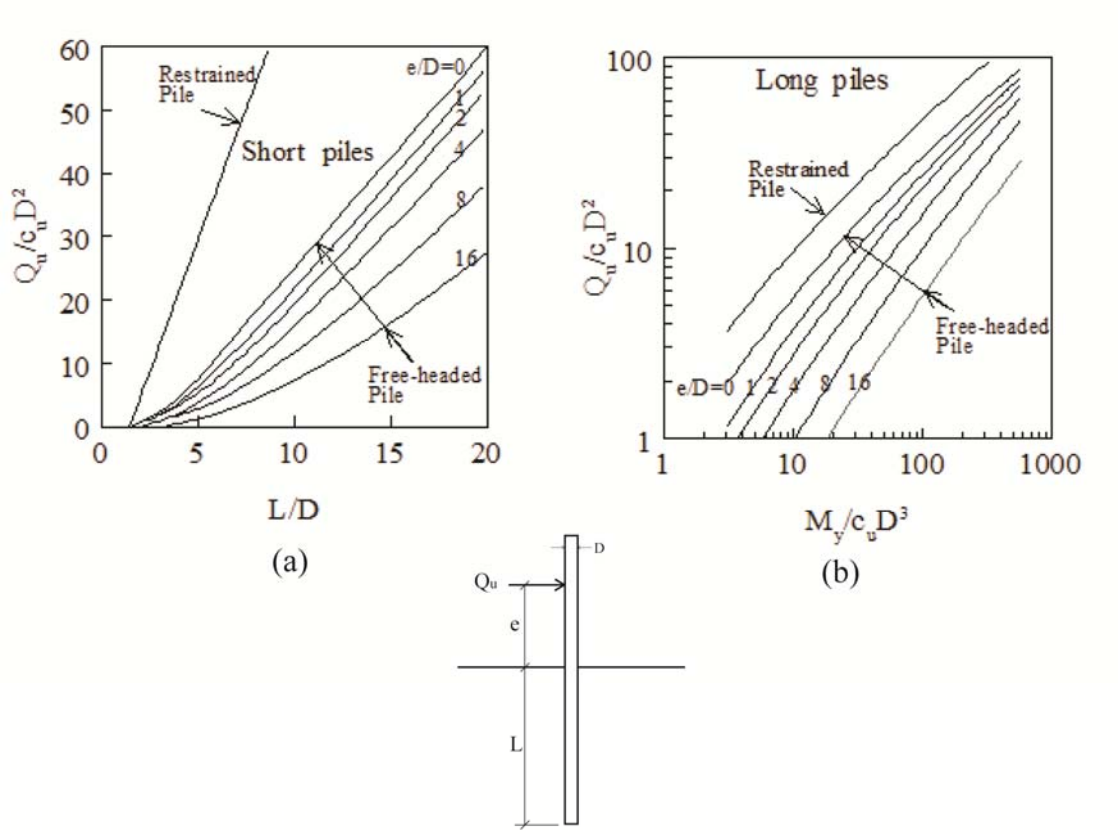

Figure 4: Broms' Method: Cohesive Soil

2.2 PRELIMINARY ANALYSIS

The finite element method is used to investigate the feasibility of the proposed pile with plate system. Because of the three-dimensional nature of a laterally loaded post system, a 3-D finite element code will be used. The finite element code used herein embodies advanced soil models capable of simulating drained and undrained loading conditions for virtually any type of soil and soil strata. It is also capable of simulating the interaction between the structure (i.e., the post with a concrete column, and the post with a welded plate) and the soil during lateral loading. The proposed finite element code has been verified by means of simulating several full-scale lateral load tests on posts with concrete columns that were performed by Ohio Department of Transportation (ODOT). Subsequent to code verification, the proposed pile with plate system was analyzed using

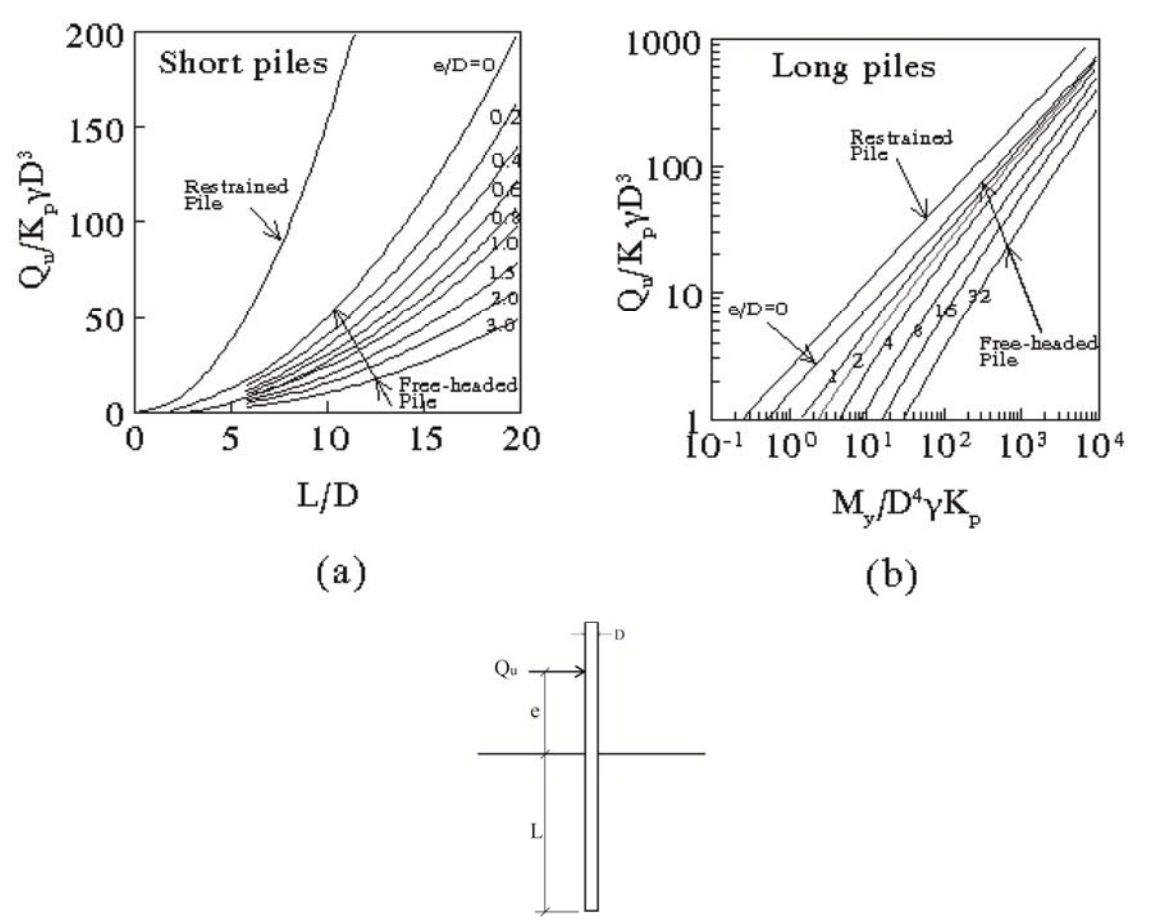

Figure 5: Broms' Method: Cohesionless Soil

a 25-mm (1-inch) thick plate. The deflections of the post at ground level were compared with those of the conventional post system as described in a subsequent Section.

A full-scale lateral load test on a post with concrete column performed by Ohio Department of Transportation (ODOT) will be analyzed herein using the proposed finite element code. The purpose of this analysis is to show that the proposed finite element analysis is capable of simulating the behavior of laterally loaded post and panel systems.

The following example describes a post with a concrete column lateral load test that was carried out by ODOT. Test results will be compared with (a) the Broms' method described earlier, and (b) finite element analysis. The concrete column is 3.66-m (12-ft)

long and 0.75-m (2.5-ft) diameter as shown in Figure 6. The above ground portion is 3.96-m (13-ft) long and is made of an HP steel section. The lateral load is applied 3.05 m (10 ft) above the ground level. The foundation soil consists of five layers with varying undrained shear strengths as indicated in the figure.

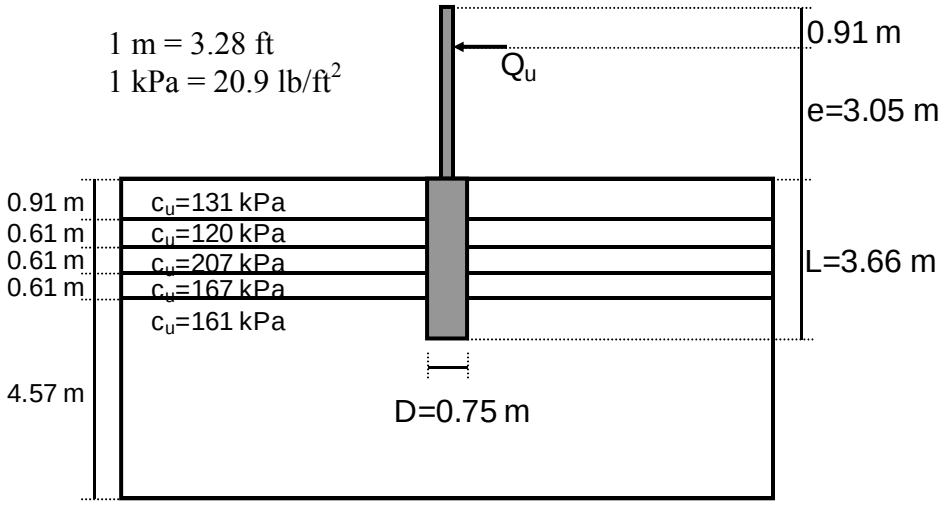

Figure 6: Ohio DOT Field Test on Laterally Loaded Post-and-Panel System

The ultimate lateral load capacity of the concrete column (short pile) will be calculated using Broms' method. Let's calculate the weighted average undrained shear strength of the five soil layers:

$c_u=(131\times0.91+120\times0.61+207\times0.61+167\times0.61+161\times0.92)/3.66=155$ kPa (3240 psf)

$L/D=3.66/0.75=4.88<20\rightarrow$short pile

$e/D=3.05/0.75\approx4$

From Figure 4a (Broms' method for short piles in cohesive soils) we obtain the normalized ultimate lateral force $Q_u/c_uD^2\approx3$. Thus, the ultimate lateral load capacity is $Q_u\approx3c_uD^2\approx3(155)(0.75)^2\approx262$ kN (60 kips).

In the realm of finite element, the analysis of a laterally loaded pile is similar to that of an axially loaded pile except for the load that is applied in the horizontal direction at or above the ground level. The lateral load can be a concentrated load, a moment, or a

combination of the two. In the case of an axially loaded pile, the finite element mesh of the pile and the surrounding soil can take advantage of axisymmetry since the geometry and the loading are both symmetrical about a vertical axis passing through the center of the pile. This simplification cannot be used for a pile that is loaded with a lateral load, since the lateral load is applied horizontally in only one direction, i.e., in a non-symmetrical manner.

Using the finite element method we will calculate the ultimate lateral load capacity of the post with concrete column system described above. We will assume undrained loading conditions and then compare the predicted lateral load-displacement curve from the finite element analysis with the field test results obtained by ODOT.

In this example a limit equilibrium solution is sought for clay strata loaded in an undrained condition by a single "pile" with a lateral load applied above ground level. Piles with lateral loads are three-dimensional by nature and will be treated as such in the following finite element analysis. Note that this problem is symmetrical about a plane that contains the vertical axis of the pile and the line of action of the lateral load. Thus, the finite element mesh of half of the pile and half the surrounding soil is considered as shown in Figures 7 and 8.

Interface elements that are capable of simulating the frictional interaction between the pile surface and the soil are used. Since this is a non-displacement (bored) pile, the excess pore water pressure after pile installation is assumed to be zero in this finite element analysis.

The three-dimensional finite element mesh, shown in Figure 8, comprises two parts: the concrete pile with the above ground HP section and the soil. The mesh is 30-m (100-ft) long in the x-direction, 15-m (50-ft) wide in the y-direction, and 7.3-m (25-ft) high in the z-direction. Mesh dimensions should be chosen in a way that the boundaries do not affect the solution. This means that the mesh must be extended in all three dimensions, and that is considered in this mesh.

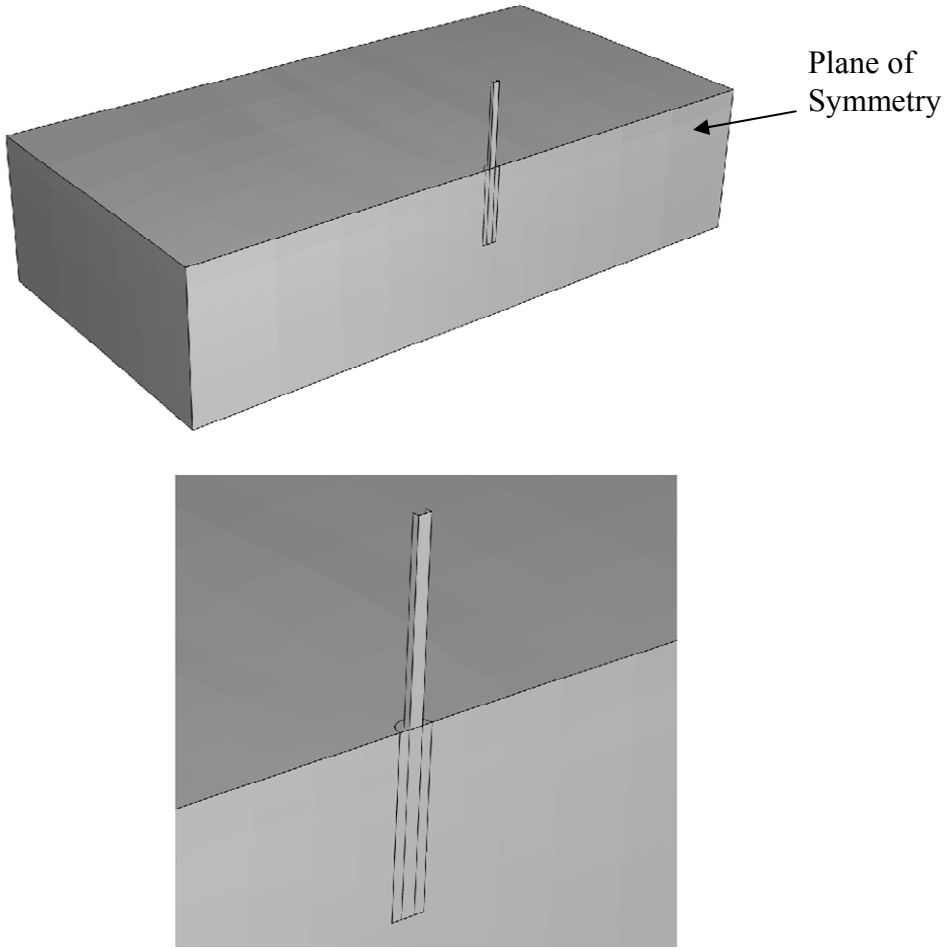

Figure 7: Geometrical Idealization of ODOT Field Test

The elastic response of the clay layers is assumed to be linear and isotropic, with a Young's modulus that is function of the undrained shear strength of each layer as indicated in Table 1. The modified Drucker-Prager/cap plasticity soil model, briefly described next, is used to simulate the plastic behavior of the soil. The model adopted the undrained shear strength c_u (Table 1) with $\phi_u=0$ to simulate the undrained behavior of the clay layers.

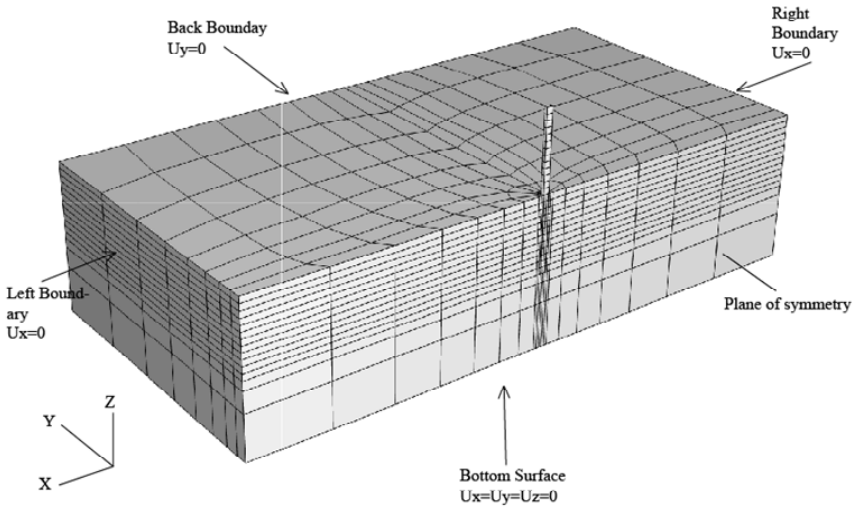

Figure 8: FEM Discretization (ODOT Test)

Table 1: Undrained Soil Properties

Soil Layer	Depth (m)	c_u (kPa)	E (MPa)
1 (top)	0-0.91	131	32.7
2	0.91-1.52	120	30
3	1.52-2.13	207	51.7
4	2.13-2.74	167	41.9
5 (bottom)	2.74-7.31	161	40.3

1 m=3.28 ft
1 kPa= 20.9 psf

2.3 MODIFIED DRUCKER-PRAGER/CAP MODEL

The Drucker-Prager/Cap plasticity model has been widely used in finite element analysis programs for a variety of geotechnical engineering applications. The cap model is appropriate to soil behavior because it is capable of considering the effect of stress history, stress path, dilatancy, and the effect of the intermediate principal stress.

The yield surface of the modified Drucker-Prager/Cap plasticity model consists of three parts: a Drucker-Prager shear failure surface, an elliptical "cap," which intersects the

mean effective stress axis at a right angle, and a smooth transition region between the shear failure surface and the cap as shown in Figure 9.

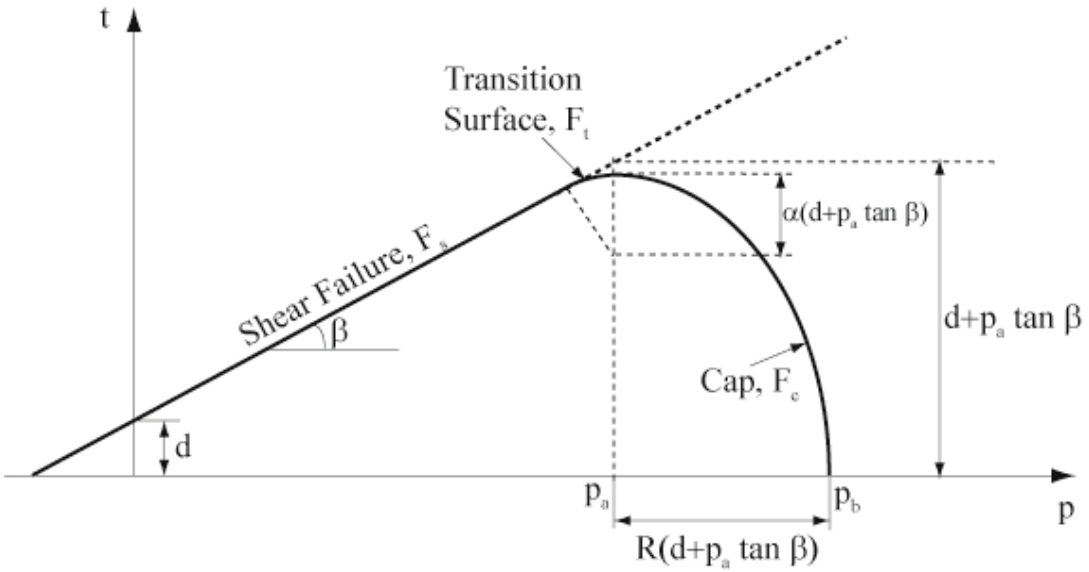

Figure 9: Modified Drucker-Prager/Cap Model in the Shear Stress Versus Mean Effective Stress Plane

The elastic behavior is modeled as linear elastic using the generalized Hooke's law. Alternatively, an elasticity model in which the bulk elastic stiffness increases as the material undergoes compression can be used to calculate the elastic strains.

The onset of the plastic behavior is determined by the Drucker-Prager failure surface and the cap yield surface. The Drucker-Prager failure surface is given by:

$$F_s = t - p\tan\beta - d = 0 \qquad (1)$$

where β is the soil's angle of friction and *d* is its cohesion in the p-t plane as indicated in Figure 9.

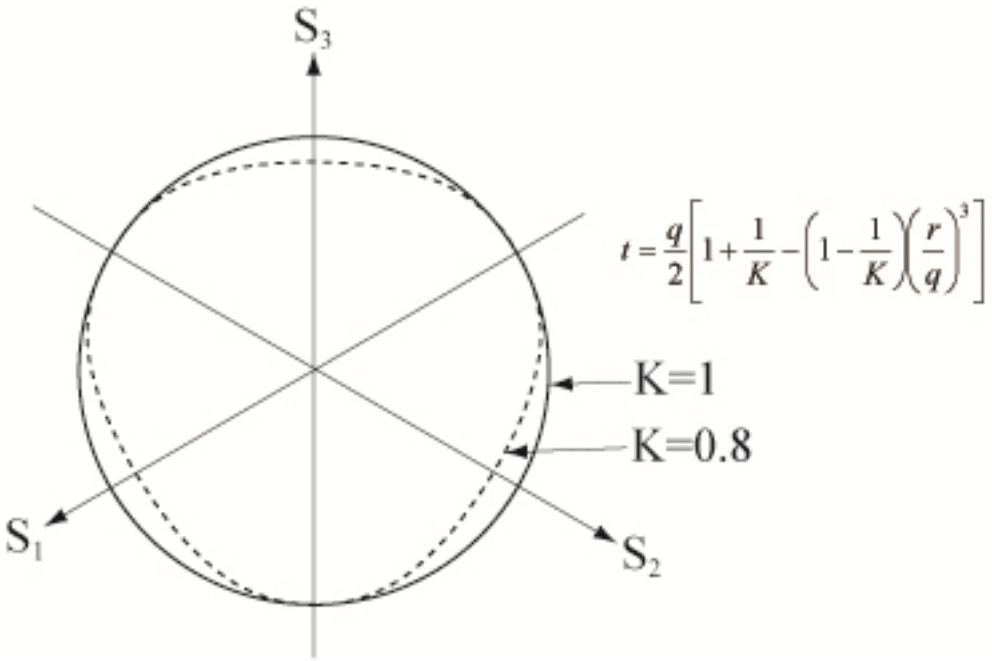

Figure 10: Modified Drucker-Prager/Cap Model in the Deviatoric Stress Space

As shown in Figure 9, the cap yield surface is an ellipse with eccentricity=*R* in the *p*-*t* plane. The cap yield surface is dependent on the third stress invariant, *r*, in the deviatoric plane as shown in Figure 10. The cap surface hardens (expands) or softens (shrinks) as a function of the volumetric plastic strain. When the stress state causes yielding on the cap, volumetric plastic strain (compaction) results causing the cap to expand (hardening). But when the stress state causes yielding on the Drucker-Prager shear failure surface, volumetric plastic dilation results causing the cap to shrink (softening). The cap yield surface is given as:

$$F_c = \sqrt{(p - p_a)^2 + [\frac{Rt}{(1 + \alpha - \alpha/\cos\beta)}]^2} - R(d + p_a \tan\beta) = 0 \qquad (2)$$

where

R is a material parameter that controls the shape of the cap

α is a small number (typically 0.01 to 0.05) used to define a smooth transition surface between the Druker-Prager shear failure surface and the cap:

$$F_t = \sqrt{(p - p_a)^2 + [t - (1 - \frac{\alpha}{\cos\beta})(d + p_a \tan\beta]^2} - \alpha(d + p_a \tan\beta) = 0 \qquad (3)$$

p_a is an "evolution parameter" that controls the hardening/softening behavior as function of the volumetric plastic strain. The hardening/softening behavior is simply described by a piecewise linear function relating the mean effective (yield) stress, p_b, and the volumetric plastic strain, $p_b = p_b(\varepsilon_{vol}^{pl})$ as shown in Figure 11. This function can be easily obtained from the results of one isotropic consolidation test with several unloading/reloading cycles. Consequently, the evolution parameter, p_a, can be calculated as:

$$p_a = \frac{p_b - Rd}{1 + R\tan\beta} \qquad (4)$$

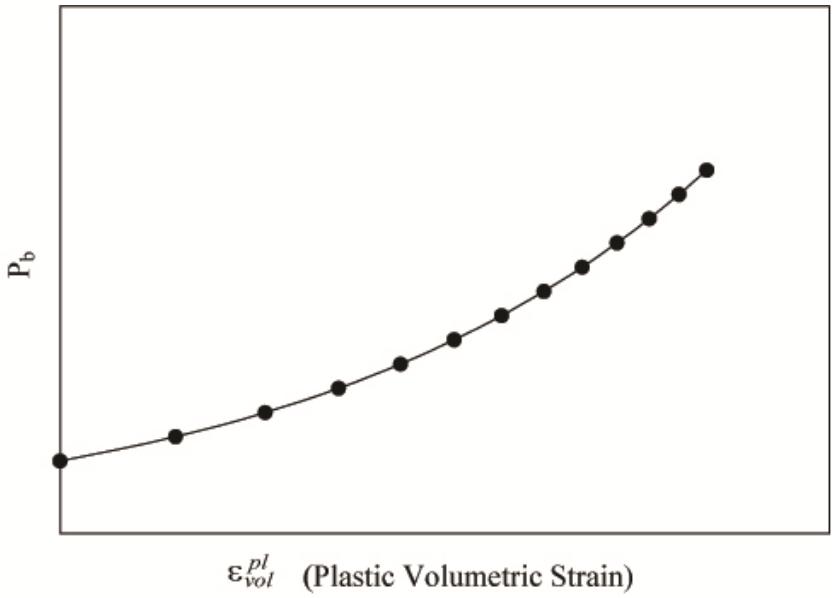

Figure 11: Hardening Curve for the Modified Drucker-Prager/Cap Model

Flow rule

In this model, the flow potential surface in the *p*-*t* plane consists of two parts as shown in Figure 12. In the cap region the plastic flow is defined by a flow potential that is identical to the yield surface, i.e., associated flow. For the Drucker-Prager failure

surface and the transition yield surface a nonassociated flow is assumed: the shape of the flow potential in the *p-t* plane is different from the yield surface shown in Figure 9.

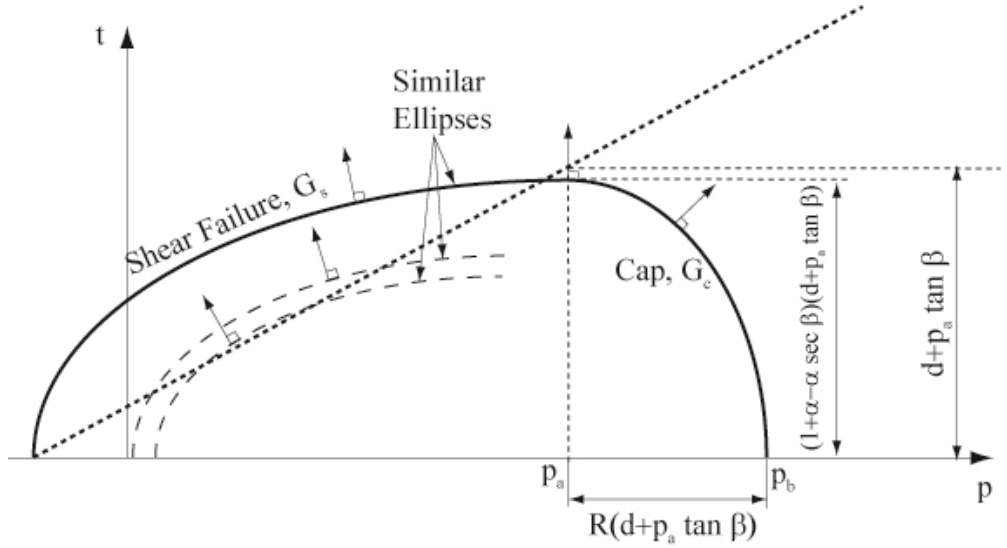

Figure 12: Flow Potential Surface in the *p-t* Plane for the Modified Drucker-Prager/Cap Model

In the cap region the elliptical flow potential surface is given as:

$$G_c = \sqrt{(p - p_a)^2 + [\frac{Rt}{(1 + \alpha - \alpha/\cos\beta)}]^2} \qquad (5)$$

The elliptical flow potential surface portion in the Drucker-Prager failure and transition regions is given as:

$$G_s = \sqrt{[(p_a - p)\tan\beta]^2 + [\frac{t}{(1 + \alpha - \alpha/\cos\beta)}]^2} \qquad (6)$$

As shown in Figure 12, the two elliptical portions, G_c and G_s, provide a continuous potential surface. Because of the nonassociated flow used in this model, the material stiffness matrix is not symmetric. Thus, an unsymmetric solver should be used in association with the Cap model.

Model Parameters

We need the results of at least three triaxial compression tests to determine the parameters d and β. The at-failure conditions taken from the tests results can be plotted in the *p*-*t* plane. A straight line is then best fitted to the three (or more) data points. The intersection of the line with the t-axis is d and the slope of the line is β.

We also need the results of one isotropic consolidation test with several unloading/reloading cycles. This can be used to evaluate the hardening/softening law as a piecewise linear function relating the hydrostatic compression yield stress, p_b, and the corresponding volumetric plastic strain, $p_b = p_b(\varepsilon_{vol}^{pl})$ (Figure 11). The unloading/reloading slope can be used to calculate the volumetric elastic strain that should be subtracted from the volumetric total strain in order to calculate the volumetric plastic strain.

2.4 FE Results versus ODOT Field Test Results

The pile lateral load capacity versus displacement curve obtained from the finite element analysis is shown in Figure 13. It is noted from the figure that the horizontal displacement increases as the lateral load is increased up to about 475-kN (106 kips) pile load at which a horizontal displacement of about 5 cm (2 inch) is encountered. Shortly after that, the pile moves laterally at a greater rate indicating that the lateral load capacity of the pile has been reached. For comparison, the pile lateral load capacity of 265 kN (60 kips), predicted by Broms' Method, is shown in Figure 13. It is noted that the finite element prediction of pile lateral load capacity is about two times greater than the capacity predicted by Broms' method.

More importantly, Figure 13 provides the load-displacement curve obtained from the field test conducted on the same pile by ODOT. The finite element results are in good agreement with the measured results. Note that the ODOT test included two cycles of loading and unloading, and that the pile failed at a lateral load of approximately 480 kN (107 kips). Also, it can be concluded from the figure that the ultimate lateral load of the

pile predicted by Broms' method seriously underestimated the measured lateral load capacity of the pile.

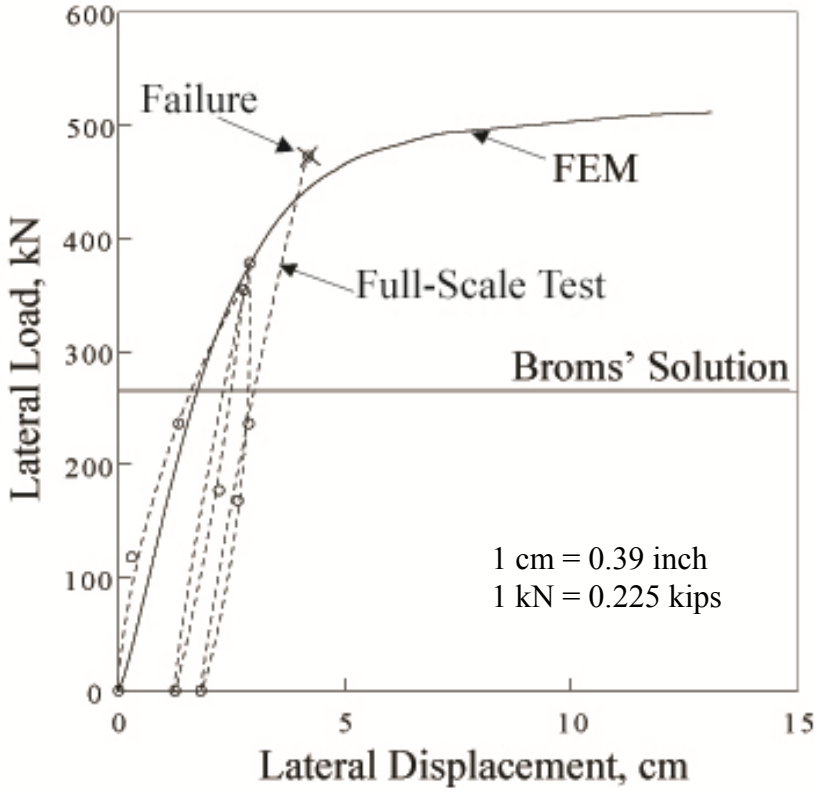

Figure 13: Comparison: FEM with Field Test Results and Brom's Method

2.5 A PRELIMINARY FEASIBILITY STUDY OF THE PROPOSED PILE WITH PLATE SYSTEM

2.5.1 Foundation Soil Type: Sand

The research team carried out a preliminary feasibility analysis of the proposed pile with plate system using the finite element code that has been verified as described in the previous Section. The preliminary feasibility analysis consisted of an objective comparison of the behavior of a conventional post with a concrete column and a post with a welded plate. The two post systems analyzed herein are identical to the proposed post systems for the field test (Figure 14). This preliminary feasibility analysis will shed some light on the proposed post system.

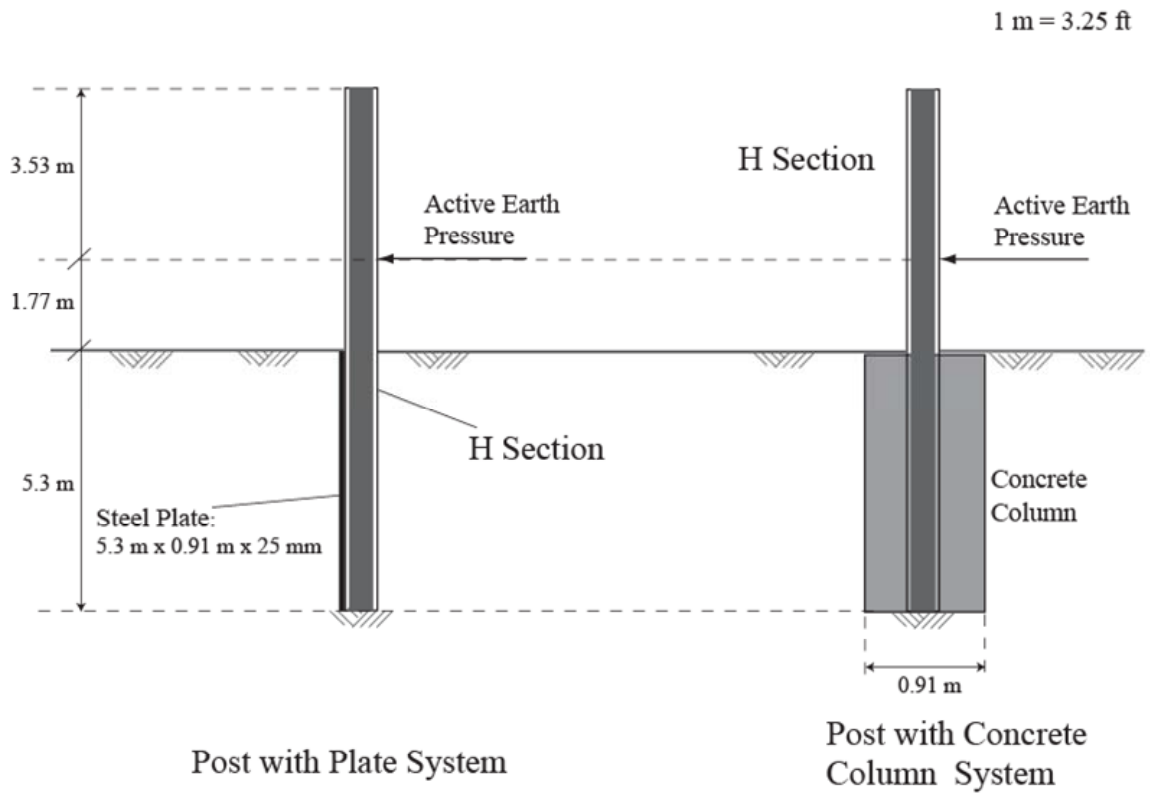

Figure 14: Comparison between Systems

As shown in Figure 14, the conventional pile with concrete pier system consists of a 5.3-m (17.5-ft) long concrete column with a diameter of 0.91 m (3 ft). The above ground H section is 5.3-m (17.5-ft) long. The proposed pile with plate system consists of a 5.3-m (17.5-ft) long, 0.91-m (3-ft) wide, 25-mm (1-inch) thick steel plate welded to a 10.6-m (35-ft) long post with an H section (5.3 m above ground). The pile with plate system model is shown in Figure 15. In both systems, the lateral load is applied at the 1/3 point measured from the ground level. This is to simulate the active force caused by the triangular distribution of the lateral earth pressure exerted by the retained soil on the concrete panel (see Figure 1). The foundation soil is assumed to be a medium dense sand with $c'=0$ and $\phi' =37°$. The 3-D finite element meshes of the two systems are not shown here.

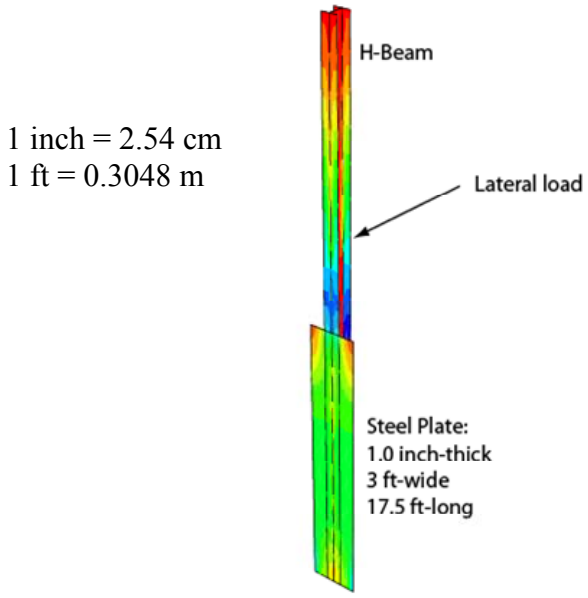

Figure 15: Alternative: Steel Plate

Figure 16 shows the predicted horizontal displacement versus applied lateral load for both post systems. In the figure, the horizontal displacement is the displacement of the post at the ground level. It is clear from the figure that the conventional post with concrete column system is much stiffer than the proposed pile with plate system. For a 5.3 m (17.5-ft) high concrete panel spanning 3 m (10 ft) between two posts, center to center, the active lateral force exerted on the concrete panel is approximately 200 kN (45 kips). From Figure 16 this lateral load will cause a horizontal displacement of 4 mm (0.16 inch) in the conventional post with concrete column system. In contrast, the same load will cause 25 mm (1 inch) of horizontal displacement in the proposed pile with plate system. This large difference in displacement is attributed to the large flexural stiffness of the concrete column in the conventional post system as compared to the flexural stiffness of the 25-mm (1-inch) thick steel plate in the proposed pile with plate system. Using typical values of Young's moduli for steel and concrete we can calculate the stiffness of the concrete column as:

$$\frac{E_{concrete} I_{column}}{L_{column}} = \frac{E_{concrete}\left(\frac{1}{4}\pi\, r^4\right)}{L_{column}} = \frac{6.0\times10^8\left(\frac{1}{4}\pi\,(1.5)^4\right)}{17.5} = 136.3\times10^6 \quad lb.ft$$

And the stiffness of the steel plate is:

$$\frac{E_{steel} I_{plate}}{L_{plate}} = \frac{E_{steel}\left(\frac{b\,t^3}{12}\right)}{L_{plate}} = \frac{4.3\times10^9 \times \frac{3}{12} \times (\frac{1}{12})^3}{17.5} = 0.036\times10^6 \quad lb.ft$$

This means that the stiffness of the concrete column is approximately 3800 times greater than the stiffness of the steel plate for this specific example.

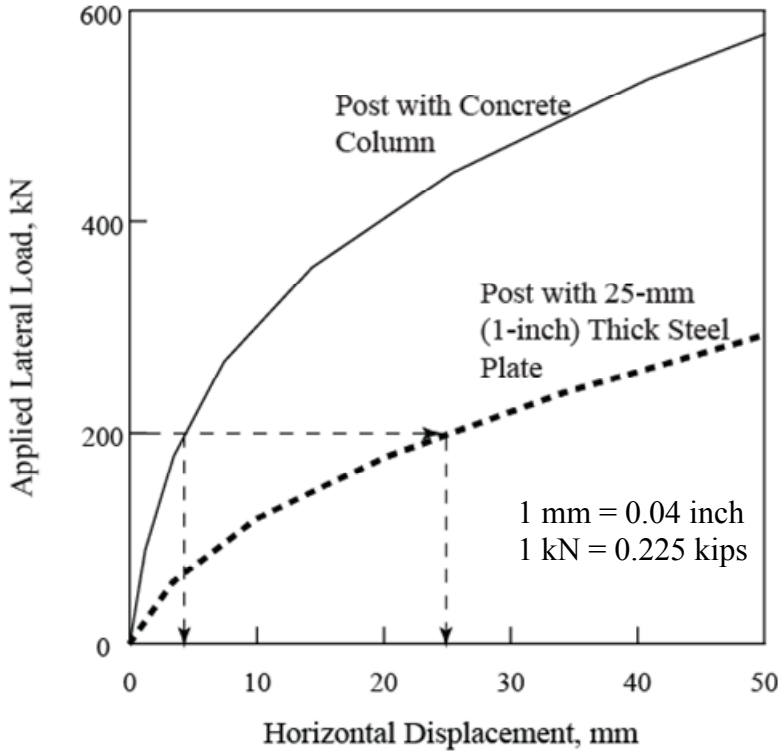

Figure 16: Comparison between Systems (Sand)

A question arises now, *is 25 mm (1 inch) of horizontal displacement tolerable for the proposed pile with plate system under a working load of 200 kN (45 kips)*? If the answer is NO then the proposed system needs to be improved. In such case, one can increase the stiffness of the plate and the stiffness of the post (H section). Note that this discussion is

only based on a single case, and many other cases need to be considered before offering remedies for the proposed system. Nevertheless, if more stiffness is needed, one can increase the thickness, and possibly the width, of the plate. Also, plate "stiffeners" can be used for added stiffness (stiffeners are welded steel sheets that are orthogonal to the plate). Anchors can also be used to reduce lateral displacements. The embedded length of the post and the welded plate can be increased as another option. Some of these options are investigated in the next Section.

2.5.2 Foundation Soil Type: Clay

The analyses described above was repeated herein four times using the same finite element mesh and the same parameters except for the foundation soil that is replaced by four different clayey soils having unconfined compressive strengths q_u = 25 kPa (520 psf; very soft clay), 37.5 kPa (780 psf; soft clay), 75 kPa (1570 psf; medium clay), and 150 kPa (3130 psf; stiff clay). Figure 17 shows the predicted horizontal displacement (at ground level) versus applied lateral load for both post systems for the four foundation soil types. It is clear from the figure that the conventional post with concrete column system is much stiffer than the proposed pile with plate system. As was done in the previous Section, Figure 17 can be used to estimate the horizontal displacement of the post at the ground level under the action of horizontal loads caused by active earth pressures.

2.6 OTHER ALTERNATIVES

The finite element analysis is extended to include four other possible systems that may be used to replace or enhance the proposed pile with plate system. These are: (1) a wide steel plate system, (2) a steel plate with stiffener system, (3) a two U-sections system, and (4) a tieback system.

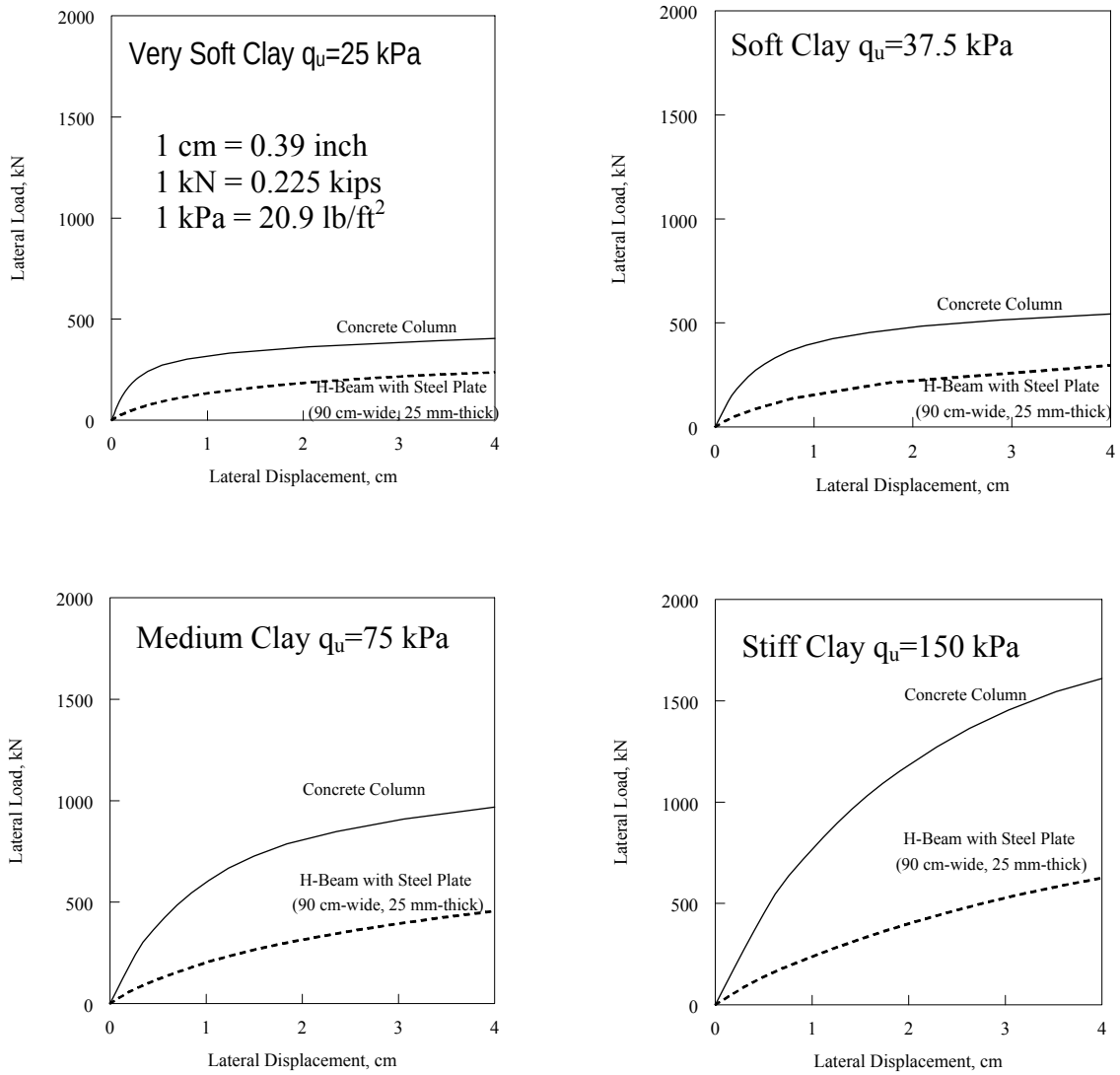

Figure 17: Comparison Between Systems for Different Soils (Clay)

2.6.1 Wide Steel Plate System

This proposed system eliminates the concrete column and replaces it with a 180 cm (6 ft)-wide, 25 mm (1 inch)-thick steel plate of the same length as the concrete column (Figure 18). This plate is welded to the "H" section and then the composite unit is driven into the ground to the required plan base elevation. The finite element analysis of this case assumes a medium clay foundation soil with q_u = 75 kPa (1570 psf). Figure 19 shows the predicted horizontal displacement at the ground level versus applied lateral load for the post-and-panel system with a concrete column, the plate system with a 90 cm

(3 ft)-wide steel plate, and the plate system with a 180 cm (6 ft)-wide steel plate. The figure clearly indicates that the wider steel plate system offers a slight improvement to the 90 cm (3 ft)-wide steel plate (i.e., the wider plate is not warranted).

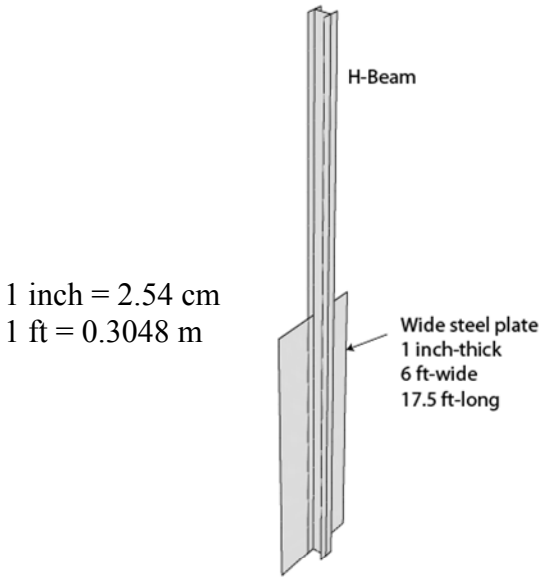

Figure 18: Alternative: Wide Steel Plate

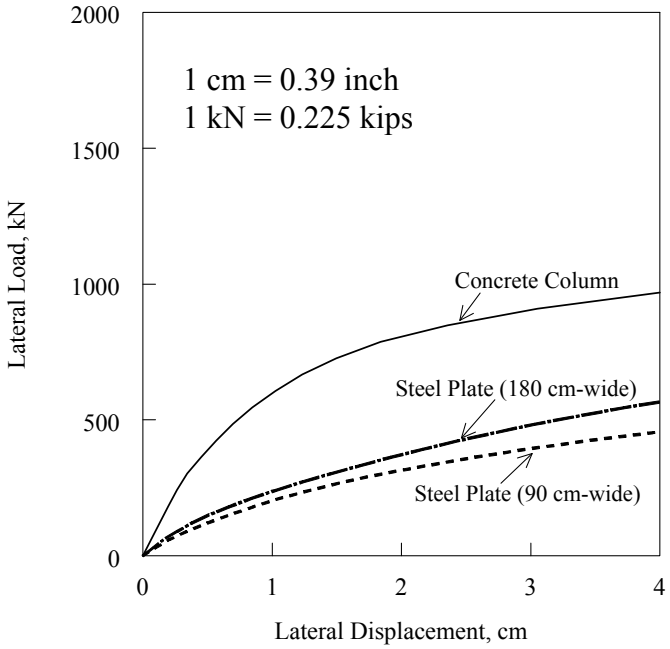

Figure 19: Alternative: Wide Steel Plate

2.6.2 A Steel Plate with Stiffener System

This system, shown in Figure 20, consists of a 90 cm (3 ft)-wide, 25 mm (1 inch)-thick steel plate that is welded to the H-beam, and a stiffener plate, 30 cm (1 ft)-wide and 25 mm (1 inch)-thick, that is orthogonally welded to the 90 cm (3 ft)-wide plate as shown in the figure. As in the previous analysis the finite element analysis of this case assumes a medium clay foundation soil with q_u = 75 kPa (1570 psf). Figure 21 shows the predicted horizontal displacement at the ground level versus applied lateral load for the post-and-panel system with a concrete column, the plate system with a 90 cm (3 ft)-wide steel plate, and the plate system with a stiffener. Again, the figure indicates that the steel plate with stiffener system offers some improvement to the 90 cm (3 ft)-wide steel plate. More improvement can be attained by increasing the width of the stiffener.

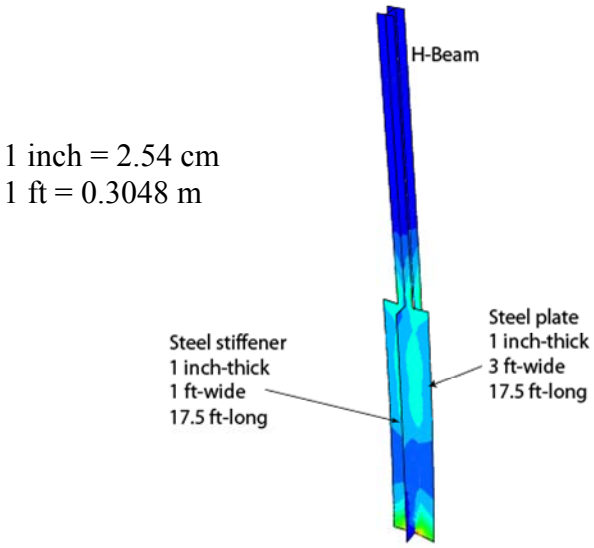

Figure 20: Alternative: Steel Plate with Stiffener

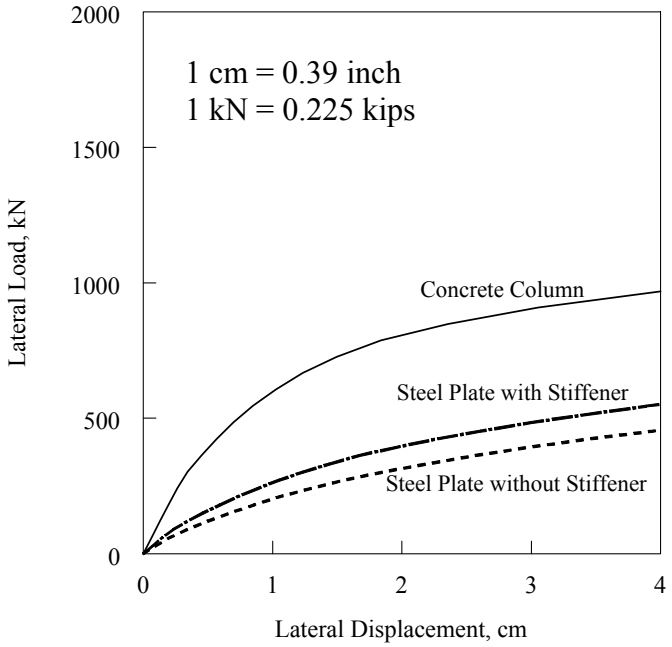

Figure 21: Alternative: Steel Plate with Stiffener

2.6.3 Two U-Sections System

Figure 22 illustrates this system that consists of two channel sections welded to the H-beam. The channel section used in this analysis is 30 cm (1 ft)-wide, 30 cm (1 ft)-deep, and 25 mm (1 inch)-thick. As in the previous analysis the finite element analysis of this case assumes a medium clay foundation soil with q_u = 75 kPa (1570 psf). Figure 23 shows the predicted horizontal displacement at the ground level versus applied lateral load for the post-and-panel system with a concrete column, the plate system with a 90 cm (3 ft)-wide steel plate, and the two U-sections system. The figure shows that the two U-sections system offers a slight improvement to the 90 cm (3 ft)-wide steel plate at early stages of loading. At loads greater than approximately 250 kN (56 kips) this improvement diminishes as shown in the figure.

2.6.4 Tieback System

This proposed system consists of a 90 cm (3 ft)-wide, 25 mm (1 inch)-thick steel plate of the same length as the concrete column (Figure 24). A tieback system consisting of a

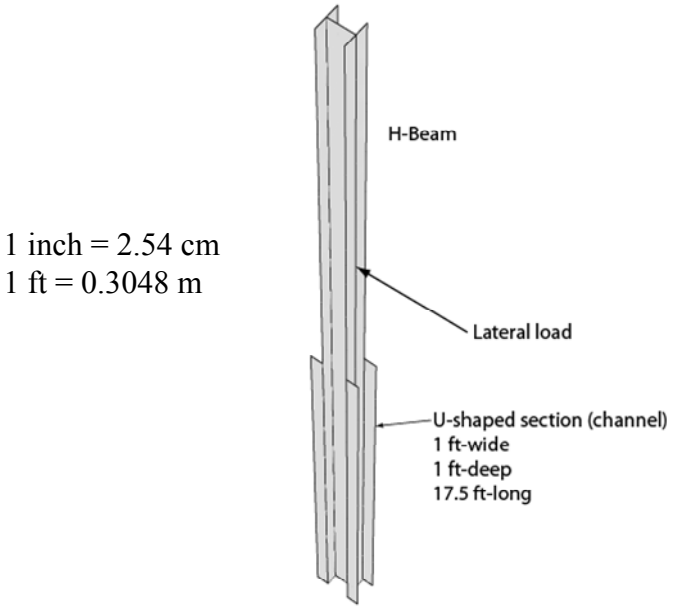

Figure 22: Alternative: Two U-Shaped Sections

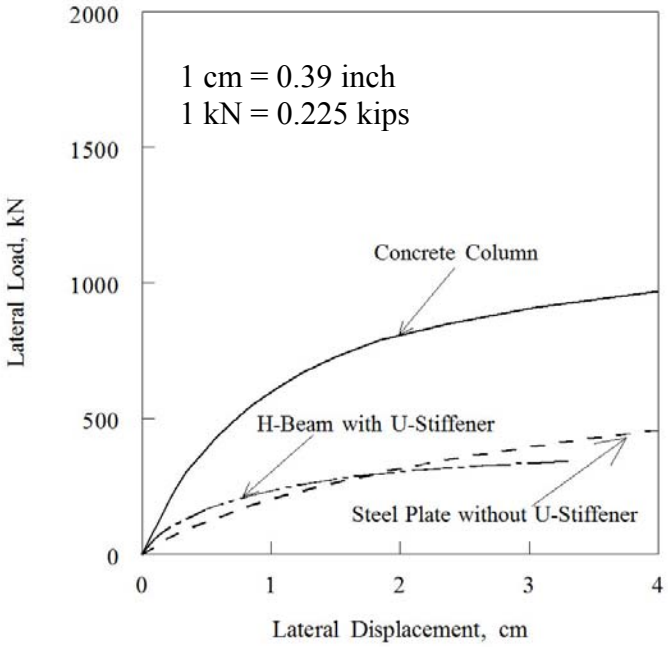

Figure 23: Alternative: Two U-Shaped Sections

steel cable attached to the H-beam 30 cm (1 ft) below the ground level at one end, and to a concrete block at the other end. The cable is attached to the H-Beam after the composite unit (H-beam and the welded steel plate) is driven into the ground to the

required plan base elevation. The finite element analysis of this case assumes a medium clay foundation soil with q_u = 75 kPa (1570 psf). Figure 25 shows the predicted horizontal displacement at the ground level versus applied lateral load for the post-and-panel system with a concrete column, the plate system with a 90 cm (3 ft)-wide steel plate, and the plate system with tieback. The figure indicates that the tieback system offers a substantial improvement on the 90 cm (3 ft)-wide steel plate.

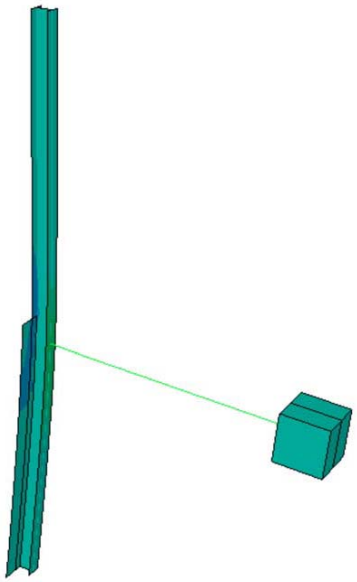

Figure 24: Alternative: Steel Plate & a Tieback

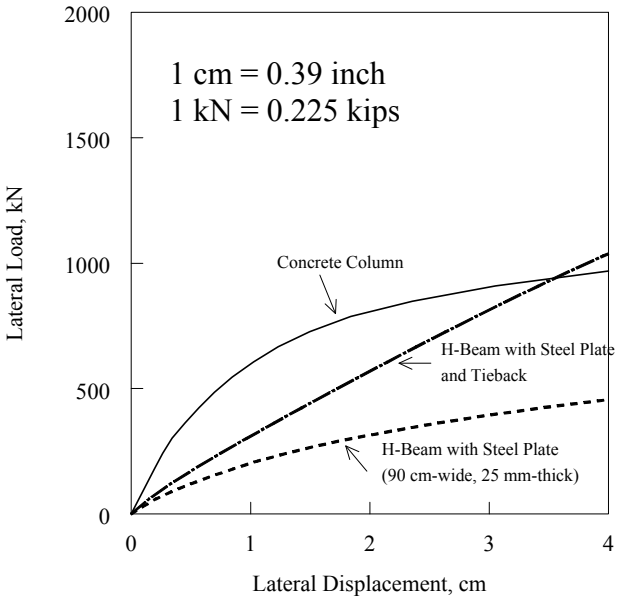

Figure 25: Alternative: Steel Plate & a Tieback

CHAPTER 3

3.1 FIELD TESTS

Two full-scale field tests were performed to investigate the performance of the proposed pile with plate system. The configuration of the field tests and instrumentation is shown in Figure 26. To obtain representative results, the length of the posts below ground level will be 5.3 m (17.5 ft). The two posts will then be loaded laterally until failure. Each post will be loaded independently, as opposed to loading one post against the other post. This is because there is a possibility that one post will fail first, thus the test has to be terminated prematurely before loading the second post to failure.

Both post systems were instrumented to determine their response to lateral loading, especially longitudinal strains and lateral deflections. The instrumentation program included inclinometers to determine lateral displacement profiles of the post in both systems. It also included strain gauges along the post of both systems to determine strain distribution. The lateral load was applied in small increments (approximately 10% of the estimated failure load). All deflection and strain measurements were taken immediately after the load increment was applied.

3.2 FIELD TEST PROCEDURE

Full-scale testing of the pile with plate system and the conventional pile with concrete pier system were performed as part of this project. The performance of the two systems is compared under otherwise nearly identical in-situ and loading conditions. The tests were performed at a site near the intersection of E. Bay Street and Lincoln Memorial Drive in Milwaukee (site belongs to the Port Authority). An aerial photo of the site is shown in Figure 27. Note the locations of borings 1 and 2 in the figure. Appendix A provides the details of the two borings. The field tests were performed in the near vicinity of boring No. 2. Of most interest is the top part of the soil since the embedded length of the test piles was 5.3 m (17.5 ft). The upper 4.3 m (14 ft) of the soil strata consisted of a dense to loose granular fill material with fine to coarse sand and gravel. This soil layer was dry in the most part except for a moist zone at the bottom. This layer

was underlain by a 1.2-m (4-ft) thick layer of a loose silty moist to wet sand. This was followed be a 1.8-m (6-ft) thick layer of a very dense sand with gravel.

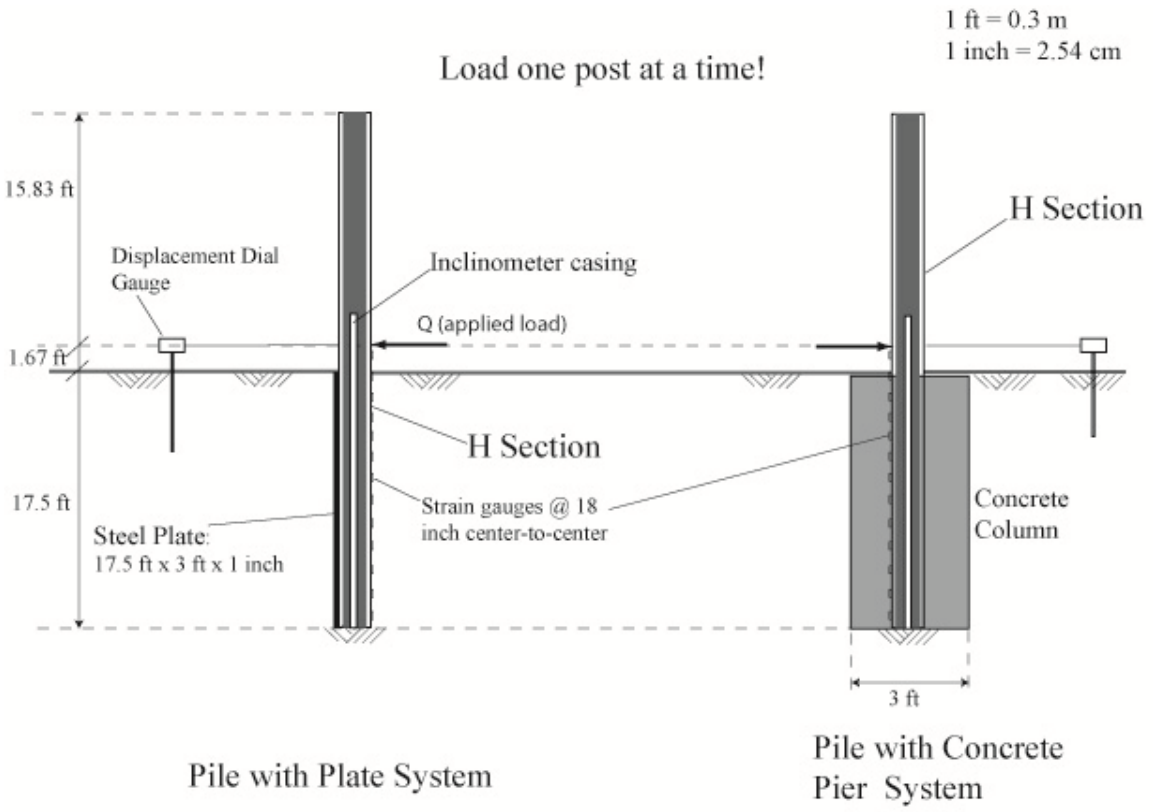

Figure 26: WisDOT Field Test

3.2.1 Test 1: Pile with Plate System

The pile with plate system, shown in Figure 28, was fabricated and then transported to the test site. The test pile (HP12×53, 50-ksi steel) was instrumented with strain gauges at the geotechnical laboratory (UWM) before being transported to the site. The strain gauges were protected using a steel channel section that was welded to the pile to prevent the gauges from being in direct contact with the soil during pile driving.

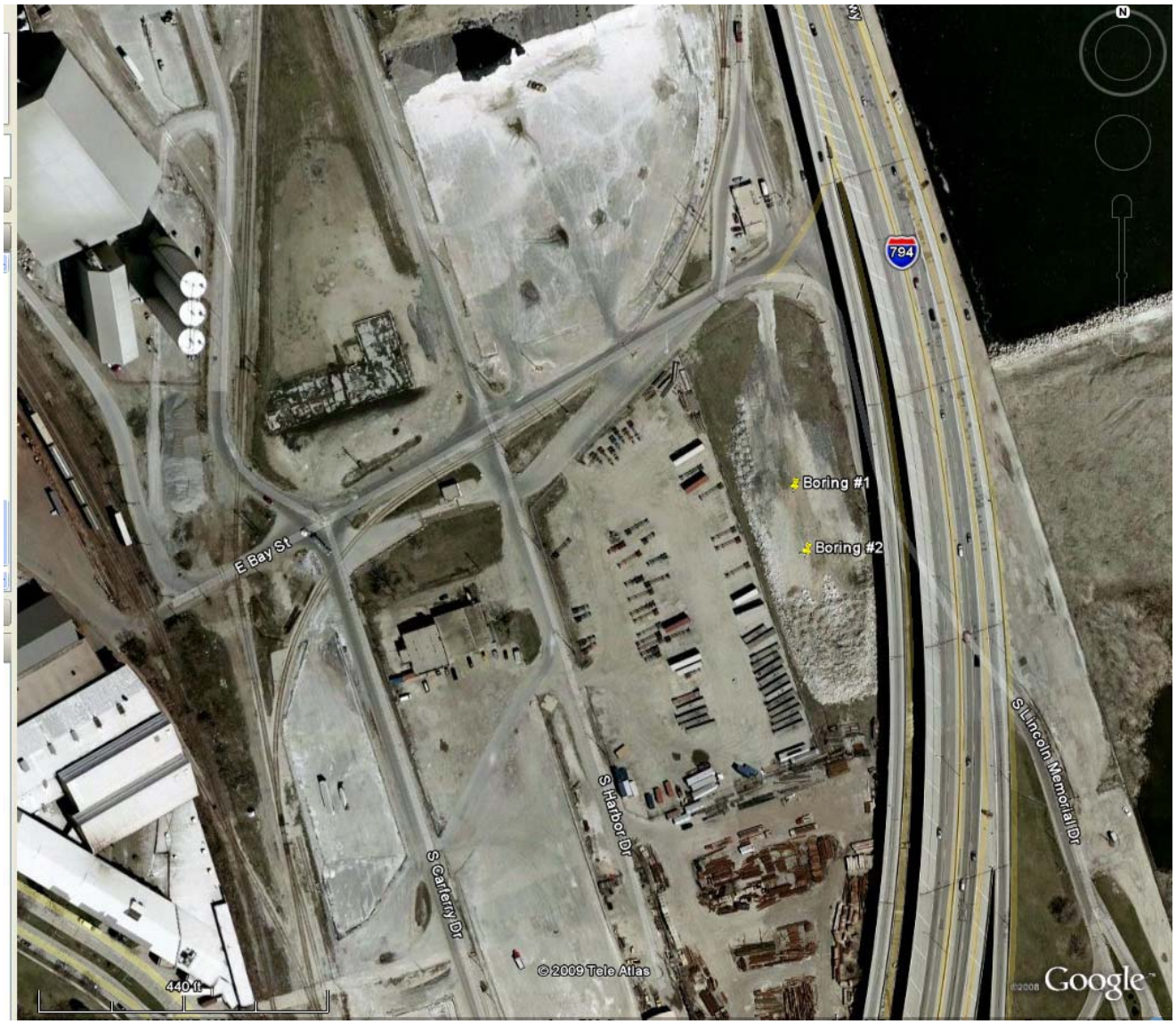

Figure 27: Borings at E. Bay Street and Lincoln Memorial Drive

Figure 28: Installation of the Pile with Steel Plate

The horizontal deflections of the pile were measured using an inclinometer as indicated in Figure 29. The inclinometer flexible casing was protected using a welded steel sleeve as shown in the same figure. The small space between the protective sleeve and the inclinometer casing was filled with grout. Inclinometer measurements were taken after each load increment application.

Figure 29: Loading Mechanism for the Pile with Steel Plate

Axial strains in the pile (H beam) were measured using 13 strain gauges. The gauges were spaced at 45 cm (18 inch) intervals center-to-center as shown in Figure 26. The top gauge is 45 cm (18 inch) above the ground level, i.e., 5 cm (2 inch) below the point of load application. Strain gauge readings were taken after the application of each load increment.

The horizontal deflection of the pile at the point of load application was measured using a displacement dial gauge mounted on a steel frame supported by four mini piles located sufficiently away from the test pile to ensure that the supporting frame is unaffected by ground subsidence associated with pile deflection during testing.

The following is a step-by-step description of the first test:

1. A 2.54-cm thick (1-inch), 0.91-m wide (3-ft), 5.3-m long (17.5-ft) steel plate was welded to the 10.7-m long (35-ft) H-beam (HP12×53) to form the proposed pile with plate system. Strain gauges and inclinometer protective sleeve were installed as shown in Figure 26.

2. The proposed plate system was driven to a depth of 5.4 m (17.5 ft) using a pneumatic hammer (Figure 28). Precautions were exercised to make sure that the pile with plate system was perfectly vertical upon driving. The actual driving of the pile was done in a few minutes.
3. Inclinometer casings were inserted inside the inclinometer protective sleeve and the space in between was grouted (see Figure 29).
4. A loading fixture with a centric hole was welded to the pile. The height of the center of the hole was 50 cm (20 inch) above ground level (see Figure 29). A 2.54-cm (1-inch) diameter steel bar was used to apply the horizontal load as shown in the same figure. A crane weighing approximately 890 kN (200,0000 lb) was situated near the pile (Figure 30) and used as a reaction mass against which a hydraulic actuator was mounted as shown in Figures 31 and 32.
5. The lateral load on the pile with plate system was increased gradually: 22.25 kN (5,000 lb), 44.5 kN (10,000 lb), 66.75 kN (15,000 lb), 111.25 kN (25,000 lb), 200.25 kN (45,000 lb), 289.25 kN (65,000 lb), 378.25 kN (85,000 lb), and 445 kN (100,000 lb). All data were collected at the conclusion of each load increment.

Figure 33 shows the measured horizontal displacements of the pile (at the point of load application) versus applied load. The figure indicates an approximately linear load-displacement behavior. At approximately 445-kN (100,000-lb) applied load, the measured lateral displacement was 3.3 cm (1.3 inch). It is to be noted that at an applied load of about 445-kN (100,000-lb), the crane that was used as a reaction mass started to slide. At that instance it was difficult to sustain the load. Nonetheless, a consequent finite element analysis of the pile with plate test indicated that the A36 steel H pile started to yield (initial yield) at approximately 445-kN (100,000-lb) applied lateral load.

Figure 30: Loading Mechanism for the Pile with Steel Plate

Figure 34 shows the profiles of lateral displacements of the pile at various loading stages. These profiles were obtained from inclinometer readings assuming that the tip of the pile is the reference point (assuming it is a stationary point). The figure indicates that most of the deflections occurred in the upper half of the pile's embedded length.

The inclinometer uppermost point is 6.1 m (20 ft) above the tip of the pile. This means that the inclinometer uppermost point is one foot higher than the location of the displacement dial gauge. It can be seen from Figure 34 that at 445-kN (100,000-lb)

lateral load, the displacement at the elevation of the displacement gauge (one foot below the top point of the inclinometer) is approximately 3.3 cm (1.3 inch). This displacement is the same as that obtained from the displacement dial gauge at the same load (see Figure 33). This shows that the inclinometer displacements in reference to the pile tip are reasonably accurate, and that the reference point (tip of the pile) was indeed stationary throughout the load test.

Figure 31: Loading Mechanism for the Pile with Steel Plate

Figure 35 shows the measured axial strains in the pile at various loading stages. It is noted from the figure that the strain at the tip of the pile and at the point of load application was always zero. The maximum measured strain at 445-kN (100,000-lb) lateral load was approximately 1,300 Micro strain and located about 127 cm (50 inch) below the point of load application. This strain can be well within the yield strain range for A36 steel (note that the yield strain and yield stress can vary widely for the same type of steel).

Finally, Figure 36 shows a substantial gap between the soil and the back of the pile at failure load. This gap started with the first lateral load increment and increased gradually as the lateral load was increased.

Figure 32: Loading Mechanism for the Pile with Steel Plate

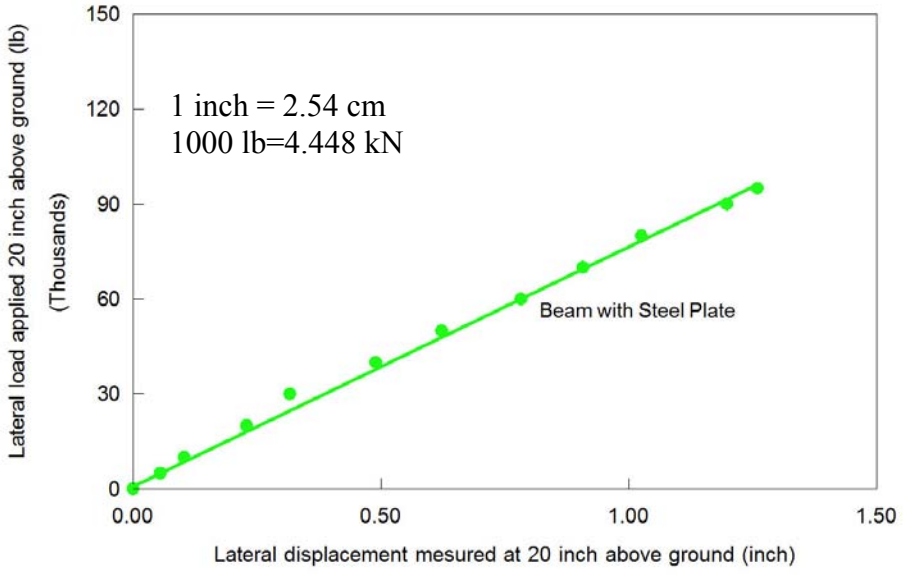

Figure 33: Measured Load versus Displacement Behavior (Pile with Steel Plate)

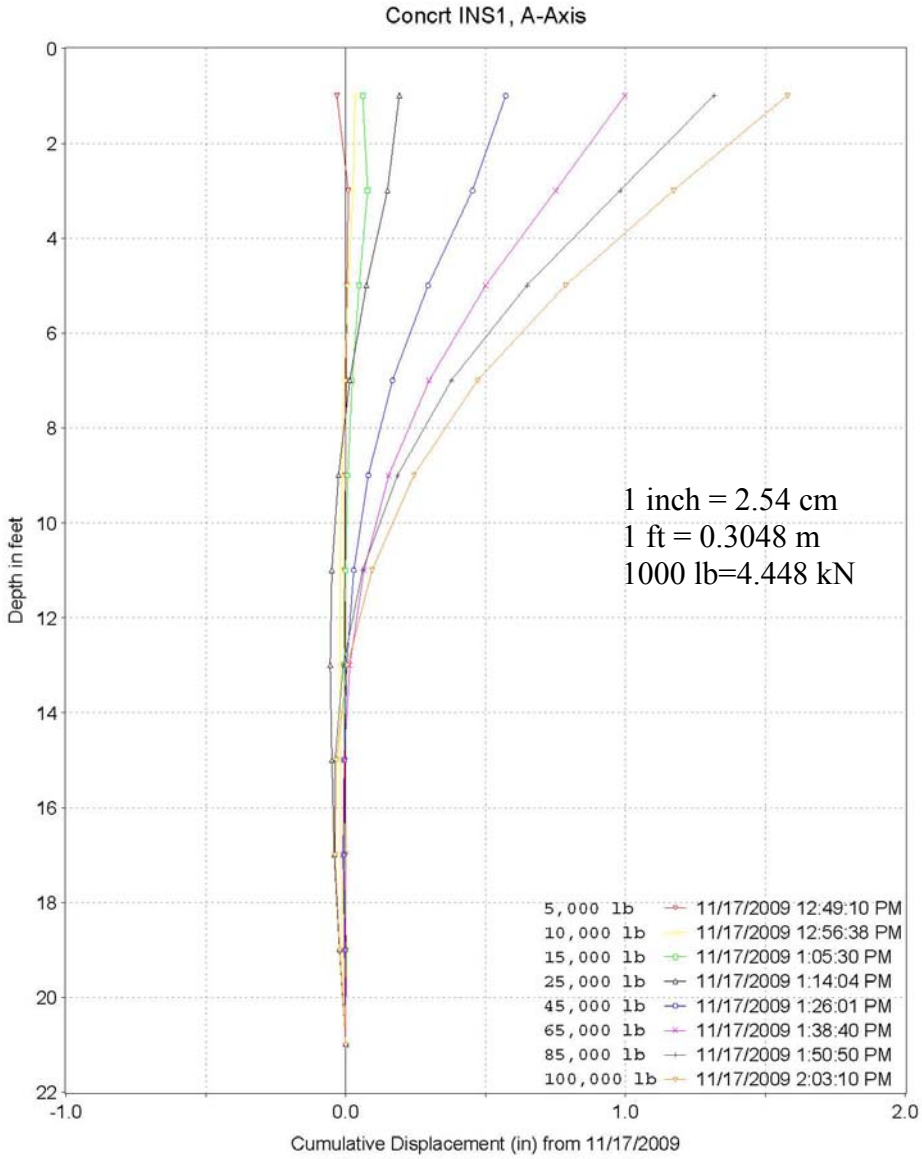

Figure 34: Measured Displacement Profiles (Pile with Steel Plate)

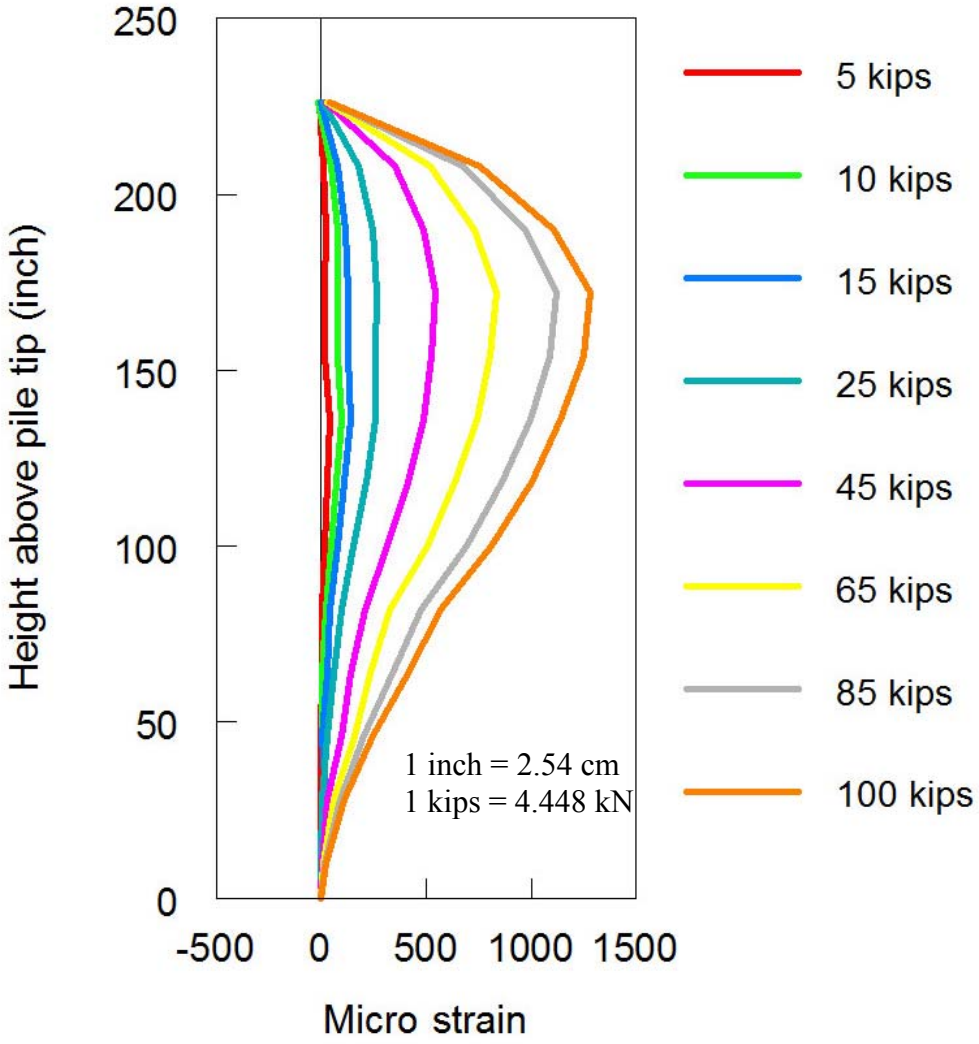

Figure 35: Measured Strains (Pile with Steel Plate)

Figure 36: Gap at 445-kN (100,000-lb)

3.2.2 Test 2: Pile with Concrete Pier

The pile with concrete pier system is schematically shown in Figure 26. The test pile (H beam) was instrumented with strain gauges at the geotechnical laboratory (UWM) before being shipped to the testing site. The strain gauges were protected using a steel channel section that was welded to the pile to prevent strain gauges from being in contact with the concrete during pile installation. The steel channel protective sleeve was made completely water proof to protect the strain gauges from moisture seeping from the fresh concrete.

The horizontal deflections of the pile were measured using an inclinometer. The inclinometer flexible casing was protected using a welded steel sleeve as was done in the

first test. The small space between the protective sleeve and the inclinometer casing was filled with grout. Inclinometer measurements were taken after each load increment application.

Axial strains in the pile (H beam) were measured using 13 strain gauges. The gauges were spaced at 45.7 cm (18 inch) intervals center-to-center as shown in Figure 26. The top gauge is 45.7 cm (18 inch) above the ground level, i.e., 5 cm (2 inch) below the point of load application. Strain gauge readings were taken after the application of each load increment.

The horizontal deflection of the pile at the point of load application was measured using a displacement dial gauge mounted on a steel frame supported by four mini piles located sufficiently away from the test pile to ensure that the supporting frame is unaffected by ground subsidence associated with pile deflection during testing.

The following is a step-by-step description of the second test:

1. A 5.3-m (17.5-ft) deep, 0.91-m (3-ft) diameter hole was drilled as shown in Figures 37 and 38. There was no need to support the excavation during construction.
2. A 10.7-m (35-ft) long H-beam (HP12×53) was positioned at the center of the hole (Figure 39).
3. Concrete was poured up to ground level as shown in Figures 39 and 40. The concrete was left to harden for 28 days.
4. Inclinometer casings were installed inside the inclinometer protective sleeve and the space in between was grouted.
5. A loading fixture with a centric hole was welded to the pile. The height of the center of the hole was 51 cm (20 inch) above ground level. A 2.54 cm (1-inch) diameter steel bar was used to apply the horizontal load. A crane weighing approximately 889 kN (200,0000 lb) was situated near the pile (Figure 41) and used as a reaction mass against which a hydraulic actuator was mounted. For

6. The lateral load on the pile with concrete pier system was increased gradually: 22.25 kN (5,000 lb), 111.25 kN (25,000 lb), 155.75 kN (45,000 lb), 289.25 kN (65,000 lb), 378.25 kN (85,000 lb), 445 kN (100,000 lb), 556.25 kN (125,000 lb), and 667.5 kN (150,000 lb) at which failure was deemed imminent. All data were collected at the conclusion of each load increment.

Figure 43 shows the measured horizontal displacements of the pile (at the point of load application) versus applied load. A highly nonlinear load-displacement behavior is noted in the figure. At approximately 667-kN (150,000-lb) applied load, the measured lateral displacement was 2.54 cm (1.0 inch). Failure was deemed imminent because of the difficulties encountered trying to maintain the hydraulic pressure in the hydraulic jack at this load level.

Figure 44 shows the deflection profiles of the pile at various loading stages. These profiles were obtained from inclinometer readings assuming that the pile tip is the reference point. The figure shows that the deflections occurred in the entire embedded length of the pile indicating some rotational tendency.

The inclinometer uppermost point is 6.1 m (20 ft) above the tip of the pile, i.e., one foot higher than the location of the displacement dial gauge. It can be seen from Figure 44 that at 667-kN (150,000-lb) lateral load, the displacement at the elevation of the displacement gauge (one foot below the top point of the inclinometer) is approximately 3 cm (1.2 inch). This displacement is slightly larger than that obtained from the displacement dial gauge at the same load (see Figure 43).

Figure 45 shows the measured axial strains in the pile at various loading stages. It is noted from the figure that the strains are mostly mobilized in the upper half of the embedded length of the pile. The maximum measured strain at 667-kN (150,000-lb) lateral load was approximately 1,400 Micro strain and located about 102 cm (40 inch)

below the point of load application. As indicated earlier, this strain can be well within the yield strain range for A36 steel (note that the yield strain and yield stress can vary widely for the same type of steel).

Figure 46 shows a gap between the soil and the back of the pier at failure load. This gap started with the first lateral load increment and increased gradually as the lateral load was increased. Figures 47 and 48 show minor cracks that appeared in the plain concrete at higher loads approaching the failure.

Figure 37: Installation of the Pile with Concrete Pier

Figure 38: Installation of the Pile with Concrete Pier

Figure 39: Installation of the Pile with Concrete Pier

Figure 40: Installation of the Pile with Concrete Pier

Figure 41: Loading Mechanism (Pile with Concrete Pier Test)

Figure 42: Loading Mechanism (Pile with Concrete Pier Test)

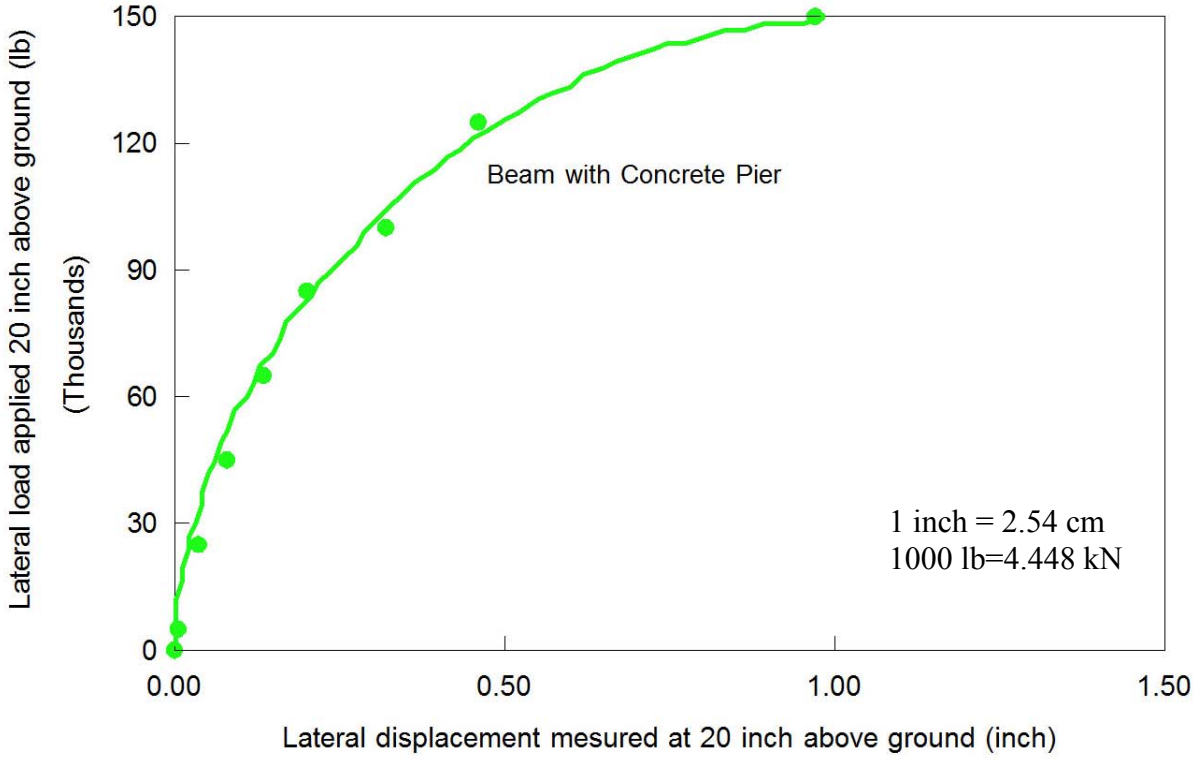

Figure 43: Measured Load versus Displacement Behavior (Pile with Concrete Pier)

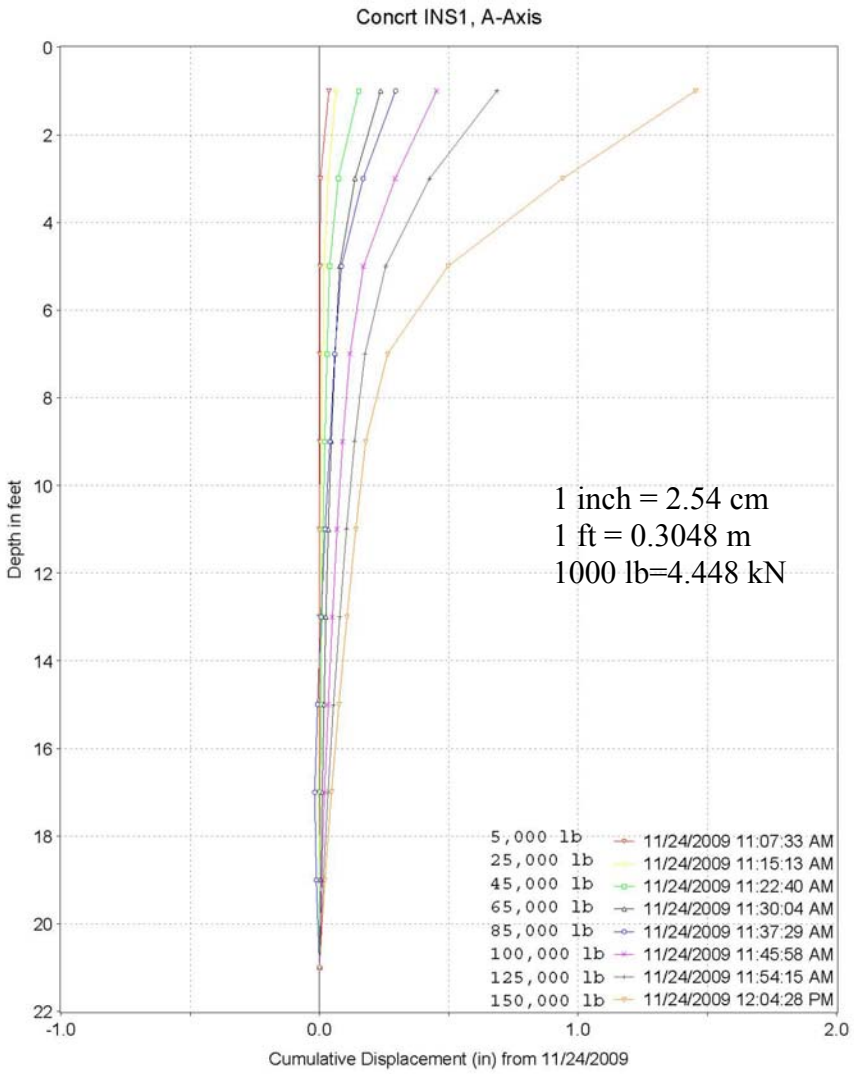

Figure 44: Measured Displacement Profiles (Pile with Concrete Pier)

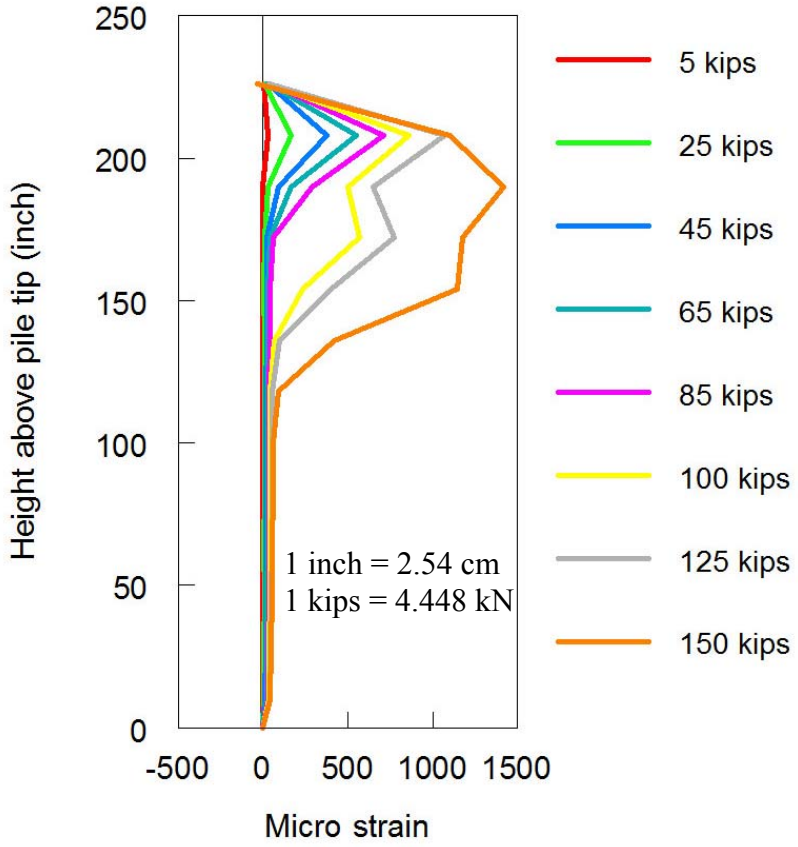

Figure 45: Measured Strains (Pile with Concrete Pier)

Figure 46: Gap at 556 kN-667 kN (125,000 lb-150,000 lb)

Figure 47: Cracking at 556 kN-667 kN (125,000 lb-150,000 lb)

Figure 48: Cracking at 556 kN-667 kN (125,000 lb-150,000 lb)

3.3 COMPARISON: PILE WITH PLATE SYSTEM VERSUS PILE WITH CONCRETE PIER SYSTEM

The field tests have shown that the pile with plate system offered several benefits such as ease of construction, reduced construction time, and lower wall costs. The fabrication of the pile with plate is fairly simple and involved welding the plate to the H beam. To further save cost one can select a plate with a standard 1.22-m (4-ft) width and use it as is (without the need for cutting). The installation of the pile with plate system was very accurate and speedy in this particular soil strata. In this particular field test, the initial alignment of the system took about five minutes. The actual driving time of the 5.3 m (17.5 ft) embedded length was 2-3 minutes in a relatively dense granular soil. There was no apparent damage to the plate during driving (please see video clip of the field test). Further field tests in difficult soils, such as dense gravely soils, may be needed to illustrate the applicability of the pile with plate system in terms of installation speed and alignment control.

The pile with plate system does not require excavation and concrete mixing equipment and their associated costs, making it a very cost-effective method. The ease of fabrication and installation in any type of weather makes this system a very attractive alternative. For example, the system can be used even during the frost season, while the pile with concrete pier can not be used due to difficulties in excavating frozen soils and the impossibility of pouring concrete without costly heating.

Figure 49 shows a comparison between the two systems in terms of their load-displacement behaviors as measured in the field tests. As indicated earlier, the behavior of the pile with plate system is approximately linear with a failure load approaching 445 kN (100,000 lb). On the other hand, the load-displacement behavior of the pile with concrete pier is nonlinear with a failure load of approximately 667 kN (150,000 lb). In terms of displacement-based performance, at 2.54 cm (1 inch) lateral displacement the pile with plate can resist a lateral load of approximately 345 kN (78,000 lb), while the pile with concrete pier can resist 667-kN (150,000-lb) lateral load at the same displacement--nearly double the load of the pile with plate system. However, the 345-kN

(78,000-lb) lateral load capacity of this particular pile with plate system makes it feasible to be used as the foundation for "post-and-panel" retaining walls, in lieu of the pile with concrete pier foundation system, as will be illustrated through examples in the parametric analyses section.

Figure 50 shows a comparison between the displacement profiles for the two systems. The figure indicates that the pile with plate system is more flexible, as expected. Figure 51 shows a comparison between the two systems in terms of measured strains. Again, the flexibility of the pile with plate system is apparent where the whole embedded length is contributing to the flexural resistance. In contrast, the strains in the pile with concrete pier are concentrated in the upper half of the embedded length, whereas the lower half endured near zero strains.

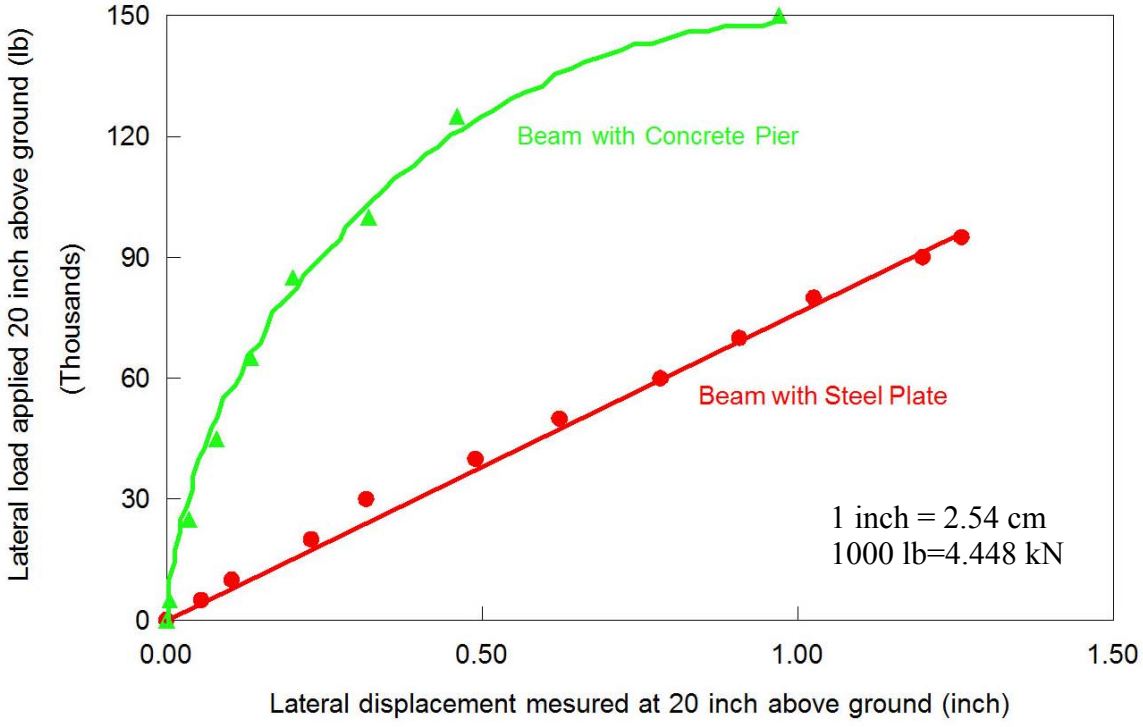

Figure 49: Comparison Between Pile with Concrete Pier and Pile with Steel Plate

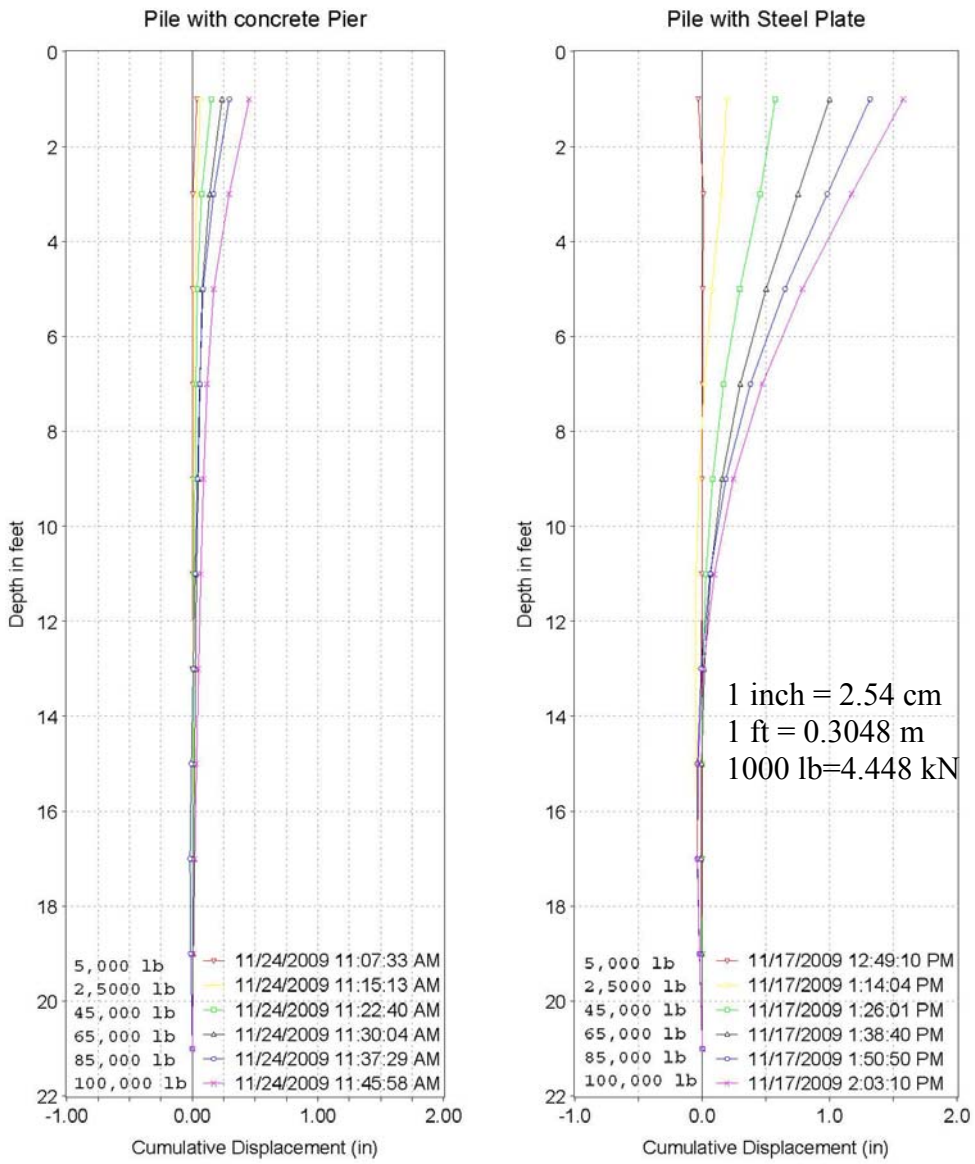

Figure 50: Displacement Comparison between Pile with Concrete Pier (Left) and Pile with Steel Plate (Right)

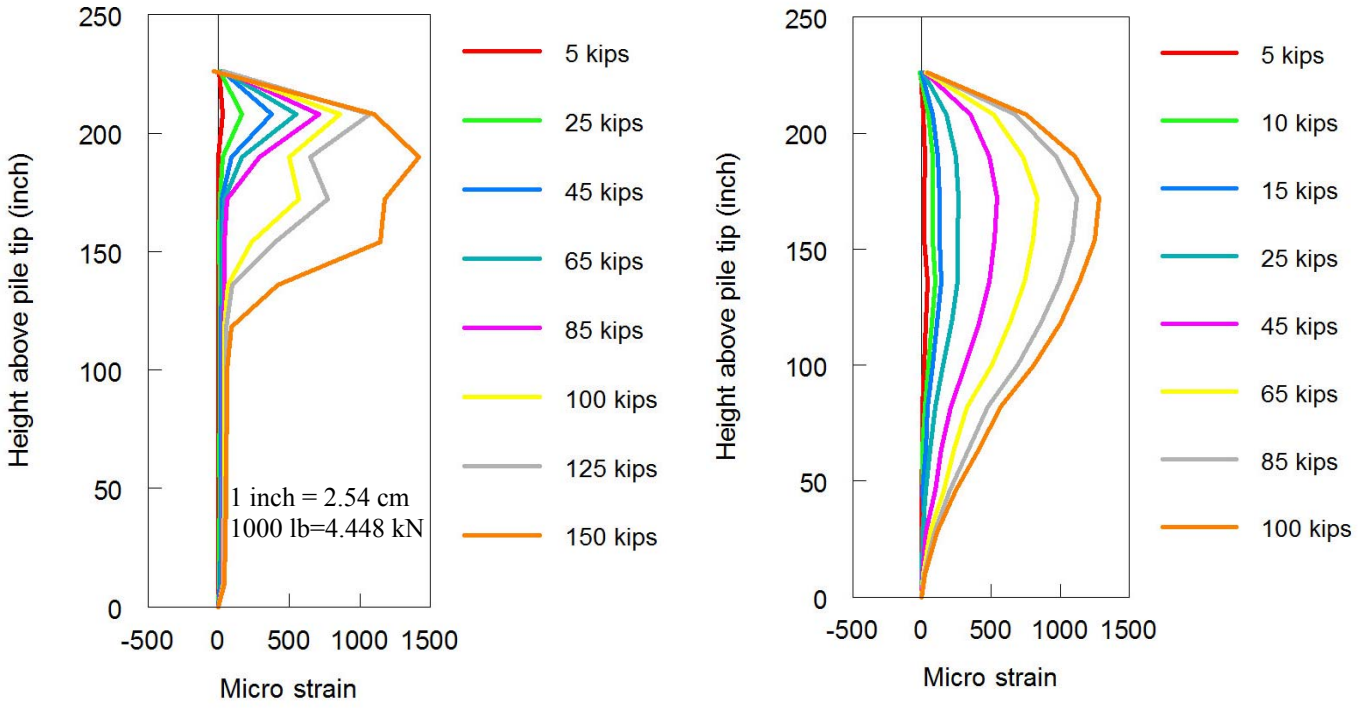

Figure 51: Strain Comparison between Pile with Concrete Pier (Left) and Pile with Steel Plate (Right)

CHAPTER 4

The following is a step-by-step procedure to obtain conventional soil parameters (ϕ', K_0, OCR) and other soil parameters relevant to the modified Drucker-Prager/Cap soil model that is embodied in the finite element program Abaqus. Subsequently, these parameters will be used in the finite element analysis of the pile with plate field test. This finite element analysis is mainly performed to verify the capability of the finite element program Abaqus in modeling this complicated boundary value problem. After verification, Abaqus will be used to perform extensive parametric analyses to establish design charts for the pile with plate system both in cohesionless and cohesive soils.

4.1 FINITE ELEMENT ANALYSIS OF THE PILE WITH PLATE FIELD TEST

As indicated earlier, the pile with plate field test was performed in the vicinity (within 3 m (10 ft)) of boring No. 2 at the Port Authority site (Figure 27). Using the data from boring No. 2 (Appendix A), the N-values at various depths were corrected to obtain the N_{60}-values. The N_{60} distribution for the top 5.5 m (18 ft) of the soil is shown in Figure 52.

A step-by-step procedure to obtain cohesionless soil parameters:

1. From SPT soundings, divide the soil into layers based on N_{60} as shown in Figure 52. For each layer determine the average unit weight, γ, and the depth, Z, of the center of the soil layer measured from the ground level.
2. Calculate the vertical effective stress, σ'_v, in the middle of the soil layer.
3. Calculate the "cone" point load, q_c, assuming $q_c(kPa)=450(N_{60})$ (Robertson and Campanella, 1983).
4. Calculate the internal friction angle of the soil: $\phi' = 17.4 + 11\log_{10}[\frac{q_c/P_a}{(\sigma'_v/P_a)^{0.5}}]$ (Kulhawy and Mayne, 1990), where P_a is the atmospheric pressure.

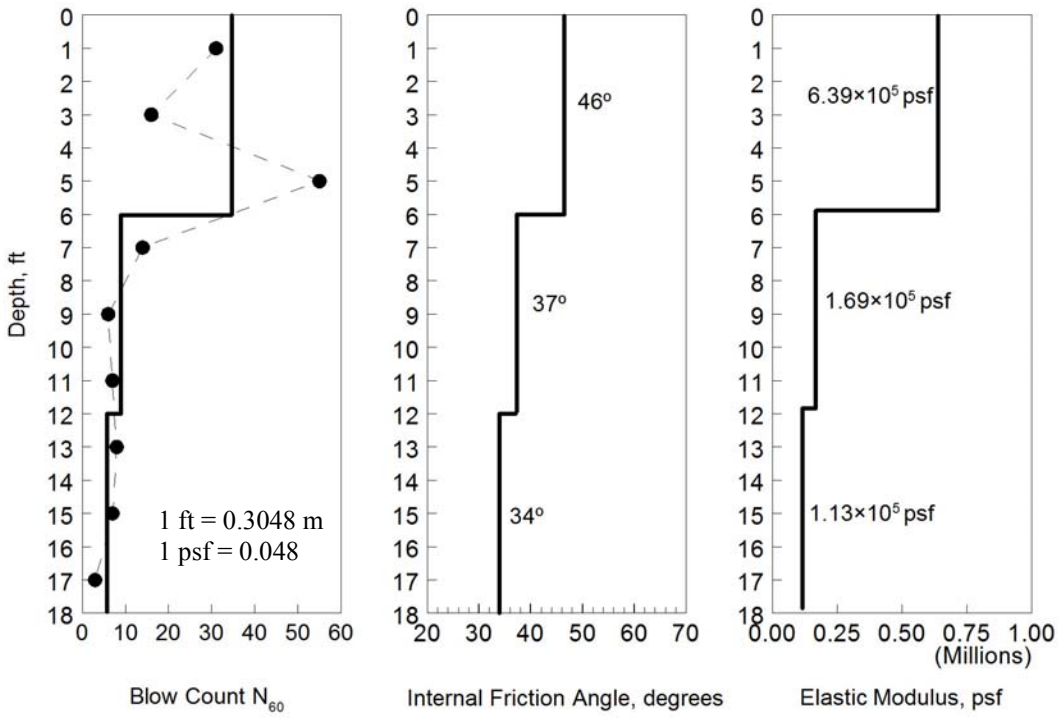

Figure 52: Soil Profile (Boring #2) in the Vicinity of the Field Tests

5. Calculate the overconsolidation ratio of the soil:

$$OCR = [\frac{0.192\,(q_c / P_a)^{0.22}}{(1-\sin\phi')(\sigma'_v / P_a)^{0.31}}]^{\frac{1}{\sin\phi'-0.27}}$$ (Mayne, 2005)

6. Calculate the at-rest lateral earth pressure coefficient of the soil:

$$K_0 = 0.192\,(\frac{q_c}{P_a})^{0.22}(\frac{P_a}{\sigma'_v})^{0.31}(OCR)^{0.27}$$ (Mayne, 2007)

7. Calculate the mean effective stress at the center of the soil layer: $p' = (\frac{1+2K_0}{3})\,\sigma'_v$

8. Calculate the preconsolidation pressure: $p'_c = p' \times (OCR)$. The preconsolidation pressure p'_c is the same as the parameter p_b in the modified Drucker-Prager/Cap soil model.

9. Using p'_c calculated above, estimate the initial volumetric plastic strain of the soil from the hardening curve shown in Figure 53.

10. Calculate the friction angle for the modified Drucker-Prager/Cap soil model:

$$\beta = \tan^{-1}[\frac{6\sin\phi'}{3-\sin\phi'}]$$

11. Calculate the cohesion constant for the modified Drucker-Prager/Cap soil model:

$d = \sqrt{3}\, c'$, where $c' = 0$ can be assumed for cohesionless soils.

12. Calculate the elastic modulus of the soil: $E \approx 2\, q_c$ (Schmertmann, 1970).

Using this procedure, the soil parameters of the three layers shown in Figure 52 were calculated as shown in Table 2. Figure 52 also shows the variation with depth of the internal friction angle and the elastic modulus of soil as calculated using the above procedure.

Table 2: Cap Model Parameters for Field Test Analyses

Z (ft)	N_{60}	K_0	OCR	ϕ' (°)	σ'_v(psf)	p'(psf)	p'_c(psf)	$\varepsilon^{pl}_{v(0)}$	β(°)	E (psf)
0-6	34	2.2	17	46	344	618	10823	0.033871	62	6.39×10^5
6-12	9	0.7	2	37	1030	818	2038	0.004419	56	1.69×10^5
12-18	6	0.4	1	34	1719	1055	1056	0.001126	54	1.13×10^5

1 ft = 0.3 m
1 psf = 0.048 kPa

The yield of the steel pile is a major failure criterion that is considered in the present analysis and the subsequent parametric analyses. Therefore, the steel H beam is assumed to behave in an elastoplastic manner in the finite element analysis. The stress-strain curve shown in Figure 54 is used in the analysis. This curve represents mild steel A36 (as opposed to A50) and it is deemed to be on the "safe side". It is noteworthy that the elastic modulus of both steel grades is the same, they only differ in their yield strength. Such a procedure can be regarded as a safety factor to account for steel strength variability. This particular curve (Figure 54) will be used later in the parametric study.

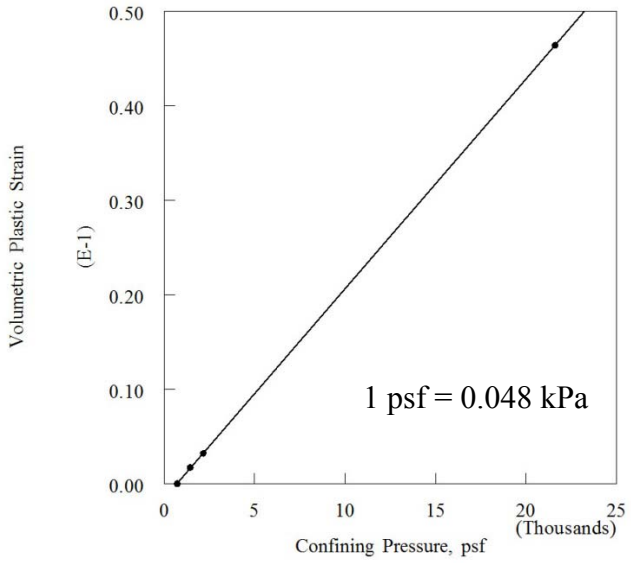

Figure 53: Assumed Hardening Curve for the Drucker-Prager/Cap Soil Model

Using the finite element method, the ultimate lateral load capacity of the pile with plate system will be calculated. Drained loading conditions are assumed. The predicted lateral load-displacement curve from the finite element analysis will be compared with the field test results described above.

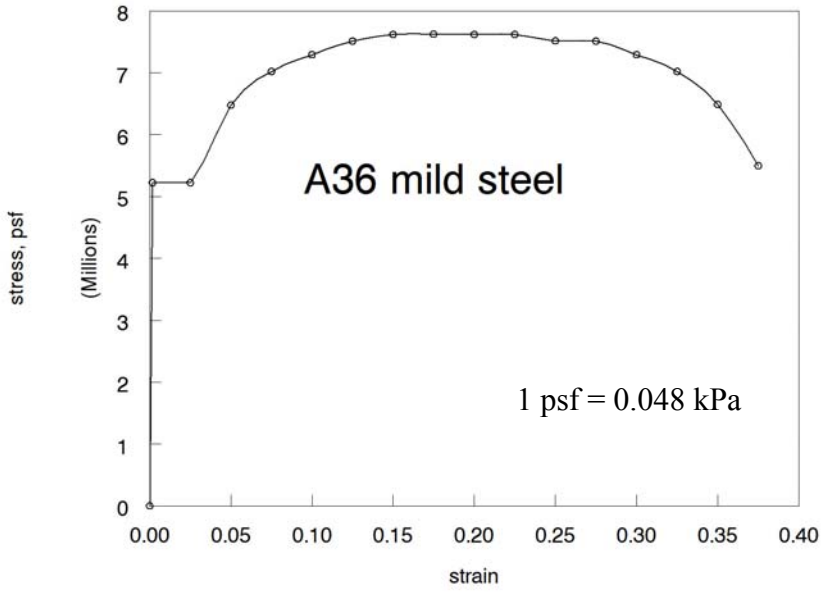

Figure 54: Stress-Strain Curve of Steel Used in the FE Analysis (Elasto-Plastic Model)

In this analysis a limit equilibrium solution is sought for granular strata loaded in a drained condition by a single “pile” with a lateral load applied above ground level. Piles with lateral loads are three-dimensional by nature and will be treated as such in the following finite element analysis. Note that this problem is symmetrical about a plane that contains the vertical axis of the pile and the line of action of the lateral load. Thus, the finite element mesh of half of the pile with plate and half the surrounding soil is considered as shown in Figure 55.

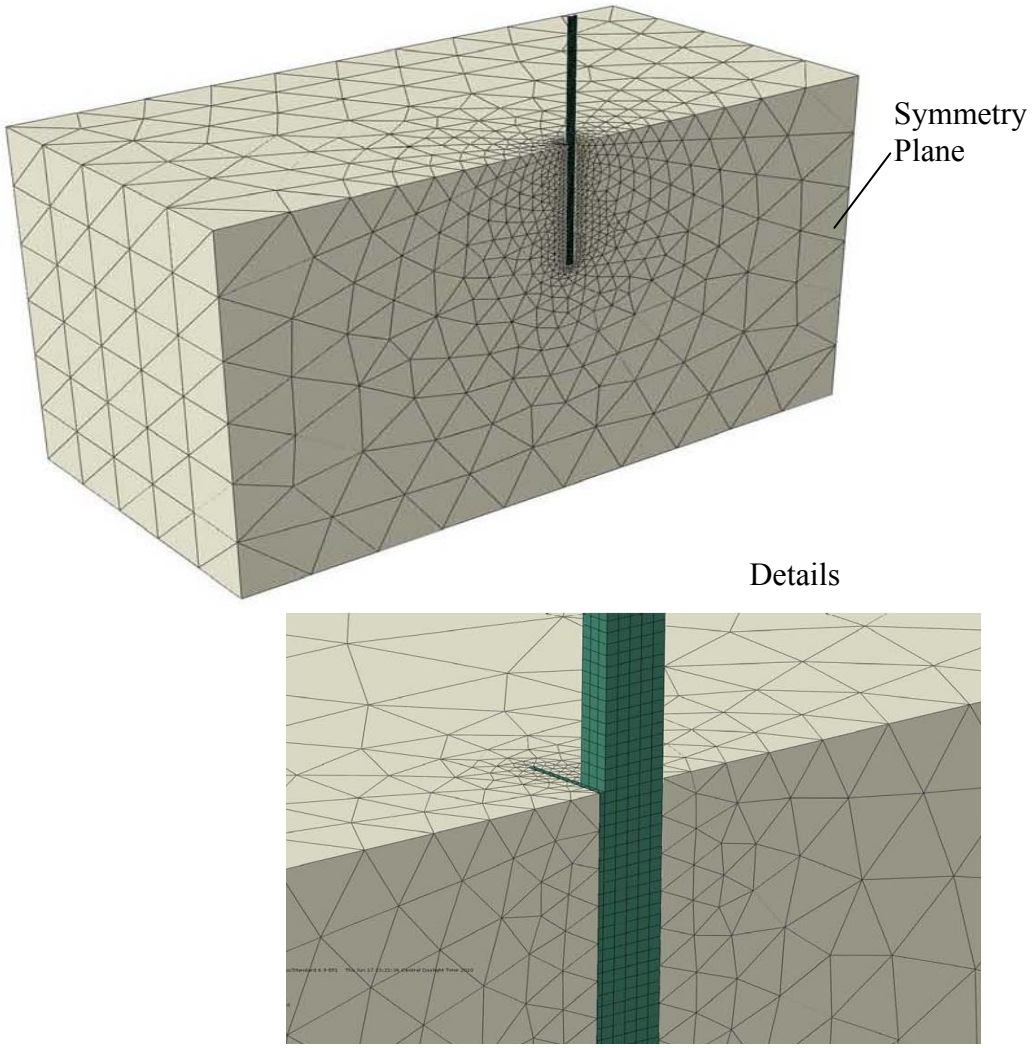

Figure 55: Finite Element Discretization of the Pile with Plate System

Since this is a partial-displacement (driven) pile with minimum soil disturbance during installation, the excess pore water pressure after pile installation is assumed to be zero in this finite element analysis.

The three-dimensional finite element mesh, shown in Figure 55, comprises two parts: the pile with plate and the soil. The mesh is 30-m (100-ft) long in the x-direction, 15-m (50-ft) wide in the y-direction, and 15-m (50-ft) high in the z-direction. Mesh dimensions are chosen in a way that the boundaries do not affect the solution. This means that the mesh must be extended in all three dimensions, and that is considered in this mesh.

The elastic response of the clay layers is assumed to be linear and isotropic, with a Young's modulus that is function of the N_{60}-value of each layer as indicated in Table 2. The modified Drucker-Prager/cap plasticity soil model is used to simulate the plastic behavior of the soil. The model adopted the soil parameters given in Table 2.

The pile lateral load versus displacement curve obtained from the finite element analysis is shown in Figure 56. As was mentioned earlier, the pile with plate field test was terminated at 445 kN (100,000-lb) lateral load because of technical difficulties encountered in the loading mechanism. Nonetheless, the calculated curve shows that the pile would have failed if the load was slightly increased above 445 kN (100,000-lb) due to the initial yielding of the A36 steel pile (H beam). Excellent agreement between the measured and the calculated results, up to 445 kN (100,000-lb), is noted in the figure.

Figure 57 shows a comparison between calculated and measured lateral displacement profiles at 25-kips, 65-kips, and 100-kips lateral loads. Excellent agreement between measured and calculated results is noted in the figure. Also, good agreement between calculated and measured strains along the embedded length of the pile is noted at the same three lateral loads as shown in Figure 58.

The good agreement between test results and finite element analyses results strongly indicate that the analytical procedure used herein is adequate for the analysis of the pile

with plate system in a granular material. It also indicates that the presented procedure for estimating conventional soil parameters and Drucker-Prager/Cap model parameters is satisfactory.

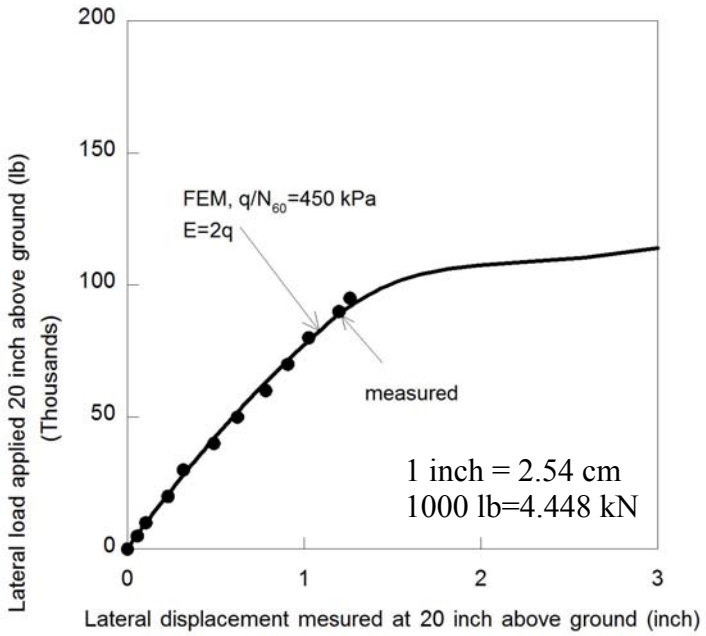

Figure 56: Comparison between Measured and Calculated Lateral Displacement (Pile with Steel Plate)

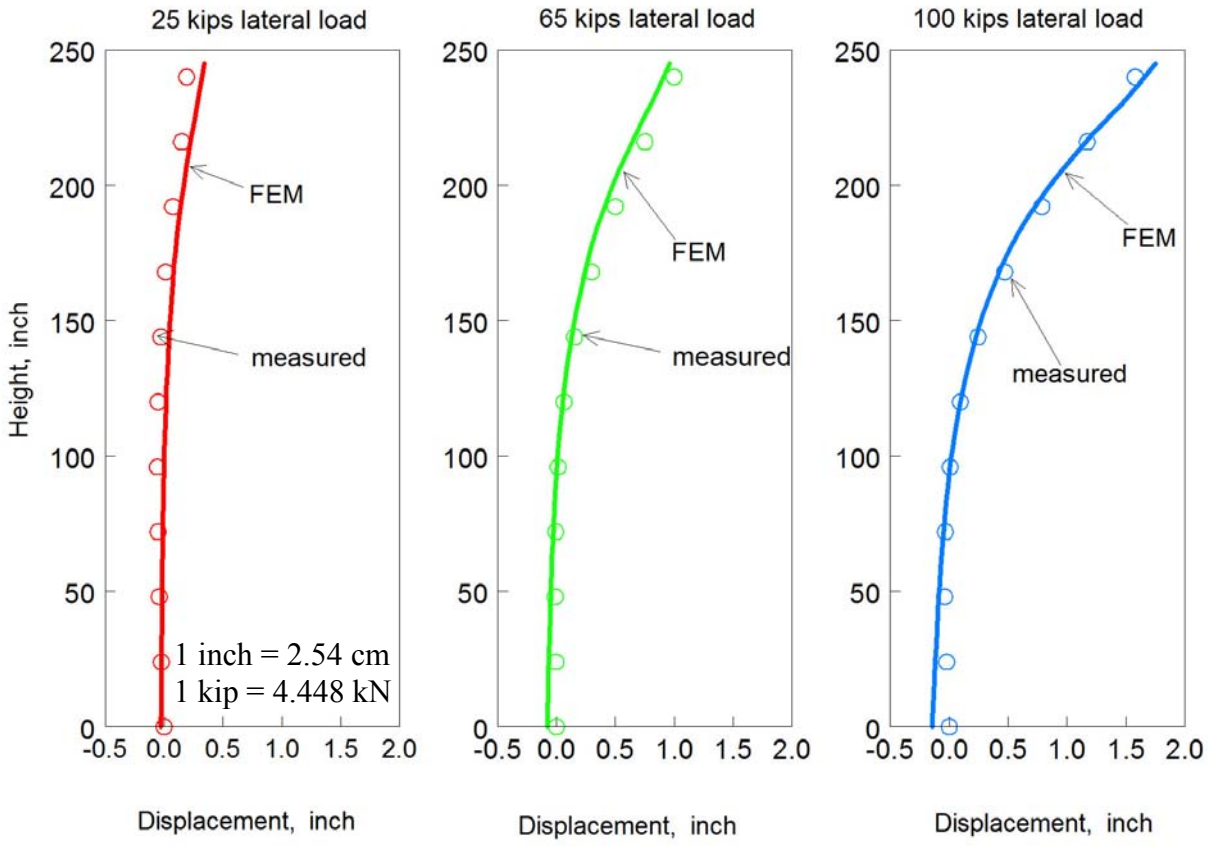

Figure 57: Comparison between Measured and Calculated Lateral Displacement Profiles (Pile with Steel Plate)

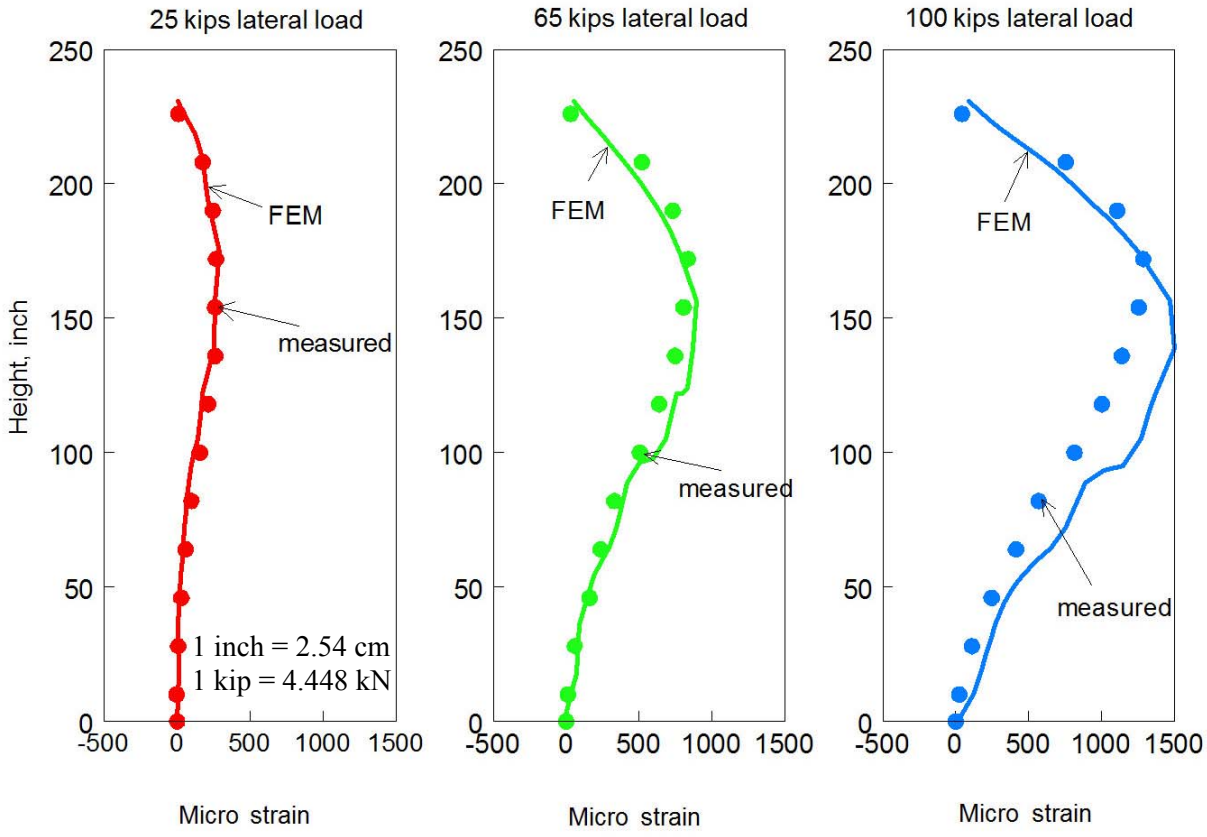

Figure 58: Comparison between Measured and Calculated Strains (Pile with Steel Plate)

4.2 DESIGN CHARTS FOR THE PILE WITH PLATE SYSTEM: COHESIONLESS SOILS

The finite element procedure, with the Drucker-Prager/Cap soil model and an elsto-plastic model for steel embodied in Abaqus, was verified against the results of a full-scale field test of the pile with plate system. The verified procedure will be used next to generate design charts for the pile with panel system in cohesionless and cohesive soils.

The present analysis utilizes five cohesionless soils with ϕ'=25º, 30º, 35º, 40º, and 45º. In the analyses, three embedded lengths of the pile with plate system are used: 3 m (10 ft), 6 m (20 ft), and 9 m (30 ft). The above-ground length of each pile is the same as its embedded length. Five eccentricity ratios are used for each pile: 0, 0.25, 0.5, 0.75, and 1.

The eccentricity ratio is defined as $\frac{e}{L}$, where e is the eccentricity (the vertical distance between the point of load application and the ground level), and L is the embedded length of the pile. To take into account all these variables, 75 analyses combinations are considered as indicated in Table 3.

Table 3: Analysis Matrix for Cohesionless Soils

L=3 m (10 ft)					
	e=0	e=0.25	e=0.5	e=0.75	e=1.0
ϕ'=25	L10ft_e0.0_Phi25	L10ft_e0.25_Phi25	L10ft_e0.5_Phi25	L10ft_e0.75_Phi25	L10ft_e1.0_Phi25
ϕ'=30	L10ft_e0.0_Phi30	L10ft_e0.25_Phi30	L10ft_e0.5_Phi30	L10ft_e0.75_Phi30	L10ft_e1.0_Phi30
ϕ'=35	L10ft_e0.0_Phi35	L10ft_e0.25_Phi35	L10ft_e0.5_Phi35	L10ft_e0.75_Phi35	L10ft_e1.0_Phi35
ϕ'=40	L10ft_e0.0_Phi40	L10ft_e0.25_Phi40	L10ft_e0.5_Phi40	L10ft_e0.75_Phi40	L10ft_e1.0_Phi40
ϕ'=45	L10ft_e0.0_Phi45	L10ft_e0.25_Phi45	L10ft_e0.5_Phi45	L10ft_e0.75_Phi45	L10ft_e1.0_Phi45
L= 6 m (20 ft)					
	e=0	e=0.25	e=0.5	e=0.75	e=1.0
ϕ'=25	L20ft_e0.0_Phi25	L20ft_e0.25_Phi25	L20ft_e0.5_Phi25	L20ft_e0.75_Phi25	L20ft_e1.0_Phi25
ϕ'=30	L20ft_e0.0_Phi30	L20ft_e0.25_Phi30	L20ft_e0.5_Phi30	L20ft_e0.75_Phi30	L20ft_e1.0_Phi30
ϕ'=35	L20ft_e0.0_Phi35	L20ft_e0.25_Phi35	L20ft_e0.5_Phi35	L20ft_e0.75_Phi35	L20ft_e1.0_Phi35
ϕ'=40	L20ft_e0.0_Phi40	L20ft_e0.25_Phi40	L20ft_e0.5_Phi40	L20ft_e0.75_Phi40	L20ft_e1.0_Phi40
ϕ'=45	L20ft_e0.0_Phi45	L20ft_e0.25_Phi45	L20ft_e0.5_Phi45	L20ft_e0.75_Phi45	L20ft_e1.0_Phi45
L= 9 m (30 ft)					
	e=0	e=0.25	e=0.5	e=0.75	e=1.0
ϕ'=25	L30ft_e0.0_Phi25	L30ft_e0.25_Phi25	L30ft_e0.5_Phi25	L30ft_e0.75_Phi25	L30ft_e1.0_Phi25
ϕ'=30	L30ft_e0.0_Phi30	L30ft_e0.25_Phi30	L30ft_e0.5_Phi30	L30ft_e0.75_Phi30	L30ft_e1.0_Phi30
ϕ'=35	L30ft_e0.0_Phi35	L30ft_e0.25_Phi35	L30ft_e0.5_Phi35	L30ft_e0.75_Phi35	L30ft_e1.0_Phi35
ϕ'=40	L30ft_e0.0_Phi40	L30ft_e0.25_Phi40	L30ft_e0.5_Phi40	L30ft_e0.75_Phi40	L30ft_e1.0_Phi40
ϕ'=45	L30ft_e0.0_Phi45	L30ft_e0.25_Phi45	L30ft_e0.5_Phi45	L30ft_e0.75_Phi45	L30ft_e1.0_Phi45

For all parametric analyses the soil is assumed to be homogeneous. The soil parameters are based on the effective stress and the friction angle calculated at the middle of the pile's embedded length. The step-be-step procedure presented in the previous section is used here to estimate soil parameters based on N_{60}-values as shown in Table 4. Also, a 2.54-cm (1-inch) thick plate welded to an H-beam (HP12×53) with the proper

embedment length is used in all analyses. A36 mild steel properties (Figure 54) are used for the beam and the plate in all analyses.

Table 4: Cap Model Parameters for Parametric Analyses (Cohesionless Soils)

Sand (10 ft pile)

Soil Description	$\phi'(^o)$	Z(ft)	N_{60}	K_0	OCR	p'(psf)	p'_c(psf)	$\varepsilon^{pl}_{v(0)}$	β (°)	E (psf)
Very loose sand	25	10/2=5	1	0.3	1	321	321	0	44	9.405E+03
Loose sand	30	10/2=5	2	0.4	1	357	357	0	50	2.822E+04
Medium sand	35	10/2=5	5	0.7	2	459	1105	0.001292	55	8.465E+04
Dense sand	40	10/2=5	12	1.1	6	613	3552	0.009494	58	2.257E+05
Very dense sand	45	10/2=5	33	1.7	12	829	9685	0.030055	61	6.207E+05

Sand (20 ft pile)

Soil Description	$\phi'(^o)$	Z(ft)	N_{60}	K_0	OCR	p'(psf)	p'_c(psf)	$\varepsilon^{pl}_{v(0)}$	β (°)	E (psf)
Very loose sand	25	20/2=10	1	0.3	1	615	615	0	45	1.505E+04
Loose sand	30	20/2=10	2	0.4	1	667	668	0	50	3.762E+04
Medium sand	35	20/2=10	6	0.5	1	782	1114	0.001321	55	1.129E+05
Dense sand	40	20/2=10	18	0.9	4	1064	4445	0.012488	59	3.386E+05
Very dense sand	45	20/2=10	46	1.3	8	1394	11702	0.036816	61	8.653E+05

Sand (30 ft pile)

Soil Description	$\phi'(^o)$	Z(ft)	N_{60}	K_0	OCR	p'(psf)	p'_c(psf)	$\varepsilon^{pl}_{v(0)}$	β (°)	E (psf)
Very loose sand	25	30/2=15	1	0.3	1	897	897	0.000593	45	1.881E+04
Loose sand	30	30/2=15	3	0.4	1	985	986	0.000891	51	5.643E+04
Medium sand	35	30/2=15	7	0.4	1	1073	1098	0.001267	54	1.317E+05
Dense sand	40	30/2=15	20	0.7	3	1423	4396	0.012322	58	3.762E+05
Very dense sand	45	30/2=15	60	1.2	7	1938	14085	0.044806	62	1.129E+06

For each of the 75 finite element analyses the finite element mesh (similar to the one shown in Figure 55) is adjusted to accommodate different soils, different pile embedded length, and different eccentricity ratios. The analytical results are presented as "Design Charts" shown in Figures 59 to 64.

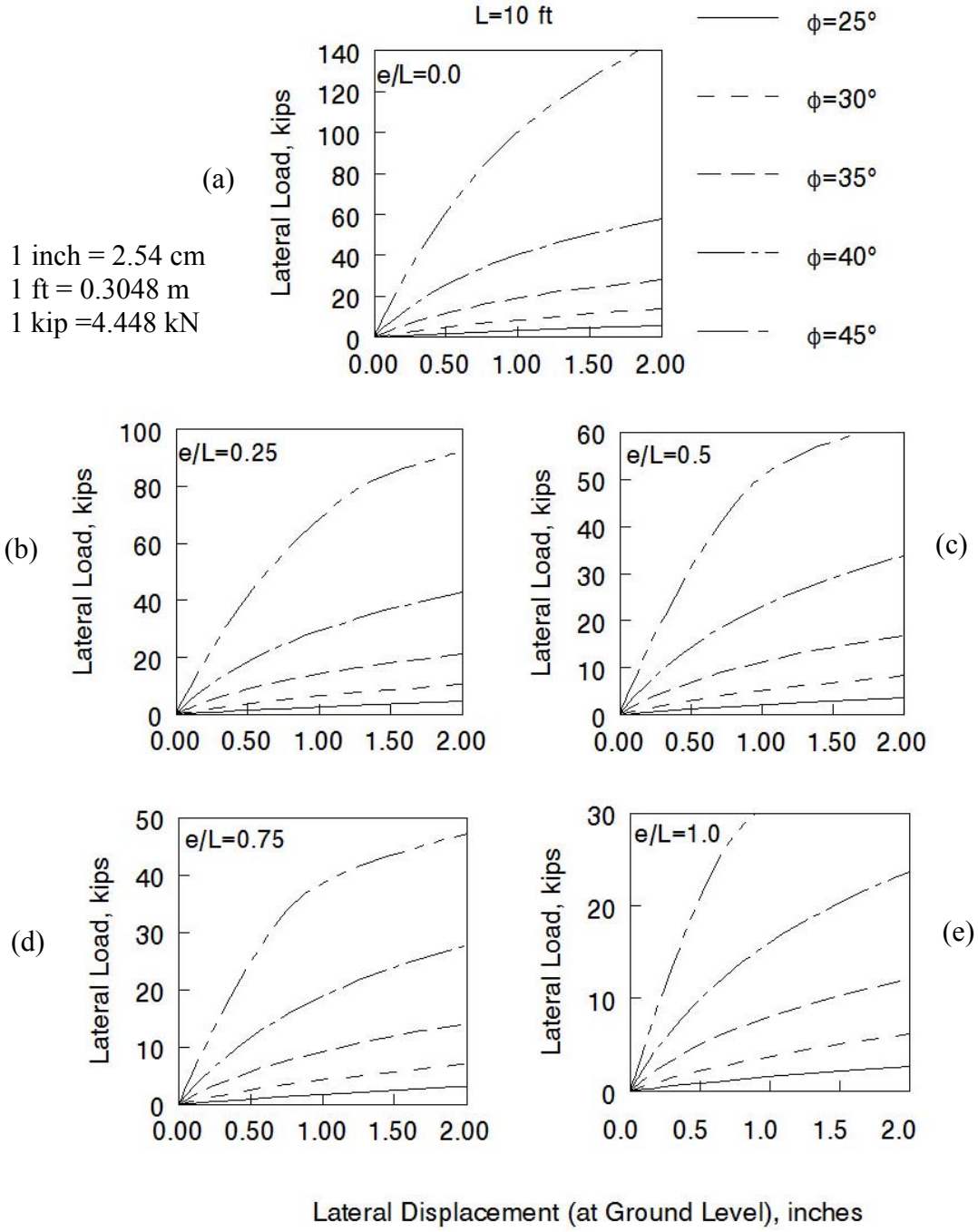

Figure 59: Design Criterion 1 for Piles in Cohesionless Soils with Embedded Length L=10 ft

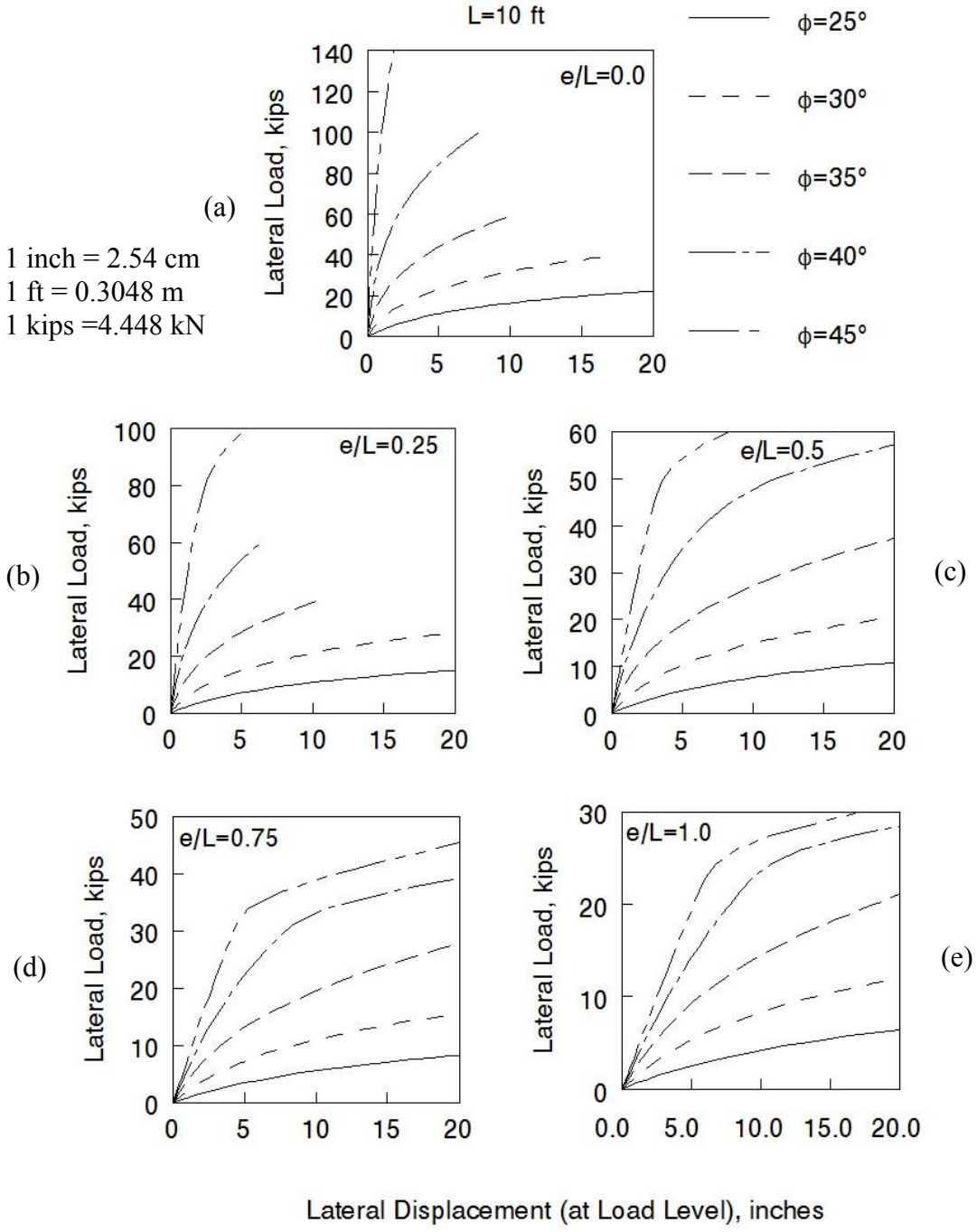

Figure 60: Design Criterion 2 for Piles in Cohesionless Soils with Embedded Length L=10 ft

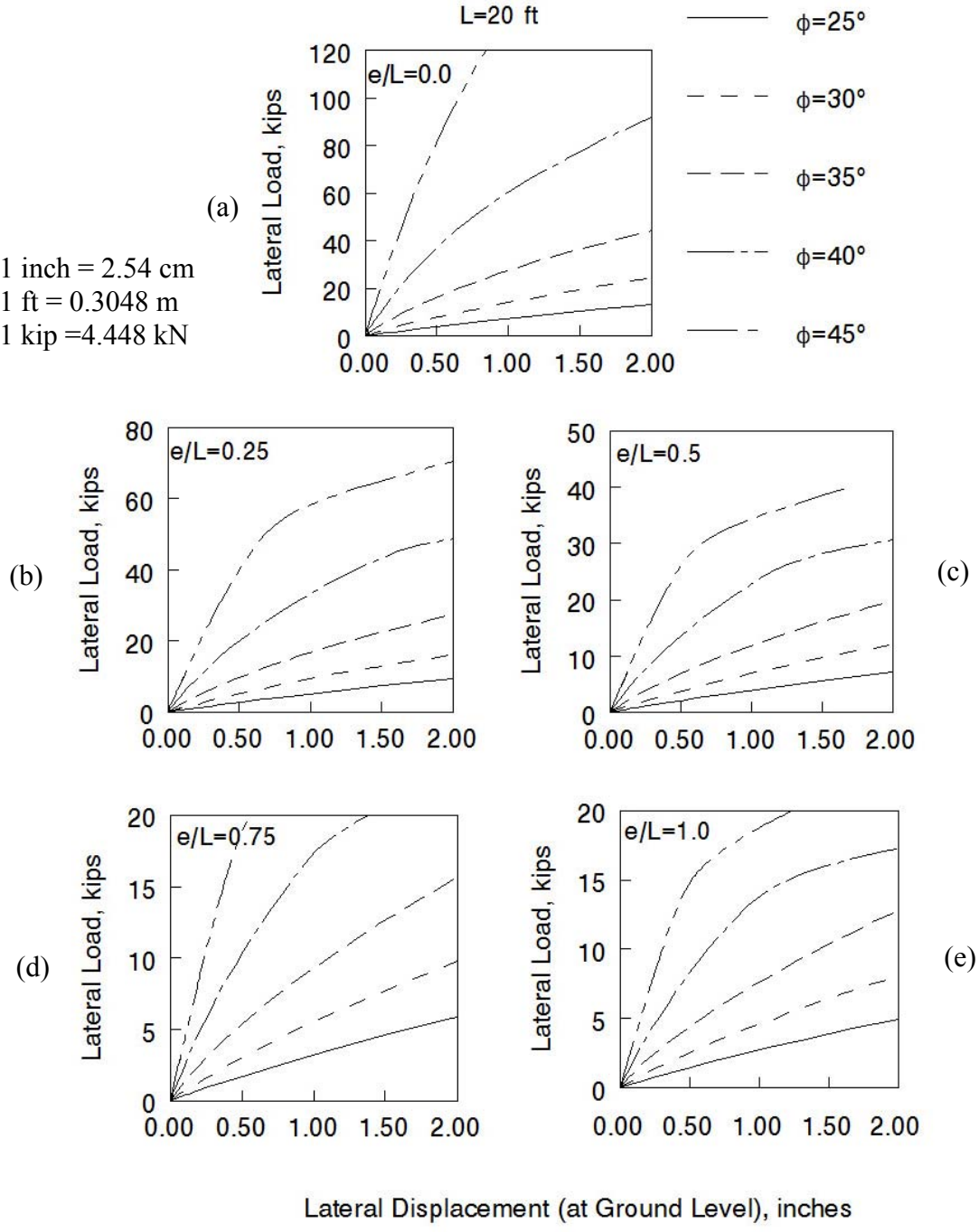

1 inch = 2.54 cm
1 ft = 0.3048 m
1 kip =4.448 kN

Figure 61: Design Criterion 1 for Piles in Cohesionless Soils with Embedded Length L=20 ft

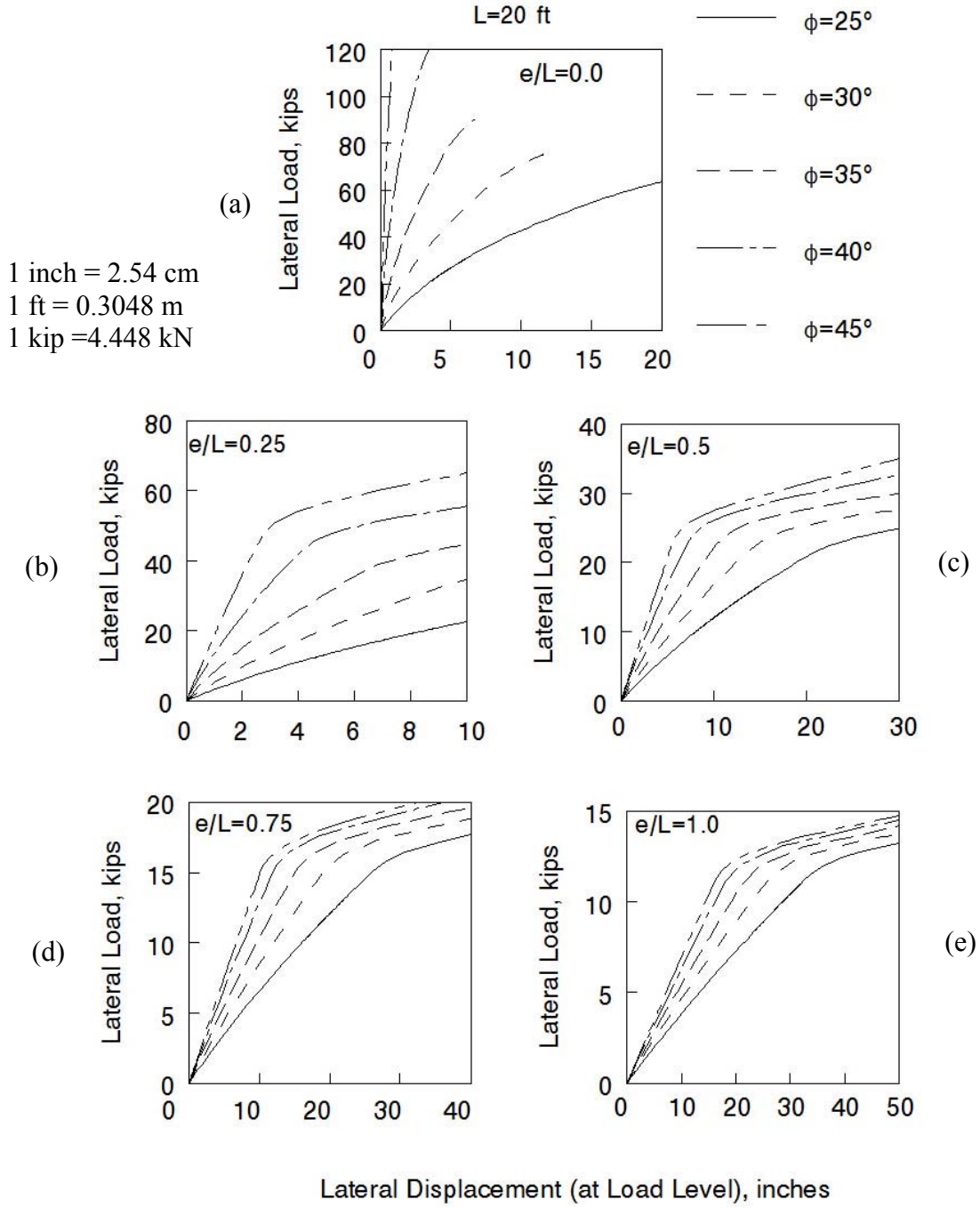

1 inch = 2.54 cm
1 ft = 0.3048 m
1 kip =4.448 kN

Figure 62: Design Criterion 2 for Piles in Cohesionless Soils with Embedded Length L=20 ft

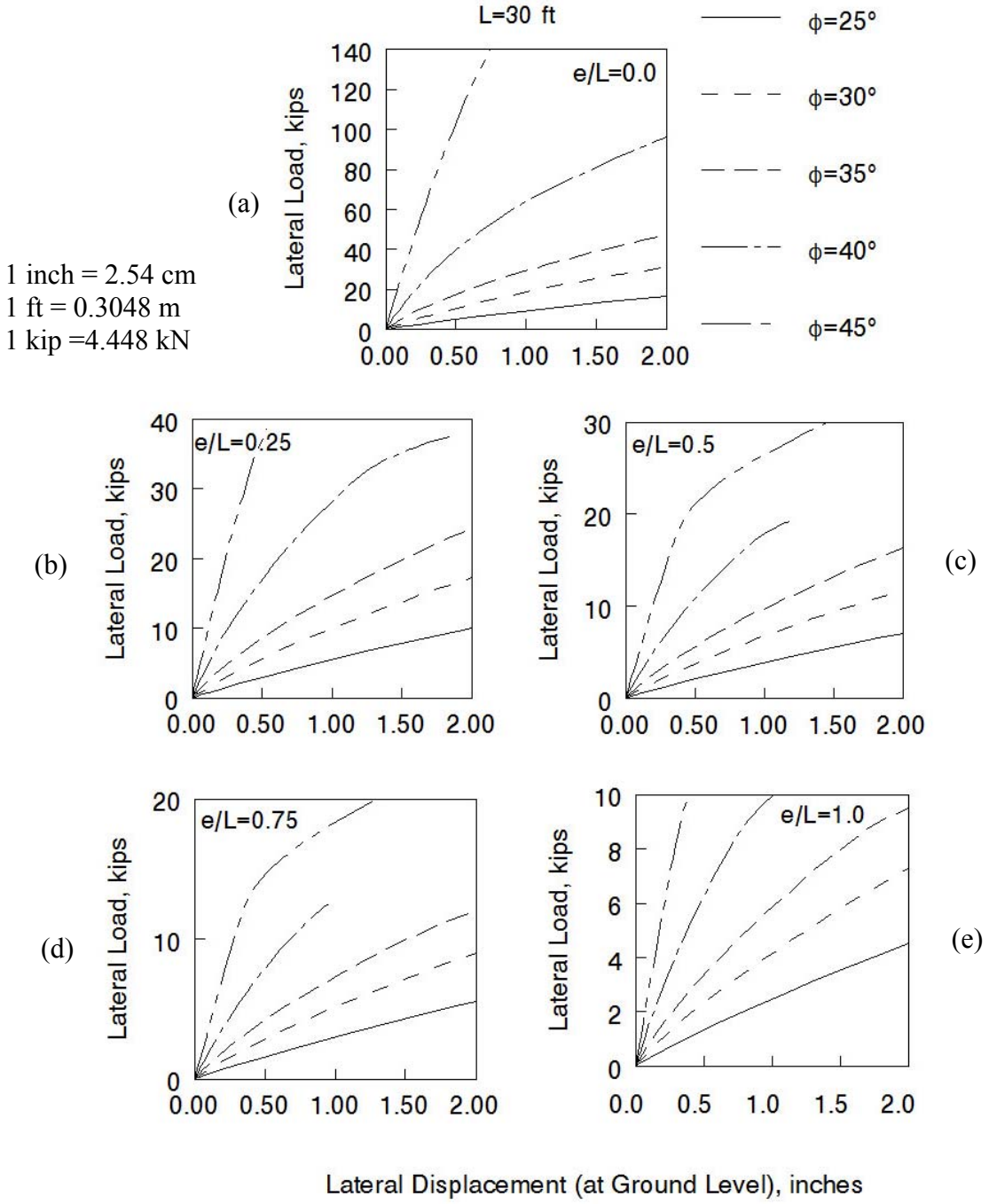

1 inch = 2.54 cm
1 ft = 0.3048 m
1 kip =4.448 kN

Figure 63: Design Criterion 1 for Piles in Cohesionless Soils with Embedded Length L=30 ft

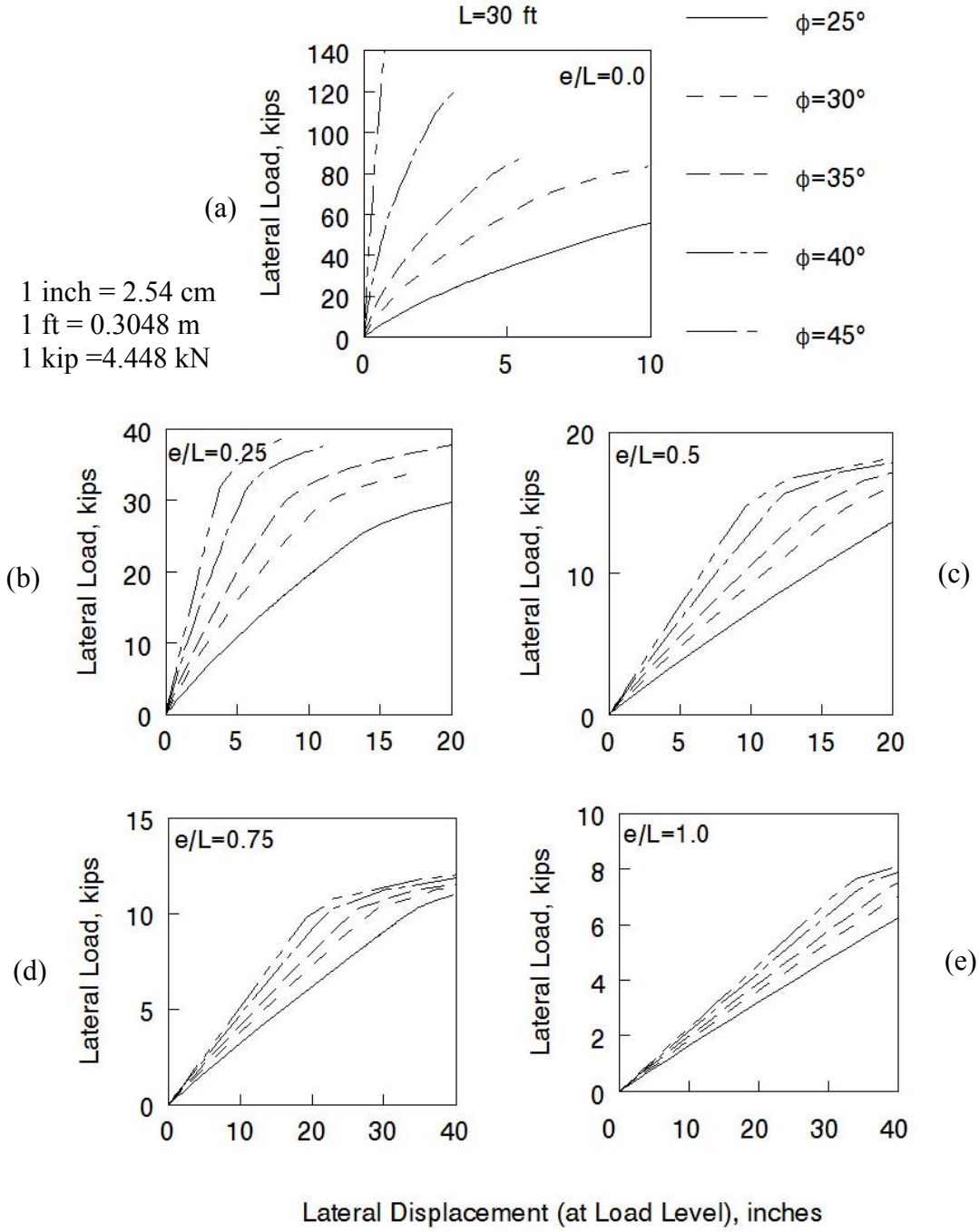

Figure 64: Design Criterion 2 for Piles in Cohesionless Soils with Embedded Length L=30 ft

4.3 PROPOSED DISPLACEMENT-BASED DESIGN METHOD

For each pile embedded length there are two sets of charts. For example, Figures 59 and 60 show the load-displacement curves for piles with 3-m (10-ft) embedded length, various soil's friction angles, and various eccentricity ratios. The first set (i.e., Figure 59) presents the applied lateral load as function of displacement at the ground level (δ_{GL}). The second set (i.e., Figure 60) presents the applied lateral load as function of displacement at the load level (δ_{LL}). In the same manner, Figures 61-62 present the results for piles with 6-m (20-ft) embedded length, and Figure 63-64 present the results for piles with 9-m (30-ft) embedded length.

The proposed displacement-based (or performance-based) design method is relevant to post-and-panel retaining walls with the pile and plate foundation system (Figure 65) and involves two simple design criteria. The use of the proposed design method is discussed assuming that the post and panel system is used for retaining wall applications. However, the design method can be also used for other post-and-panel applications including highway sound barriers.

Just as in any soil retaining system design, the height of the retaining wall, H, the characteristics of the backfill soil (c'_b, ϕ'_b, and γ_b), and the average characteristics of the foundation soil (ϕ', and γ) need to be determined beforehand. The design begins by assuming a pile's embedded length, L, and a reasonable pile-to-pile distance, L_x (Figure 65). Calculate the applied active lateral earth thrust on one pile: $Q_{app} = \frac{1}{2} K_a \gamma_b H^2 L_x$.

Also, calculate the eccentricity: $e = H/3$.

1. Design Criterion 1: Select a reasonable allowable displacement of the pile at ground level, say δ_{GL}= 2.54 cm (1 inch). Using the design charts in Figures 59, 61, and 63 for piles with embedded lengths of 3 m (10 ft), 6 m (20 ft), and 9 m (30 ft), respectively, determine the allowable lateral load for a specified embedded length, soil's friction angle, and eccentricity ratio. If the allowable load is greater than (or equal) to the applied load, proceed to Design Criterion 2. If

2. Design Criterion 2: After determining the allowable lateral load from Design Criterion 1, determine the at-load-level displacement, δ_{LL}, using the design charts in Figures 60, 62, and 64 for piles with embedded lengths of 3 m (10 ft), 6 m (20 ft), and 9 m (30 ft), respectively. From geometrical considerations (the above-ground pile length, H, and the eccentricity, e) and using the estimated displacements δ_{LL} and δ_{GL}, determine the tilt of the above-ground portion of the pile. Accept the design if pile tilt is within acceptable limits (1 to 2 %). If tilt is excessive, then modify L, or L_x, or both L and L_x. Go back to Design Criterion 1.

When the calculated tilt of the pile is large (greater than 2%) the pile with plate foundation system can be driven at a negative tilt (i.e., towards the backfill). This will cause the wall to be near vertical after the placement of the backfill soil. This procedure is not tested yet but it seems fairly feasible.

The use of the proposed design method in cohesionless soils is illustrated in the next two examples.

Example 1 (Post-and-panel system with a pile with plate foundation in sand):
As shown in Figure 65 the post-and-panel system with a pile with plate foundation type is used to retain a 4.6-m (15-ft) high backfill. The embedded length of the pile with plate is 6.1 m (20 ft). The friction angle of the sandy foundation soil is 40º as was obtained from correlations with the average N_{60} value of 12. The backfill soil unit weight and strength parameters are shown in the figure. Calculate the required distance between piles center-to-center. Assume δ_{GL}= 2.54 cm (1 inch).

Solution (English units):
Given: L=20 ft, H=15 ft, ϕ'=40º, δ_{GL}= 1 inch

L_x=?

$$e = \frac{H}{3} = \frac{15}{3} = 5\ ft$$

$$\frac{e}{L} = \frac{5}{20} = 0.25$$

For L=20 ft, ϕ'=40º, $\frac{e}{L} = 0.25$, and δ_{GL}= 1 inch, use Figure 61b (detailed in Figure 66) to obtain $Q_{all} \approx 33.7$ kips.

Set $Q_{app}=Q_{all}$, therefore: $Q_{app} = \frac{1}{2} K_a \gamma_b H^2 L_x \rightarrow L_x = \frac{2Q_{app}}{K_a \gamma_b H^2}$

or, $L_x = \frac{2 \times 33700}{0.283 \times 100 \times 15^2} = 10.6\ ft$

where, $K_a = \frac{1 - \sin \phi_b'}{1 + \sin \phi_b'} = \frac{1 - \sin 34°}{1 + \sin 34°} = 0.283$

Use L_x=10 ft.

Performance Issues:

From Figure 62b (detailed in Figure 66) we can estimate the lateral displacement at load level, $\delta_{LL} \approx$ 3 inch, corresponding to Q_{app}=33.7 kips. It is noted from Figure 62b that Q_{app}=33.7 kips is below the load that causes the initial yielding of the pile.

From Figure 65 one can estimate the slope of the above-ground portion of the pile and the lateral deflection at the end of the pile, δ_{top}.

$$Slope \approx \frac{3-1}{5 \times 12} \approx 3.3\%$$

$$\frac{\delta_{top} - 1}{15 \times 12} \approx \frac{3-1}{5 \times 12} \rightarrow \delta_{top} \approx 7\ inches$$

As indicated earlier, when the calculated tilt (slope) of the pile is large, as in this example, the pile with plate foundation system can be driven at a negative tilt (i.e.,

towards the backfill). This will cause the wall to be near vertical after the placement of the backfill soil.

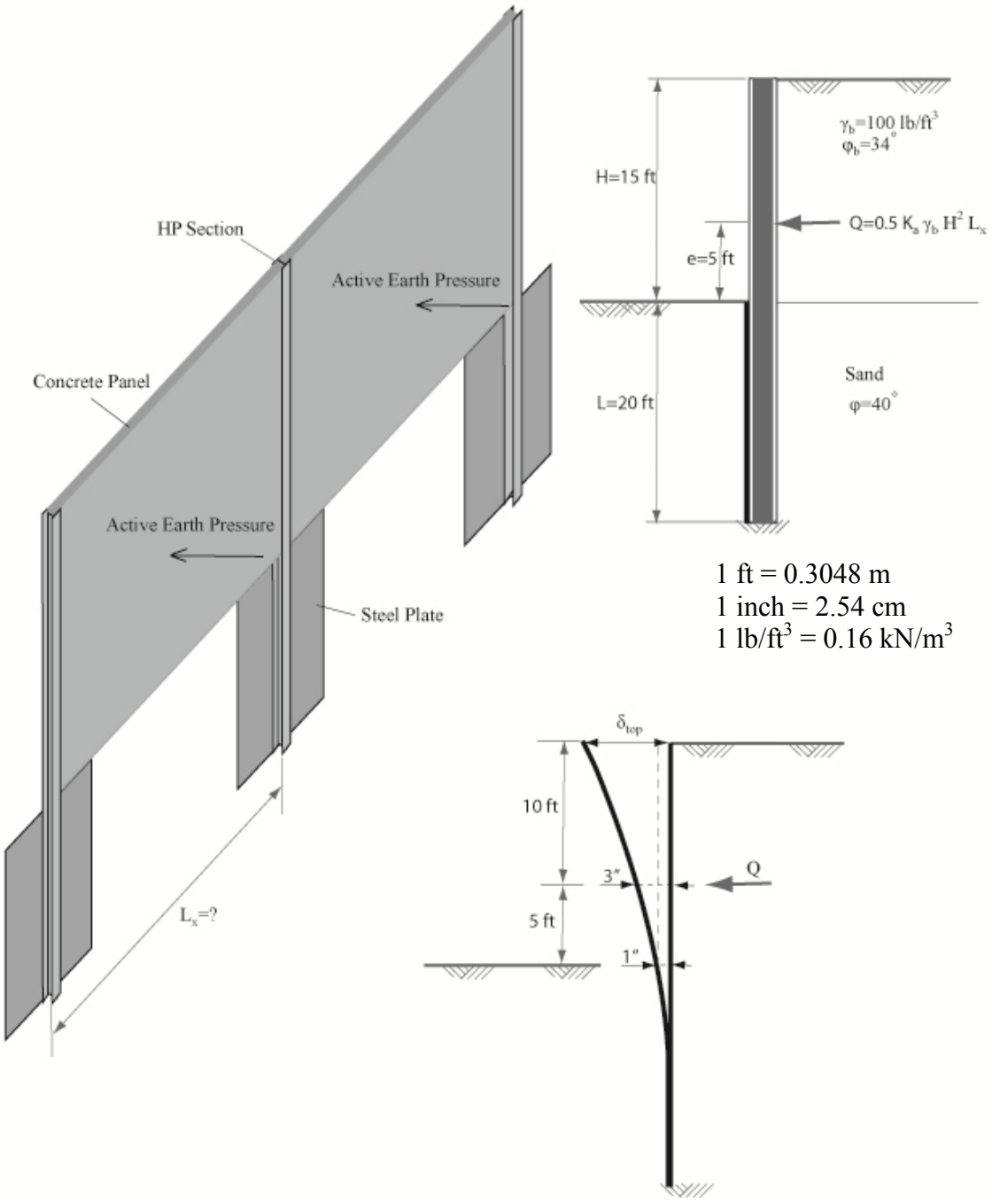

Figure 65: Design Example 1--Pile in Sand

1 inch = 2.54 cm
1 kip =4.448 kN

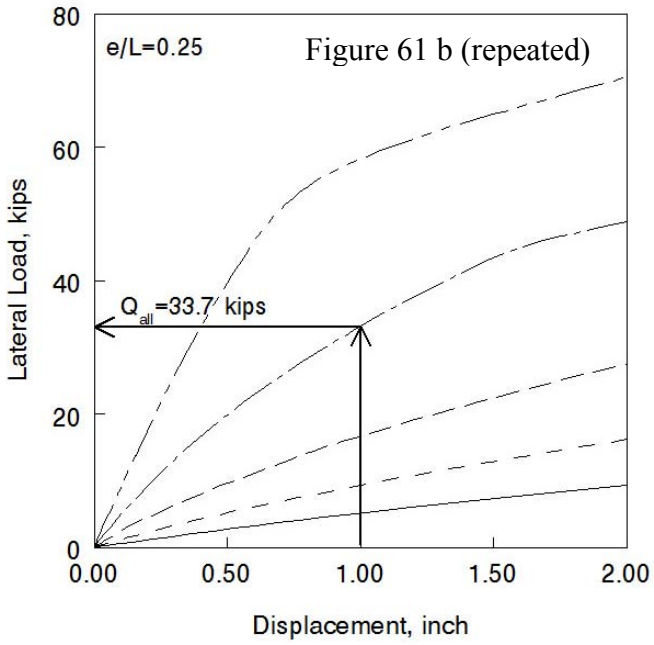

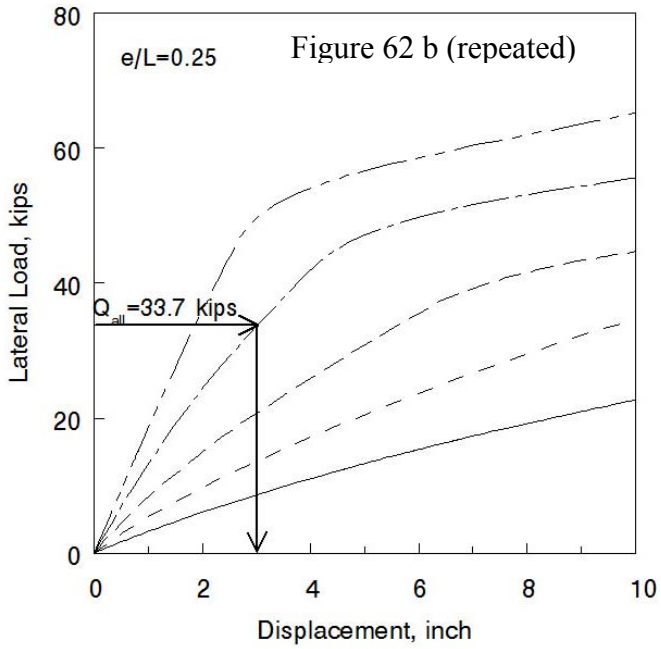

Figure 66: Design Example 1--Solution

Example 2 (Post-and-panel system with a pile with plate foundation in sand):

Figure 67 shows a post-and-panel system with a pile with plate foundation type that is used to retain a 2.3 m (7.5-ft) high backfill. The friction angle of the sandy foundation soil is 35º. The backfill soil unit weight and strength parameters are shown in the figure. The distance between piles center-to-center is L_x=6.1 m (20 ft). Calculate the required embedded length of the pile with plate foundation. The lateral deflection of the pile at ground level should not exceed 2.54 cm (1 inch).

Solution (English units):

Given: H=7.5 ft, ϕ'=35º, δ_{GL}= 1 inch, and L_x=20 ft

$$Q_{app} = \frac{1}{2} K_a \gamma_b H^2 L_x = 0.5 \times 0.238 \times 110 \times 7.5^2 \times 20 = 14.7 \; kips$$

where, $K_a = \frac{1-\sin\phi_b'}{1+\sin\phi_b'} = \frac{1-\sin 38°}{1+\sin 38°} = 0.238$

$$e = \frac{H}{3} = \frac{7.5}{3} = 2.5 \; ft$$

Try L=10 ft

$$\frac{e}{L} = \frac{2.5}{10} = 0.25$$

For L=10 ft, ϕ'=35º, $\frac{e}{L} = 0.25$, and δ_{GL}= 1 inch, use Figure 59b to obtain $Q_{all} \approx 14.7$ kips.

Therefore, $Q_{app} \approx Q_{all}$, and the suggested embedded length L=10 ft is acceptable.

Performance Issues:

From Figure 60b we can estimate the lateral displacement at load level, $\delta_{LL} \approx$ 1.49 inch, corresponding to Q_{app}=14.7 kips. It is noted from Figure 60b that Q_{app}=14.7 kips is below the load that causes the initial yielding of the pile.

From Figure 67 we can estimate the slope of the above-ground portion of the pile and the lateral deflection at the end of the pile, δ_{top}.

$$Slope \approx \frac{1.49-1}{2.5\times 12} \approx 1.6\% \rightarrow \text{Okay!}$$

$$\frac{\delta_{top}-1}{7.5\times 12} \approx \frac{1.49-1}{2.5\times 12} \rightarrow \delta_{top} \approx 2.47\ inches \rightarrow \text{Okay!}$$

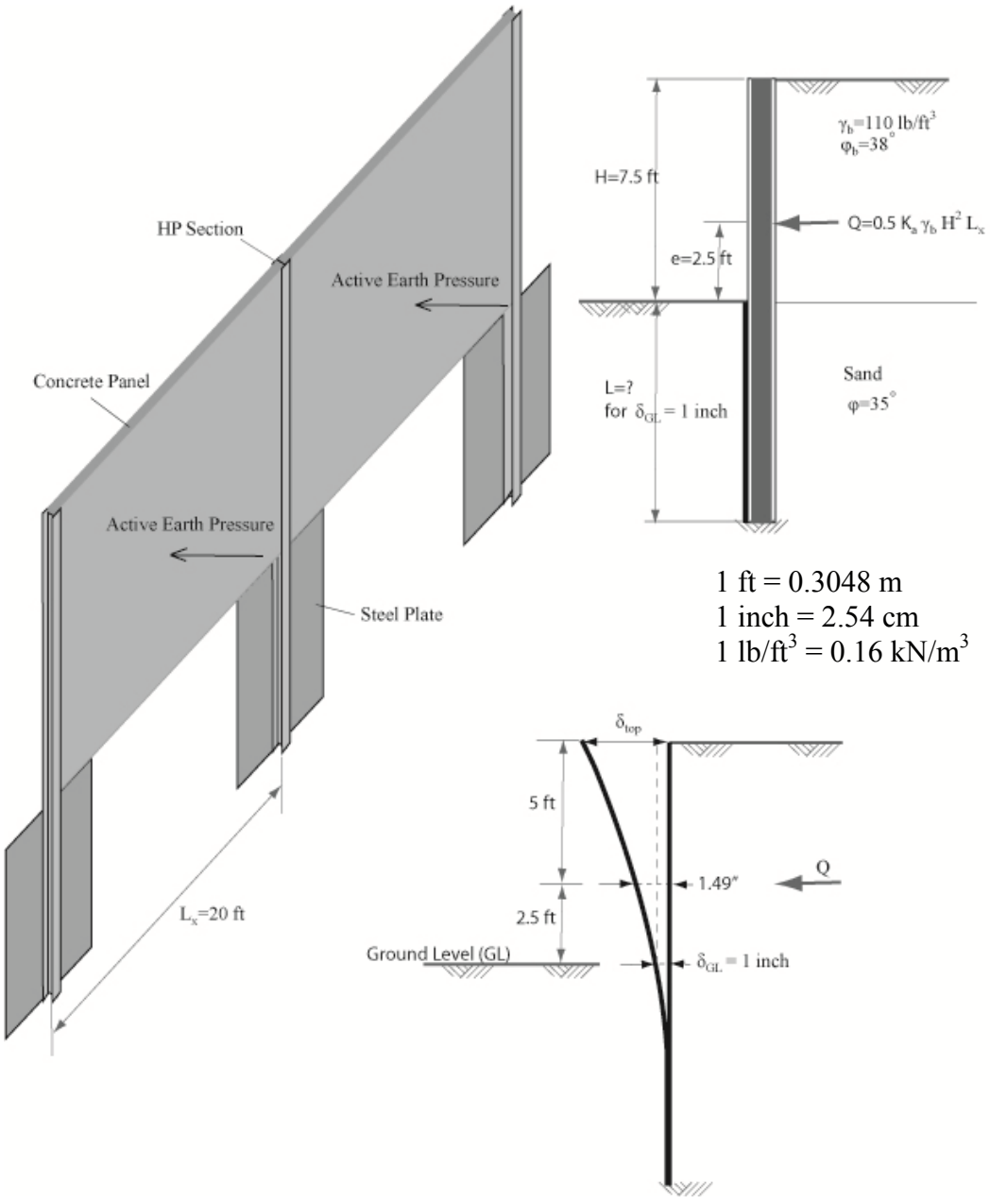

Figure 67: Design Example 2--Pile in Sand

4.4 DESIGN CHARTS FOR THE PILE WITH PLATE SYSTEM: COHESIVE SOILS

Five cohesive soils with c_u=16.7 kPa (350 psf), 30 kPa (625 psf), 65 kPa (1350 psf), 125 kPa (2600 psf), and 210 kPa (4400 psf) are used in this parametric study. As was done in the previous analyses for cohesionless soils, three embedded lengths of the pile with plate system are used: 3 m (10 ft), 6 m (20 ft), and 9 m (30 ft). The above-ground length of each pile is the same as its embedded length. Five eccentricity ratios are used for each pile: 0, 0.25, 0.5, 0.75, and 1. In total, 75 analyses combinations are considered as indicated in Table 5.

Table 5: Analysis Matrix for Cohesive Soils

L= 3 m (10 ft)					
	e=0	e=0.25	e=0.5	e=0.75	e=1.0
c_u=350 psf	L10ft_e0.0_cu1	L10ft_e0.25_cu1	L10ft_e0.5_cu1	L10ft_e0.75_cu1	L10ft_e1.0_cu1
c_u =625 psf	L10ft_e0.0_cu2	L10ft_e0.25_cu2	L10ft_e0.5_cu2	L10ft_e0.75_cu2	L10ft_e1.0_cu2
c_u =1350 psf	L10ft_e0.0_cu3	L10ft_e0.25_cu3	L10ft_e0.5_cu3	L10ft_e0.75_cu3	L10ft_e1.0_cu3
c_u =2600 psf	L10ft_e0.0_cu4	L10ft_e0.25_cu4	L10ft_e0.5_cu4	L10ft_e0.75_cu4	L10ft_e1.0_cu4
c_u =4400 psf	L10ft_e0.0_cu5	L10ft_e0.25_cu5	L10ft_e0.5_cu5	L10ft_e0.75_cu5	L10ft_e1.0_cu5
L=6 m (20 ft)					
	e=0	e=0.25	e=0.5	e=0.75	e=1.0
c_u=350 psf	L20ft_e0.0_cu1	L20ft_e0.25_cu1	L20ft_e0.5_cu1	L20ft_e0.75_cu1	L20ft_e1.0_cu1
c_u =625 psf	L20ft_e0.0_cu2	L20ft_e0.25_cu2	L20ft_e0.5_cu2	L20ft_e0.75_cu2	L20ft_e1.0_cu2
c_u =1350 psf	L20ft_e0.0_cu3	L20ft_e0.25_cu3	L20ft_e0.5_cu3	L20ft_e0.75_cu3	L20ft_e1.0_cu3
c_u =2600 psf	L20ft_e0.0_cu4	L20ft_e0.25_cu4	L20ft_e0.5_cu4	L20ft_e0.75_cu4	L20ft_e1.0_cu4
c_u =4400 psf	L20ft_e0.0_cu5	L20ft_e0.25_cu5	L20ft_e0.5_cu5	L20ft_e0.75_cu5	L20ft_e1.0_cu5
L=9 m (30 ft)					
	e=0	e=0.25	e=0.5	e=0.75	e=1.0
c_u=350 psf	L30ft_e0.0_cu1	L30ft_e0.25_cu1	L30ft_e0.5_cu1	L30ft_e0.75_cu1	L30ft_e1.0_cu1
c_u =625 psf	L30ft_e0.0_cu2	L30ft_e0.25_cu2	L30ft_e0.5_cu2	L30ft_e0.75_cu2	L30ft_e1.0_cu2
c_u =1350 psf	L30ft_e0.0_cu3	L30ft_e0.25_cu3	L30ft_e0.5_cu3	L30ft_e0.75_cu3	L30ft_e1.0_cu3
c_u =2600 psf	L30ft_e0.0_cu4	L30ft_e0.25_cu4	L30ft_e0.5_cu4	L30ft_e0.75_cu4	L30ft_e1.0_cu4
c_u =4400 psf	L30ft_e0.0_cu5	L30ft_e0.25_cu5	L30ft_e0.5_cu5	L30ft_e0.75_cu5	L30ft_e1.0_cu5

For all parametric analyses the soil is assumed to be homogeneous. A step-be-step procedure, presented below, is used here to estimate soil parameters based on N_{60}-values as shown in Table 6.

Table 6: Cap Model Parameters for Parametric Analyses (Cohesive Soils)

Soil Description	c_u (psf)	N_{60}	d (psf)	E (psf)
Very soft clay	350	1	600	2.265E+04
Soft clay	625	3	1087	5.173E+04
Medium clay	1350	8	2346	1.505E+05
Stiff clay	2600	20	4521	3.743E+05
Very stiff clay	4400	41	7608	7.712E+05

A step-by-step procedure to obtain cohesive soil parameters:

1. From SPT soundings, divide the soil into layers based on N_{60}. Calculate the weighted average of the N_{60}-value for the soil strata.
2. Calculate the undrained cohesion of the soil strata: $c_u\ (kPa) = 29(N_{60})^{0.72}$ (Hara et al, 1971).
3. As a safety precaution, use a modified undrained cohesion $(c_u)_{mod}$, such that: $(c_u)_{\text{mod}}\ (kPa) = \frac{c_u\ (kPa)}{2} = \frac{29(N_{60})^{0.72}}{2}$. This safety factor is introduced herein because of the lack of experience using the proposed pile with plate system in cohesive soils.
4. Calculate the cohesion constant for the modified Drucker-Prager/Cap soil model: $d = \sqrt{3}\ (c_u)_{\text{mod}}$.
5. Calculate the friction angle for the modified Drucker-Prager/Cap soil model: $\beta = \tan^{-1}[\frac{6\sin\phi_u}{3-\sin\phi_u}] = 0$, where ϕ_u is the undrained friction angle of the soil (=0).
6. Reasonable elastic modulus of the soil can be assumed. The values given in Table 6 are on the lower bound of elastic moduli for clays based on the written literature.

As was done in the parametric analyses for cohesionless soils, a 2.54 cm (1-inch) thick plate welded to an H-beam (HP12×53) with the proper embedment length is used in all analyses. A36 mild steel properties (Figure 54) are used for the beam and the plate in all analyses. For each of the 75 finite element analyses indicated in Table 5, the finite element mesh (similar to the one shown in Figure 55) is adjusted to accommodate different soils, different pile embedded length, and different eccentricity ratios. The analytical results are presented as "Design Charts" shown in Figures 68 to 73.

The proposed two-criteria displacement-based design method, described above, can also be used for the design of post-and-panel retaining walls with the pile and plate foundation system embedded in cohesive soils. As described earlier, the method involves two simple design criteria. Figures 68, 70, and 72 are associated with design criterion 1, whereas Figures 69, 71, and 73 are associated with design criterion 2. The use of the proposed design method in a cohesive soil is illustrated in the next example.

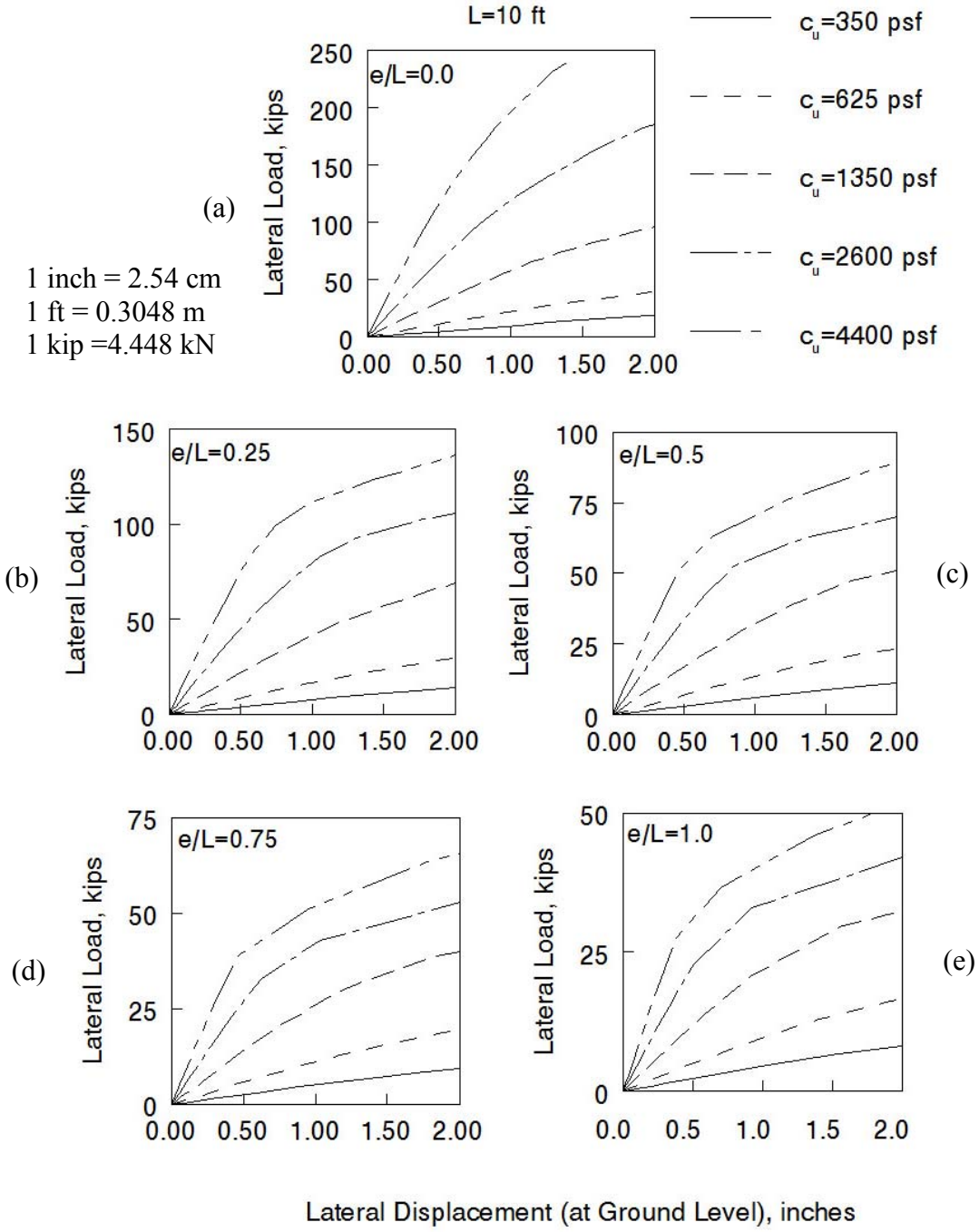

Figure 68: Design Criterion 1 for Piles in Cohesive Soils with Embedded Length L=10 ft

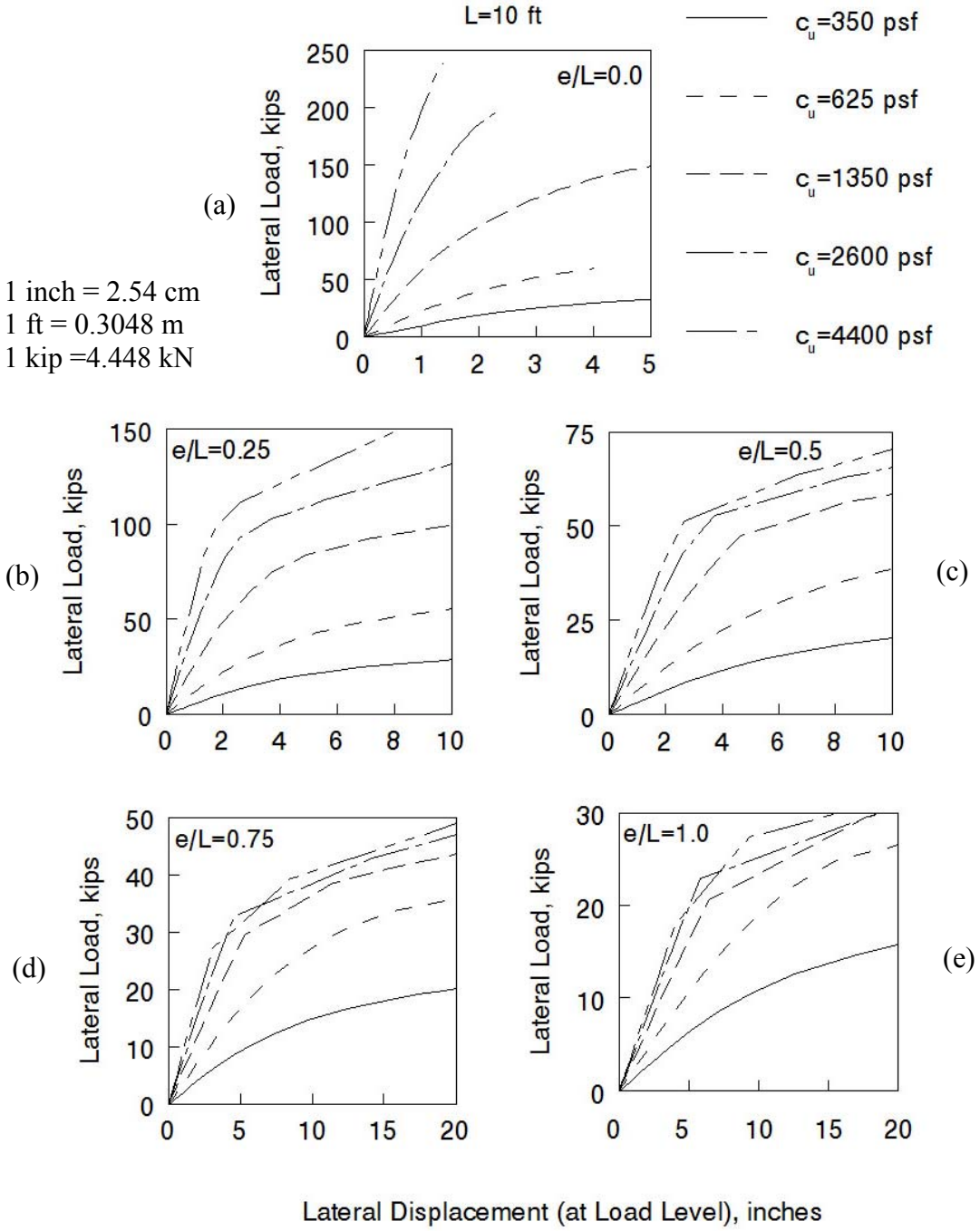

Figure 69: Design Criterion 2 for Piles in Cohesive Soils with Embedded Length L=10 ft

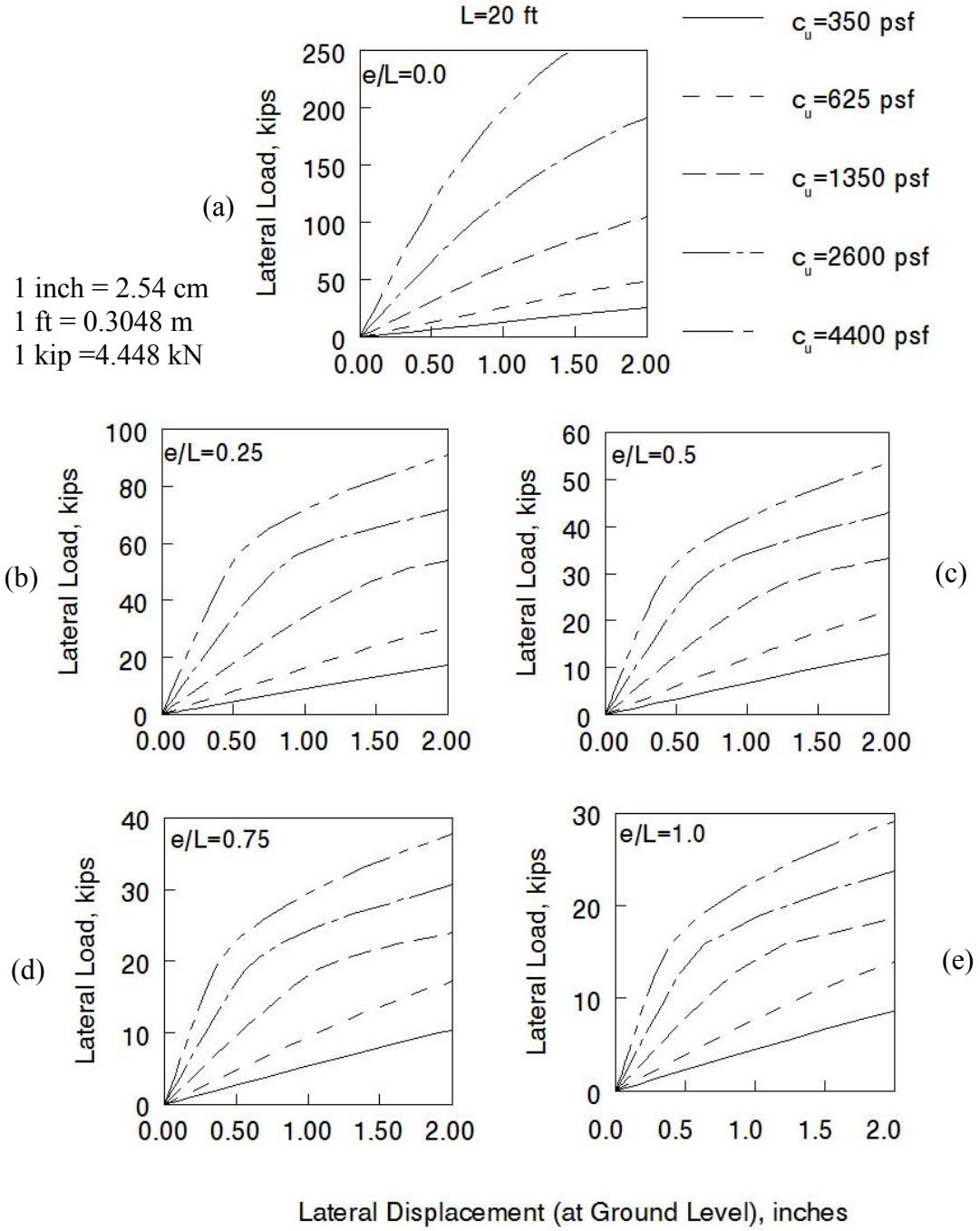

Figure 70: Design Criterion 1 for Piles in Cohesive Soils with Embedded Length L=20 ft

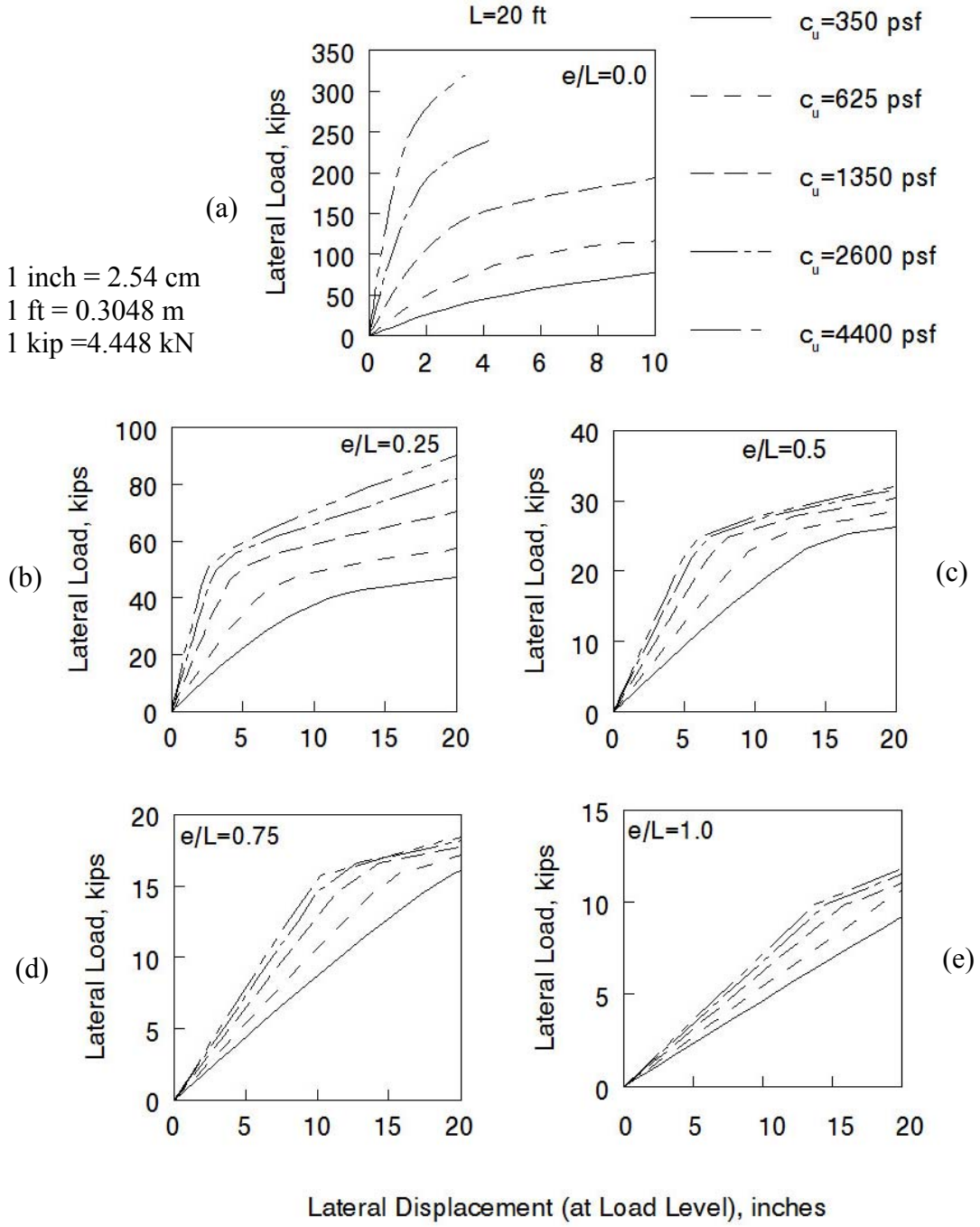

Figure 71: Design Criterion 2 for Piles in Cohesive Soils with Embedded Length L=20 ft

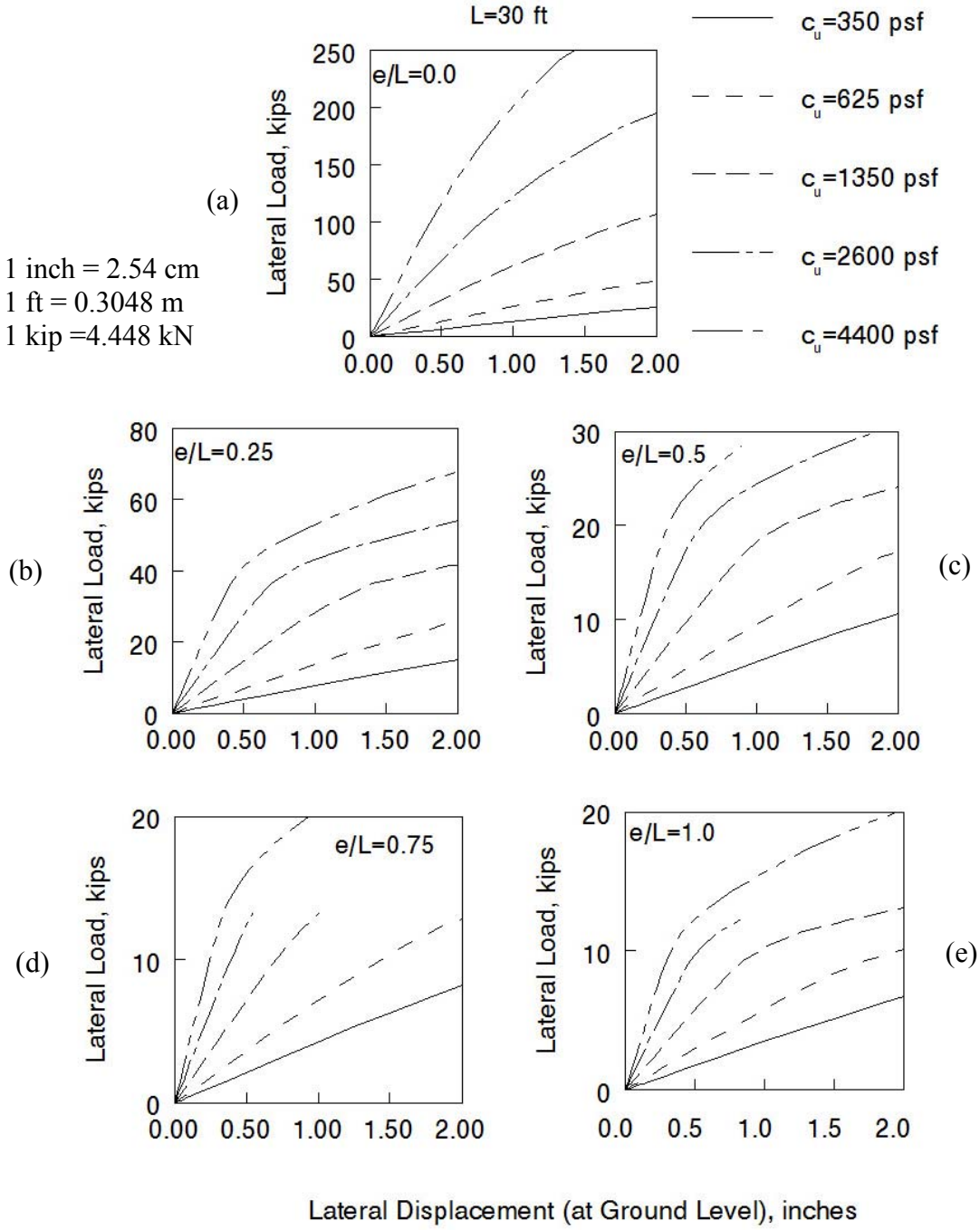

1 inch = 2.54 cm
1 ft = 0.3048 m
1 kip =4.448 kN

Figure 72: Design Criterion 1 for Piles in Cohesive Soils with Embedded Length L=30 ft

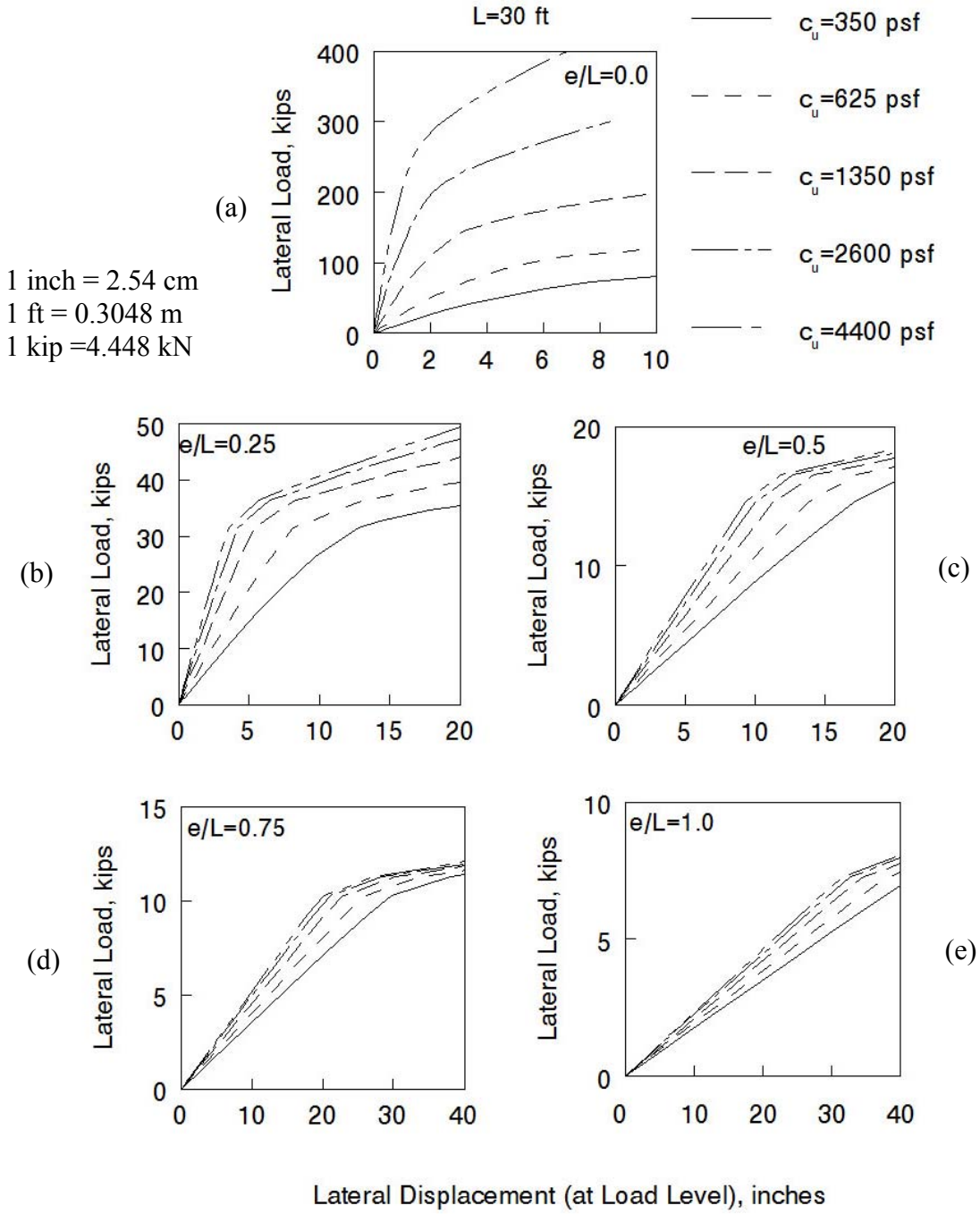

Figure 73: Design Criterion 2 for Piles in Cohesive Soils with Embedded Length L=30 ft

Example 3 (Post-and-panel system with a pile with plate foundation in clay):

As shown in Figure 74 the post-and-panel system with a pile with plate foundation type is used to retain a 4.6-m (15-ft) high backfill. The embedded length of the pile with plate is 6.1 m (20 ft). The average undrained cohesion of the clayey foundation soil is 1350 psf as was obtained from correlations with the average N_{60} value of the soil strata in the vicinity of the embedded length of the foundation system. The backfill soil unit weight and strength parameters are shown in the figure. Calculate the required distance between piles center-to-center. Assume δ_{GL}= 2.54 cm (1 inch).

Solution (English units):

Given: L=20 ft, H=15 ft, c_u=1350 psf, δ_{GL}= 1 inch

L_x=?

$$e = \frac{H}{3} = \frac{15}{3} = 5\ ft$$

$$\frac{e}{L} = \frac{5}{20} = 0.25$$

For L=20 ft, c_u=1350 psf, $\frac{e}{L} = 0.25$, and δ_{GL}= 1 inch, use Figure 70b to obtain $Q_{all} \approx 36$ kips.

Set $Q_{app}=Q_{all}$, therefore: $Q_{app} = \frac{1}{2} K_a \gamma_b H^2 L_x \rightarrow L_x = \frac{2Q_{app}}{K_a \gamma_b H^2}$

or, $L_x = \frac{2 \times 36000}{0.283 \times 100 \times 15^2} = 11.3\ ft$

where, $K_a = \frac{1 - \sin\phi_b'}{1 + \sin\phi_b'} = \frac{1 - \sin 34°}{1 + \sin 34°} = 0.283$

Use L_x=10 ft.

Performance Issues:

From Figure 71b we can estimate the lateral displacement at load level, $\delta_{LL} \approx 3.1$ inch, corresponding to Q_{app}=36 kips. It is noted from Figure 71b that Q_{app}=36 kips is below the load that causes the initial yielding of the pile.

From Figure 74 one can estimate the slope of the above-ground portion of the pile and the lateral deflection at the end of the pile, δ_{top}.

$$Slope \approx \frac{3.1-1}{5\times 12} \approx 3.5\%$$

$$\frac{\delta_{top}-1}{15\times 12} \approx \frac{3.1-1}{5\times 12} \rightarrow \delta_{top} \approx 7.3\ inches$$

Since the calculated tilt (slope) of the pile is large, the pile with plate foundation system can be driven at a negative tilt (i.e., towards the backfill). This will cause the wall to be near vertical after the placement of the backfill soil.

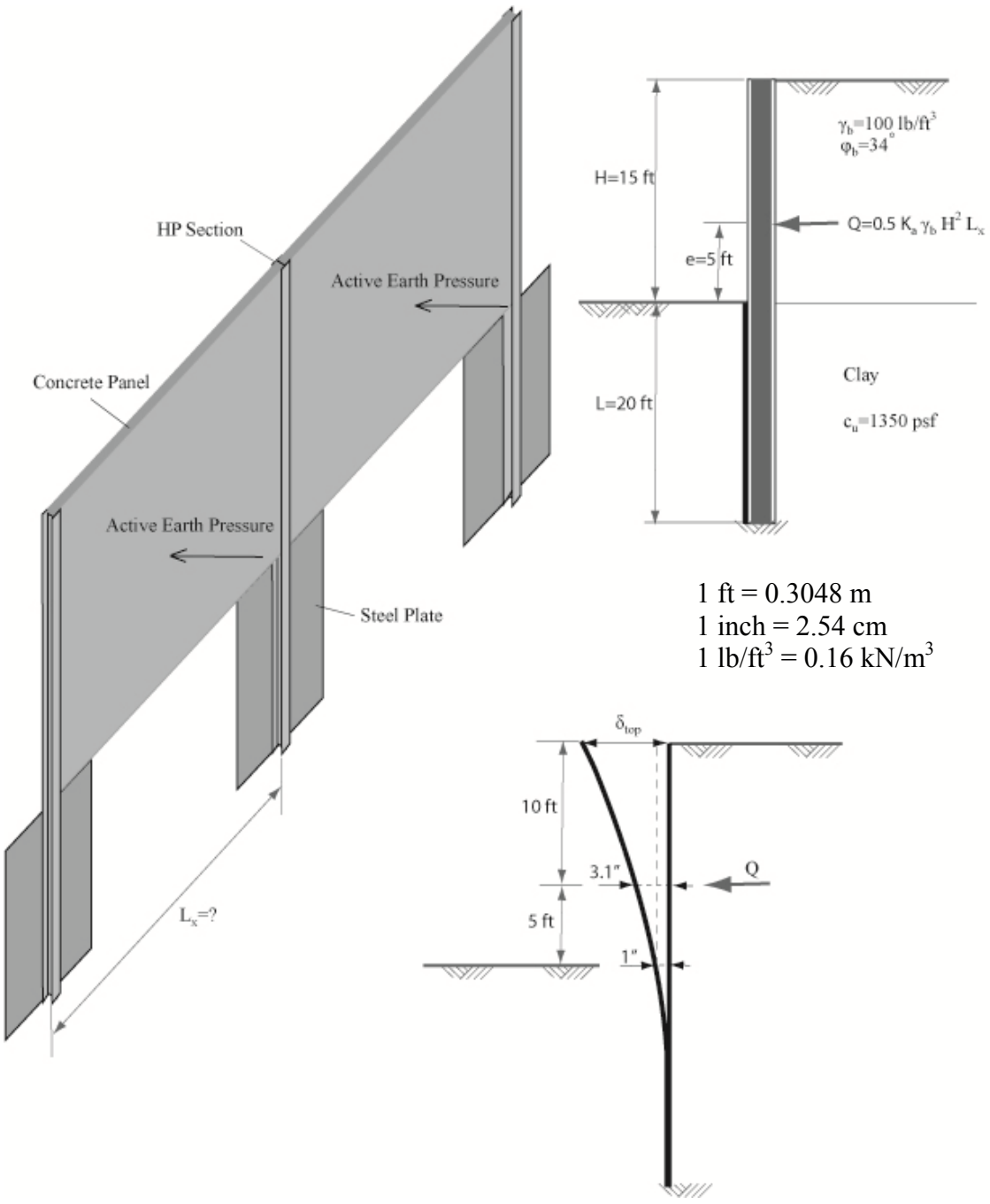

Figure 74: Design Example 3--Pile in Clay

REFERENCES

Broms, B.B. (1964). "Design of Laterally Loaded Piles," *Journal of the Soil Mechanics and Foundation Division, American Society of Civil Engineers*, Vol. 91, No. SM3, pp. 79-99.

Davisson, M.T., and Gill, H.L. (1963). "Laterally Loaded Piles in a Layered Soil System," *Journal of the Soil Mechanics and Foundation Division, American Society of Civil Engineers*, Vol. 89, No. SM3, pp. 63-94.

Hara, A., Ohta, T., and Niwa, M. (1971). "Shear Modulus and Shear Strength of Cohesive Soils," Soils and Foundations, Vol. 14, No. 3, pp. 1-12.

Kulhawy, F.H., and Myane, P.W. (1990). Manual on Estimating Soil Properties for Foundation Design, Electric Power Research Institute, Palo Alto, California.

Matlock, H., and Reese, L.C. (1960). "Generalized Solution for Laterally Loaded Piles," *Journal of the Soil Mechanics and Foundation Division, American Society of Civil Engineers*, Vol. 86, No. SM5, pp. 63-91.

Meyerhof, G. G. (1995). "Behavior of Pile Foundations under Special Loading Conditions: 1994 R.M. Hardy Keynote Address," *Canadian Geotechnical Journal*, Vol. 32, No. 2, pp. 204-222.

Robertson, P.K., and Campanella, R.G. (1983). "Interpretation of Cone Penetration Tests. Part I: Sand, " Canadian Geotechnical Journal, Vol. 20, No. 4, pp. 718-733.

Schmertmann, J.H. (1970). Static cone to compute static settlement over sand. ASCE Journal of Soil Mechanics & Foundations Division 96 (3), 1011-1043.

Appendix A
Site Investigation

Borings at E. Bay Street and Lincoln Memorial Drive

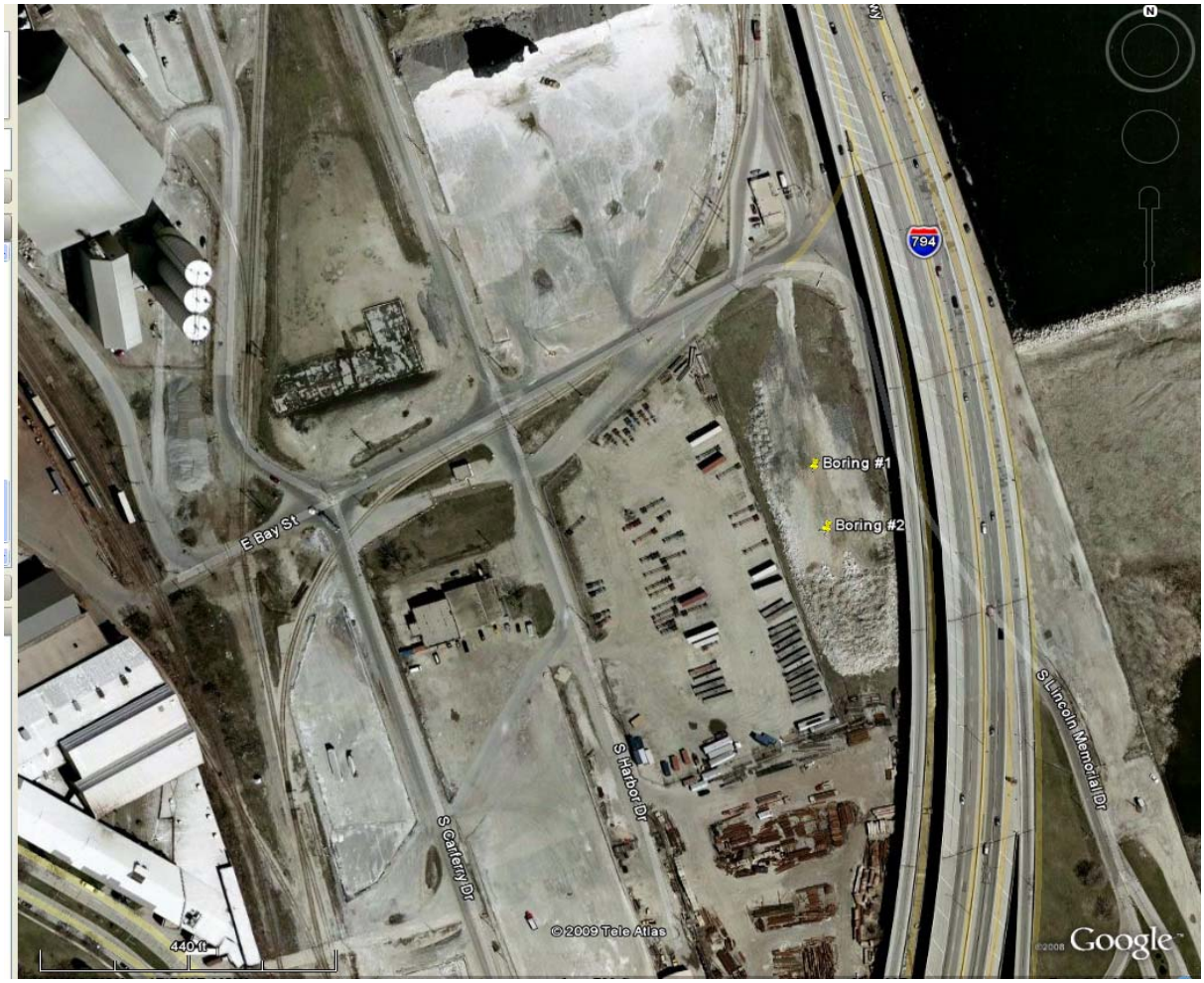

HNTB
ENGINEERS ARCHITECTS PLANNERS
11414 West Park Place, Ste. 300, Milwaukee, WI 53224
Phone (414) 359-2300 Fax (414) 359-2310

SOIL BORING LOG

BORING NUMBER: **B-1**

PROJECT NAME: Wisconsin Highway Research Project		DATE DRILLING STARTED: 4/6/2009	DRILLING METHOD: wash boring
PROJECT NUMBER: 41991		DATE DRILLING ENDED: 4/7/2009	DRILL RIG:
BORING DRILLED BY: FIRM: WisDOT CREW CHIEF: Skolos	FIELD LOG: Skolos LAB LOG / QC: SDM/DAJ	NORTHING: EASTING:	BOREHOLE DIAMETER: 4 in. SURFACE ELEVATION: Feet

Number and Type	Recovery (in)	Blow Counts	N - Value	Depth (ft) / Elevation	Soil Description and Geological Origin for Each Major Unit	USCS	Graphic	Well Diagram	Unconfined Compressive Strength (Qu or **Qp**) (tsf)	Liquid Limit	Plasticity Index	Moisture Content (%)	Comments
SPT - 1	24		32		Dense, gray to brown GRANULAR FILL, fine to coarse sand and gravel, moist								
SPT - 2	24		11										
					Hard, brown CLAY/SILT FILL, little fine gravel, moist								
SPT - 3	24		11	**5**	Very loose to loose, dark brown to black silty SAND, little to some fine to coarse gravel, trace organics, moist to wet (Possible Fill)								
SPT - 4	12		7	▽									
SPT - 5	24		1										
				10									
SPT - 6	0		6										No recovery @ 10-12 feet sample interval
SPT - 7	24		9		- with trace fine gravel	SM							
SH - 8	0			**15**									No recovery in Shelby Tube
SPT - 9	24		2										
SPT - 10	24		19										
				20	Medium dense to very dense well-graded SAND with silt, trace organics (marine shells), moist	SW-SM							

WATER OBSERVATION DATA

▽	WATER ENCOUNTERED DURING DRILLING: 8 ft.		CAVE DEPTH AT COMPLETION: ft.	WET ☐ DRY ☐
▼	WATER LEVEL AT COMPLETION: ft.	■	CAVE DEPTH AFTER HOURS: ft., hrs.	WET ☐ DRY ☐
▼	WATER LEVEL AFTER HOURS: ft., hrs.		NOTE: Bolded Unconfined Compressive Strength values denote a Qp test.	

NOTE: Stratification lines between soil types represent the approximate boundary; gradual transition between in-situ soil layers should be expected.

HNTB GEOTECH SBL WHRP 2009 BORINGS.GPJ HNTB-WIDNR.GDT 5/20/09

HNTB
ENGINEERS ARCHITECTS PLANNERS
11414 West Park Place, Ste. 300, Milwaukee, WI 53224
Phone (414) 359-2300 Fax (414) 359-2310

SOIL BORING LOG

PROJECT NAME: Wisconsin Highway Research Project		DATE DRILLING STARTED: 4/6/2009	BORING NUMBER: B-1
PROJECT NUMBER: 41991		DATE DRILLING ENDED: 4/7/2009	DRILLING METHOD: wash boring
BORING DRILLED BY: FIRM: WisDOT CREW CHIEF: Skolos	FIELD LOG: Skolos LAB LOG / QC: SDM/DAJ	NORTHING EASTING	DRILL RIG BOREHOLE DIAMETER: 4 in. SURFACE ELEVATION: Feet

Number and Type	Recovery (in)	Blow Counts	N - Value	Depth (ft) / Elevation	Soil Description and Geological Origin for Each Major Unit	USCS	Graphic	Well Diagram	Unconfined Compressive Strength (Qu or Qp) (tsf)	Liquid Limit	Plasticity Index	Moisture Content (%)	Comments
SPT - 11	18		56		Medium dense to very dense well-graded SAND with silt, trace organics (marine shells), moist - with little coarse gravel and less silt	SW-SM							
				25									
SPT - 12	18		12		Stiff, brown CLAY, trace fine to coarse gravel, little fine sand, moist				**1.75**				
				30									
SPT - 13	18		15			CH			**1.75**				
				35									
SPT - 14	18		11		- with little to some silt - Shelby Tube collected @ 36.5-39 feet				**1.5**				
				40									

WATER OBSERVATION DATA

WATER ENCOUNTERED DURING DRILLING: 8 ft.		CAVE DEPTH AT COMPLETION: ft.	WET ☐ DRY ☐
WATER LEVEL AT COMPLETION: ft.		CAVE DEPTH AFTER HOURS: ft., hrs.	WET ☐ DRY ☐
WATER LEVEL AFTER HOURS: ft., hrs.		NOTE: Bolded Unconfined Compressive Strength values denote a Qp test.	

NOTE: Stratification lines between soil types represent the approximate boundary; gradual transition between in-situ soil layers should be expected.

HNTB GEOTECH SBL WHRP 2009 BORINGS.GPJ HNTB-WIDNR.GDT 5/20/09

HNTB
ENGINEERS ARCHITECTS PLANNERS
11414 West Park Place, Ste. 300, Milwaukee, WI 53224
Phone (414) 359-2300 Fax (414) 359-2310

SOIL BORING LOG

BORING NUMBER: B-1

PROJECT NAME: Wisconsin Highway Research Project
PROJECT NUMBER: 41991
DATE DRILLING STARTED: 4/6/2009
DATE DRILLING ENDED: 4/7/2009
DRILLING METHOD: wash boring
DRILL RIG:

BORING DRILLED BY: FIRM: WisDOT; CREW CHIEF: Skolos
FIELD LOG: Skolos
LAB LOG / QC: SDM/DAJ
NORTHING:
EASTING:
BOREHOLE DIAMETER: 4 in.
SURFACE ELEVATION: Feet

Number and Type	Recovery (in)	Blow Counts	N - Value	Depth (ft) / Elevation	Soil Description and Geological Origin for Each Major Unit	USCS	Graphic	Well Diagram	Unconfined Compressive Strength (Qu or Qp) (tsf)	Liquid Limit	Plasticity Index	Moisture Content (%)	Comments
					Stiff, brown CLAY, trace fine to coarse gravel, little fine sand, moist								
SPT - 15	18		10						1				
				45									
SPT - 16	18		1.25						1.25				
						CH							
				50									
SPT - 17	18		14						1.5				
				55									
SPT - 18	18		19		Very stiff to hard, brownish gray silty CLAY, little fine sand, moist				2.5				
						CL							
				60									

WATER OBSERVATION DATA

▽	WATER ENCOUNTERED DURING DRILLING: 8 ft.		CAVE DEPTH AT COMPLETION: ft.	WET ☐ DRY ☐
▼	WATER LEVEL AT COMPLETION: ft.		CAVE DEPTH AFTER HOURS: ft., hrs.	WET ☐ DRY ☐
▼	WATER LEVEL AFTER HOURS: ft., hrs.		NOTE: Bolded Unconfined Compressive Strength values denote a Qp test.	

NOTE: Stratification lines between soil types represent the approximate boundary; gradual transition between in-situ soil layers should be expected.

HNTB GEOTECH SBL WHRP 2009 BORINGS.GPJ HNTB-WIDNR.GDT 5/20/09

HNTB
ENGINEERS ARCHITECTS PLANNERS
11414 West Park Place, Ste. 300, Milwaukee, WI 53224
Phone (414) 359-2300 Fax (414) 359-2310

SOIL BORING LOG

BORING NUMBER: **B-1**

PROJECT NAME: Wisconsin Highway Research Project		DATE DRILLING STARTED: 4/6/2009	DRILLING METHOD: wash boring
PROJECT NUMBER: 41991		DATE DRILLING ENDED: 4/7/2009	DRILL RIG:
BORING DRILLED BY: FIRM: WisDOT CREW CHIEF: Skolos	FIELD LOG: Skolos LAB LOG / QC: SDM/DAJ	NORTHING: EASTING:	BOREHOLE DIAMETER: 4 in. SURFACE ELEVATION: Feet

Number and Type	Recovery (in)	Blow Counts	N - Value	Depth (ft) / Elevation	Soil Description and Geological Origin for Each Major Unit	USCS	Graphic	Well Diagram	Unconfined Compressive Strength (Qu or **Qp**) (tsf)	Liquid Limit	Plasticity Index	Moisture Content (%)	Comments
					Very stiff to hard, brownish gray silty CLAY, little fine sand, moist								
SPT - 19	18		24		- with wet silt seam				**0.5**				
				65									
SPT - 20	18		28						**3.5**				
						CL							
				70									
SPT - 21	18		40						**4.5**				
				75									
SPT - 22	18		27		Medium dense, gray silty SAND with clay, wet				**0.5**				
						SM							
				80									

WATER OBSERVATION DATA

▽	WATER ENCOUNTERED DURING DRILLING: 8 ft.	CAVE DEPTH AT COMPLETION: ft.	WET ☐ DRY ☐
▼	WATER LEVEL AT COMPLETION: ft.	CAVE DEPTH AFTER HOURS: ft., hrs.	WET ☐ DRY ☐
▼	WATER LEVEL AFTER HOURS: ft., hrs.	NOTE: Bolded Unconfined Compressive Strength values denote a Qp test.	

NOTE: Stratification lines between soil types represent the approximate boundary; gradual transition between in-situ soil layers should be expected.

HNTB GEOTECH SBL WHRP 2009 BORINGS.GPJ HNTB-WIDNR.GDT 5/20/09

HNTB
ENGINEERS ARCHITECTS PLANNERS
11414 West Park Place, Ste. 300, Milwaukee, WI 53224
Phone (414) 359-2300 Fax (414) 359-2310

SOIL BORING LOG

BORING NUMBER: **B-1**

PROJECT NAME: Wisconsin Highway Research Project		DATE DRILLING STARTED: 4/6/2009	DRILLING METHOD: wash boring
PROJECT NUMBER: 41991		DATE DRILLING ENDED: 4/7/2009	DRILL RIG:
BORING DRILLED BY: FIRM: WisDOT CREW CHIEF: Skolos	FIELD LOG: Skolos LAB LOG / QC: SDM/DAJ	NORTHING: EASTING:	BOREHOLE DIAMETER: 4 in. SURFACE ELEVATION: Feet

Number and Type	Recovery (in)	Blow Counts	N - Value	Depth (ft) / Elevation	Soil Description and Geological Origin for Each Major Unit	USCS	Graphic	Well Diagram	Unconfined Compressive Strength (Qu or **Qp**) (tsf)	Liquid Limit	Plasticity Index	Moisture Content (%)	Comments
					Medium dense, gray silty SAND with clay, wet	SM							
SPT - 23	18		27		Medium dense, gray well-graded GRAVEL with sand, little to some silt, wet	GW-GM							
					End of Boring @ 82 feet								
				85									
				90									
				95									
				100									

WATER OBSERVATION DATA

▽	WATER ENCOUNTERED DURING DRILLING: 8 ft.		CAVE DEPTH AT COMPLETION: ft.	WET ☐ DRY ☐
▼	WATER LEVEL AT COMPLETION: ft.	■	CAVE DEPTH AFTER HOURS: ft., hrs.	WET ☐ DRY ☐
▼	WATER LEVEL AFTER HOURS: ft., hrs.		NOTE: Bolded Unconfined Compressive Strength values denote a Qp test.	

NOTE: Stratification lines between soil types represent the approximate boundary; gradual transition between in-situ soil layers should be expected.

HNTB GEOTECH SBL WHRP 2009 BORINGS.GPJ HNTB-WIDNR.GDT 5/20/09

HNTB
ENGINEERS ARCHITECTS PLANNERS
11414 West Park Place, Ste. 300, Milwaukee, WI 53224
Phone (414) 359-2300 Fax (414) 359-2310

SOIL BORING LOG

BORING NUMBER: **B-2**

PROJECT NAME: Wisconsin Highway Research Project		DATE DRILLING STARTED: 4/7/2009	DRILLING METHOD: wash boring
PROJECT NUMBER: 41991		DATE DRILLING ENDED: 4/8/2009	DRILL RIG:
BORING DRILLED BY: FIRM: WisDOT CREW CHIEF: Skolos	FIELD LOG: Skolos LAB LOG / QC: SDM/DAJ	NORTHING: EASTING:	BOREHOLE DIAMETER: 4 in. SURFACE ELEVATION: Feet

Number and Type	Recovery (in)	Blow Counts	N - Value	Depth (ft) / Elevation	Soil Description and Geological Origin for Each Major Unit	USCS	Graphic	Well Diagram	Unconfined Compressive Strength (Qu or **Qp**) (tsf)	Liquid Limit	Plasticity Index	Moisture Content (%)	Comments
SPT - 1	24		37		Dense to loose, light brown to black GRANULAR FILL, fine to coarse sand and gravel, dry to moist								
SPT - 2	24		19		- with black foundry sand and glass fragments								
SPT - 3	24		65	**5**	- with nails and foundry sand								
SPT - 4	24		16		- with slag and foundry sand								
SPT - 5	24		7	**10**									
SPT - 6	12		8		- with petroleum odor								
SPT - 7	6		9										
SPT - 8	6		8	**15**	Loose, black to gray silty SAND, moist to wet (Possible Fill)	SM							Petroleum odor noted @ 14-20 feet
SPT - 9	24		4										
SPT - 10	2		100	**20**	Very dense, light to dark gray SAND with gravel, fine to coarse sand and gravel, some silt, cemented concrete fragments, wet (Possible Fill)	SW-SM							

WATER OBSERVATION DATA

▽	WATER ENCOUNTERED DURING DRILLING: ft.	▨	CAVE DEPTH AT COMPLETION: ft. WET ☐ DRY ☐
▼	WATER LEVEL AT COMPLETION: ft.	■	CAVE DEPTH AFTER HOURS: ft., hrs. WET ☐ DRY ☐
▼	WATER LEVEL AFTER HOURS: ft., hrs.		NOTE: Bolded Unconfined Compressive Strength values denote a Qp test.

NOTE: Stratification lines between soil types represent the approximate boundary; gradual transition between in-situ soil layers should be expected.

HNTB GEOTECH SBL WHRP 2009 BORINGS.GPJ HNTB-WIDNR.GDT 5/20/09

HNTB
ENGINEERS ARCHITECTS PLANNERS
11414 West Park Place, Ste. 300, Milwaukee, WI 53224
Phone (414) 359-2300 Fax (414) 359-2310

SOIL BORING LOG

PROJECT NAME: Wisconsin Highway Research Project		DATE DRILLING STARTED: 4/7/2009	BORING NUMBER: B-2
PROJECT NUMBER: 41991		DATE DRILLING ENDED: 4/8/2009	DRILLING METHOD: wash boring
BORING DRILLED BY: FIRM: WisDOT CREW CHIEF: Skolos	FIELD LOG: Skolos LAB LOG / QC: SDM/DAJ	NORTHING EASTING	DRILL RIG BOREHOLE DIAMETER: 4 in. SURFACE ELEVATION: Feet

Number and Type	Recovery (in)	Blow Counts	N - Value	Depth (ft) / Elevation	Soil Description and Geological Origin for Each Major Unit	USCS	Graphic	Well Diagram	Unconfined Compressive Strength (Qu or Qp) (tsf)	Liquid Limit	Plasticity Index	Moisture Content (%)	Comments
SPT - 11	24		65		Very dense, light to dark gray SAND with gravel, fine to coarse sand and gravel, some silt, cemented concrete fragments, wet (Possible Fill)	SW-SM							
SPT - 12	24		101										
SPT - 13	24		14	25	Medium, grayish brown CLAY, some fine sand, little fine gravel, moist								
				30									
SPT - 14	18		15		- with trace fine gravel	CH							
				35									
SPT - 15	18		15										
				40									

WATER OBSERVATION DATA

▽	WATER ENCOUNTERED DURING DRILLING: ft.	▨	CAVE DEPTH AT COMPLETION: ft. WET ☐ DRY ☐
▼	WATER LEVEL AT COMPLETION: ft.	■	CAVE DEPTH AFTER HOURS: ft., hrs. WET ☐ DRY ☐
▼	WATER LEVEL AFTER HOURS: ft., hrs.		NOTE: Bolded Unconfined Compressive Strength values denote a Qp test.

NOTE: Stratification lines between soil types represent the approximate boundary; gradual transition between in-situ soil layers should be expected.

HNTB GEOTECH SBL WHRP 2009 BORINGS.GPJ HNTB-WIDNR.GDT 5/20/09

HNTB
ENGINEERS ARCHITECTS PLANNERS
11414 West Park Place, Ste. 300, Milwaukee, WI 53224
Phone (414) 359-2300 Fax (414) 359-2310

SOIL BORING LOG

PROJECT NAME: Wisconsin Highway Research Project		DATE DRILLING STARTED: 4/7/2009	BORING NUMBER: B-2
PROJECT NUMBER: 41991		DATE DRILLING ENDED: 4/8/2009	DRILLING METHOD: wash boring
BORING DRILLED BY: FIRM: WisDOT CREW CHIEF: Skolos	FIELD LOG: Skolos LAB LOG / QC: SDM/DAJ	NORTHING EASTING	DRILL RIG BOREHOLE DIAMETER: 4 in. SURFACE ELEVATION: Feet

Number and Type	Recovery (in)	Blow Counts	N - Value	Depth (ft) / Elevation	Soil Description and Geological Origin for Each Major Unit	USCS	Graphic	Well Diagram	Unconfined Compressive Strength (Qu or Qp) (tsf)	Liquid Limit	Plasticity Index	Moisture Content (%)	Comments
					Medium, grayish brown CLAY, some fine sand, little fine gravel, moist								
SPT - 16	18		12										
				45		CH							
SPT - 17	18		12						0.5				
				50									
SPT - 18	18		18		Soft, gray silty CLAY, little to some fine sand, moist				0.25				
						CL							
				55									
SPT - 19	18		22		Very stiff to hard, gray silty CLAY, litte to some fine sand, moist to wet				2.5				
						CL							
				60									

WATER OBSERVATION DATA

▽	WATER ENCOUNTERED DURING DRILLING: ft.	▨	CAVE DEPTH AT COMPLETION: ft. WET ☐ DRY ☐
▼	WATER LEVEL AT COMPLETION: ft.	■	CAVE DEPTH AFTER HOURS: ft., hrs. WET ☐ DRY ☐
▼	WATER LEVEL AFTER HOURS: ft., hrs.		NOTE: Bolded Unconfined Compressive Strength values denote a Qp test.

NOTE: Stratification lines between soil types represent the approximate boundary; gradual transition between in-situ soil layers should be expected.

HNTB GEOTECH SBL WHRP 2009 BORINGS.GPJ HNTB-WIDNR.GDT 5/20/09

HNTB
ENGINEERS ARCHITECTS PLANNERS
11414 West Park Place, Ste. 300, Milwaukee, WI 53224
Phone (414) 359-2300 Fax (414) 359-2310

SOIL BORING LOG

PROJECT NAME: Wisconsin Highway Research Project		DATE DRILLING STARTED: 4/7/2009	BORING NUMBER: B-2
PROJECT NUMBER: 41991		DATE DRILLING ENDED: 4/8/2009	DRILLING METHOD: wash boring
BORING DRILLED BY: FIRM: WisDOT CREW CHIEF: Skolos	FIELD LOG: Skolos LAB LOG / QC: SDM/DAJ	NORTHING EASTING	DRILL RIG BOREHOLE DIAMETER: 4 in. SURFACE ELEVATION: Feet

Number and Type	Recovery (in)	Blow Counts	N - Value	Depth (ft) / Elevation	Soil Description and Geological Origin for Each Major Unit	USCS	Graphic	Well Diagram	Unconfined Compressive Strength (Qu or Qp) (tsf)	Liquid Limit	Plasticity Index	Moisture Content (%)	Comments
SPT - 20	18		19		Very stiff to hard, gray silty CLAY, litte to some fine sand, moist to wet	CL			**1.75**				
				65									
SPT - 21	18		17						**2.25**				
				70									
SPT - 22	18		20		- wet @ 71 feet				**2.5**				
				75									
SPT - 23	18		32		- with trace fine gravel				**4**				
				80									

WATER OBSERVATION DATA

▽	WATER ENCOUNTERED DURING DRILLING: ft.	▨	CAVE DEPTH AT COMPLETION: ft. WET ☐ DRY ☐
▼	WATER LEVEL AT COMPLETION: ft.	■	CAVE DEPTH AFTER HOURS: ft., hrs. WET ☐ DRY ☐
▼	WATER LEVEL AFTER HOURS: ft., hrs.		NOTE: Bolded Unconfined Compressive Strength values denote a Qp test.

NOTE: Stratification lines between soil types represent the approximate boundary; gradual transition between in-situ soil layers should be expected.

HNTB GEOTECH SBL WHRP 2009 BORINGS.GPJ HNTB-WIDNR.GDT 5/20/09

HNTB
ENGINEERS ARCHITECTS PLANNERS
11414 West Park Place, Ste. 300, Milwaukee, WI 53224
Phone (414) 359-2300 Fax (414) 359-2310

SOIL BORING LOG

BORING NUMBER: **B-2**

PROJECT NAME: Wisconsin Highway Research Project		DATE DRILLING STARTED: 4/7/2009	DRILLING METHOD: wash boring
PROJECT NUMBER: 41991		DATE DRILLING ENDED: 4/8/2009	DRILL RIG:
BORING DRILLED BY: FIRM: WisDOT CREW CHIEF: Skolos	FIELD LOG: Skolos LAB LOG / QC: SDM/DAJ	NORTHING: EASTING:	BOREHOLE DIAMETER: 4 in. SURFACE ELEVATION: Feet

Number and Type	Recovery (in)	Blow Counts	N - Value	Depth (ft) / Elevation	Soil Description and Geological Origin for Each Major Unit	USCS	Graphic	Well Diagram	Unconfined Compressive Strength (Qu or **Qp**) (tsf)	Liquid Limit	Plasticity Index	Moisture Content (%)	Comments
SPT - 24	18		43		Very stiff to hard, gray silty CLAY, litte to some fine sand, moist to wet	CL			**4.5**				
					End of Boring @ 81.5 feet								
				85									
				90									
				95									
				100									

WATER OBSERVATION DATA

▽	WATER ENCOUNTERED DURING DRILLING: ft.		CAVE DEPTH AT COMPLETION: ft.	WET ☐ DRY ☐
▼	WATER LEVEL AT COMPLETION: ft.	■	CAVE DEPTH AFTER HOURS: ft., hrs.	WET ☐ DRY ☐
▼	WATER LEVEL AFTER HOURS: ft., hrs.		NOTE: Bolded Unconfined Compressive Strength values denote a Qp test.	

NOTE: Stratification lines between soil types represent the approximate boundary; gradual transition between in-situ soil layers should be expected.

HNTB GEOTECH SBL WHRP 2009 BORINGS.GPJ HNTB-WIDNR.GDT 5/20/09

LABORATORY SOIL TEST REQUEST SHEET

Project Location: Wisconsin Highway Research Project (WHRP)

Job No. 41991

DATE 5/14/2009

Boring	Sample	Depth (ft)	Type sample	Water content (ASTM D2216)	Atterberg limits (ASTM D4318)	Grain size (ASTM D422)	Combined Sieve & Hydrometer (ASTM D422)	% Passing No. 200 Sieve (ASTM D1140)	Unit Weight Determination (ASTM D2937)	Incremental Consolidation w/1 unload/reload cycle (ASTM D2435)	Direct Shear Test (ASTM D3080)	Organic Content by Ignition (ASTM D2974)	Unconfined Compression w/ Stress Strain Plot (ASTM 2166)	Triaxial UU with Stress Strain Plot (ASTM D2850)	Triaxial CD Test (ASTM D4767)	Triaxial CIU w/pp Test (ASTM D4767)	Hydraulic Conductiviy (ASTM D5084)	Specific Gravity (ASTM D854)	Lab Pocket Penetrometer	Lab Torvane Shear	PH (ASTM D4972)	Standard Proctor (ASTM D698)	Modified Proctor (ASTM D1557)	CBR (ASTM D1883)	Remarks/Comments
B-1	7	12-14.0	SS			1																			
B-1	11	20-21.5	SS			1																			
B-1	14	35-36.5	SS		1																				
B-1	10	60.5-62	SS		1																				
B-1	ST	36.5-39	ST		1								1												
B-2	2	2-4.0	SS			1																			
B-2	11	24-26	SS			1																			
B-2	ST	26-28	ST		1								1												
B-2	18	50-51.5	SS		1																				
B-2	20	60-61.5	SS		1																				

Boring B-1 Sample S-14
Natural Moisture Content = 16.00 %

Liquid Limit Test			
Test No.	1	2	3
W1	38.74	38.63	38.32
W2	48.51	48.47	49.56
W3	46.88	46.90	47.82
w%	20.02	18.98	18.32
N	20	24	29

Liquid Limit % =	18.98

Plastic Limit Test			
Test No.	1	2	3
W1	38.86	38.70	
W2	40.49	40.58	
W3	40.32	40.37	
w%	11.64	12.57	

Plastic Limit % =	12.11

Plasticity Index, PI =	6.87

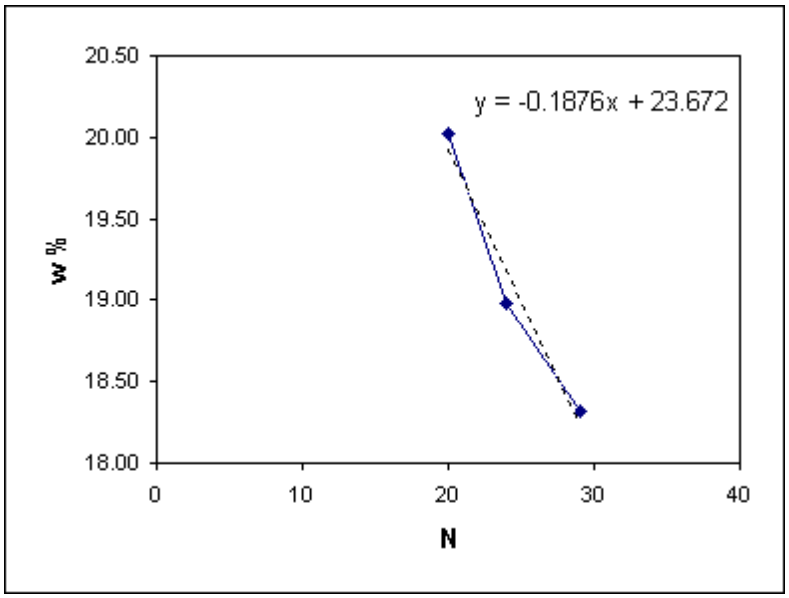

Boring B-1 Sample S-20
Natural Moisture Content = 14.16 %

Liquid Limit Test			
Test No.	1	2	3
W1	38.76	38.35	38.87
W2	61.72	65.34	65.07
W3	57.53	60.71	60.76
w%	22.32	20.71	19.69
N	16	24	33

Liquid Limit % =	20.81

Plastic Limit Test			
Test No.	1	2	3
W1	38.20	38.69	
W2	42.05	42.67	
W3	41.59	42.18	
w%	13.57	14.04	

Plastic Limit % =	13.80

Plasticity Index, PI =	7.01

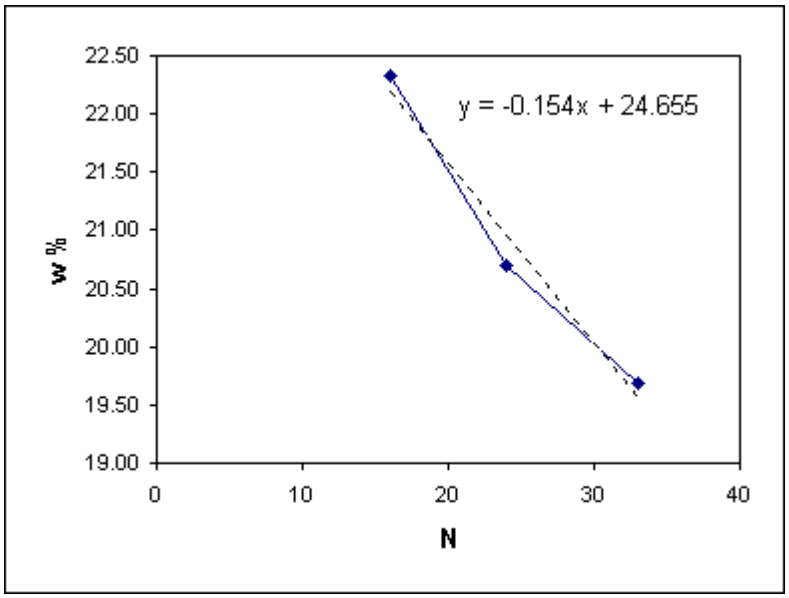

Boring B-2 Sample S-18
Natural Moisture Content = 15.92 %

Liquid Limit Test			
Test No.	1	2	3
W1	31.53	31.64	31.66
W2	61.60	64.35	61.24
W3	56.68	59.19	56.60
w%	19.56	18.73	18.60
N	17	23	34

Liquid Limit % =	18.95

Plastic Limit Test			
Test No.	1	2	3
W1	38.70	31.71	
W2	42.98	34.96	
W3	42.48	34.63	
w%	13.23	11.30	

Plastic Limit % =	12.26

Plasticity Index, PI =	6.69

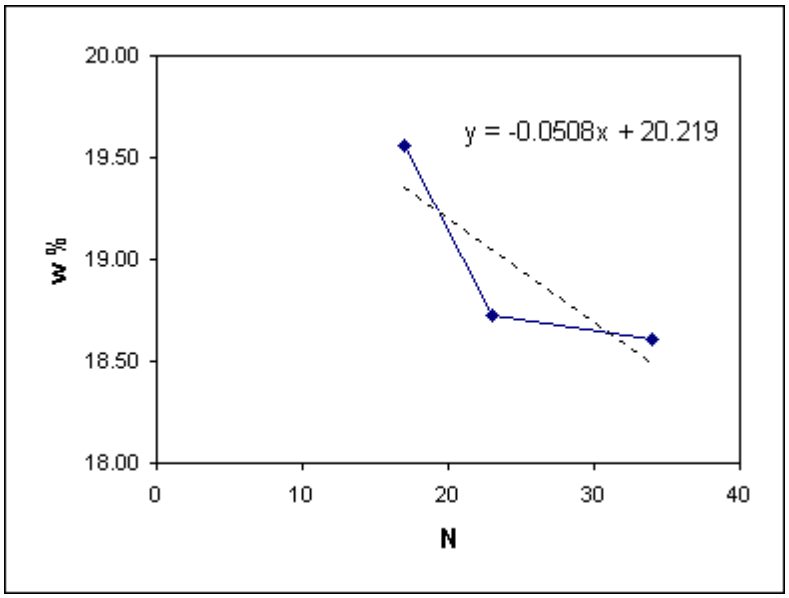

Boring B-2 Sample S-20
Natural Moisture Content = 15.21 %

Liquid Limit Test			
Test No.	1	2	3
W1	38.72	38.21	38.27
W2	48.31	49.48	50.25
W3	46.62	47.65	48.36
w%	21.39	19.39	18.73
N	15	26	35

Liquid Limit % =	19.88

Plastic Limit Test			
Test No.	1	2	3
W1	38.33	38.58	
W2	40.64	39.56	
W3	40.39	39.45	
w%	12.14	12.64	

Plastic Limit % =	12.39

Plasticity Index, PI =	7.49

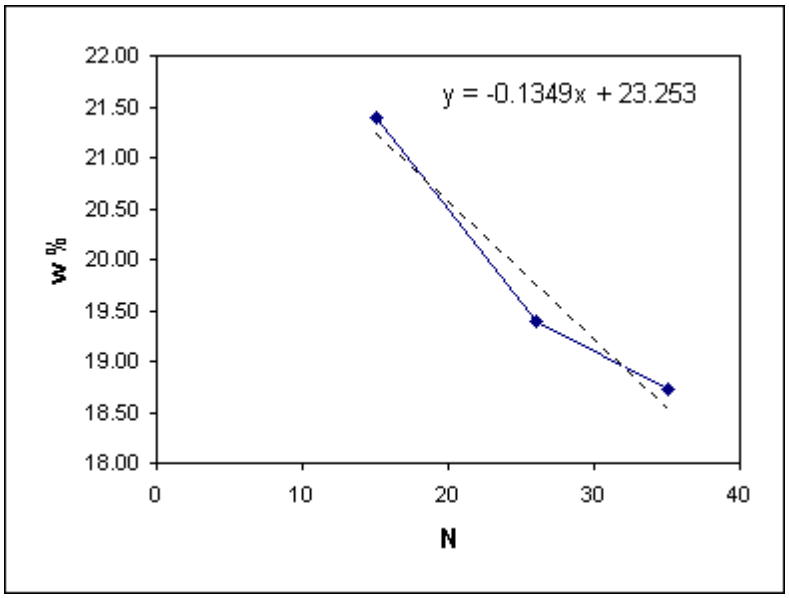

Boring B-1 Sample ST
Natural Moisture Content = 14.80 %

Liquid Limit Test			
Test No.	1	2	3
W1	38.69	38.66	38.64
W2	64.93	67.76	69.85
W3	60.63	63.07	65.01
w%	19.60	19.21	18.35
N	22	28	32

Liquid Limit % =	19.34

Plastic Limit Test			
Test No.	1	2	3
W1	38.43	38.84	
W2	41.66	43.01	
W3	41.28	42.53	
w%	13.33	13.01	

Plastic Limit % =	13.17

Plasticity Index, PI =	6.16

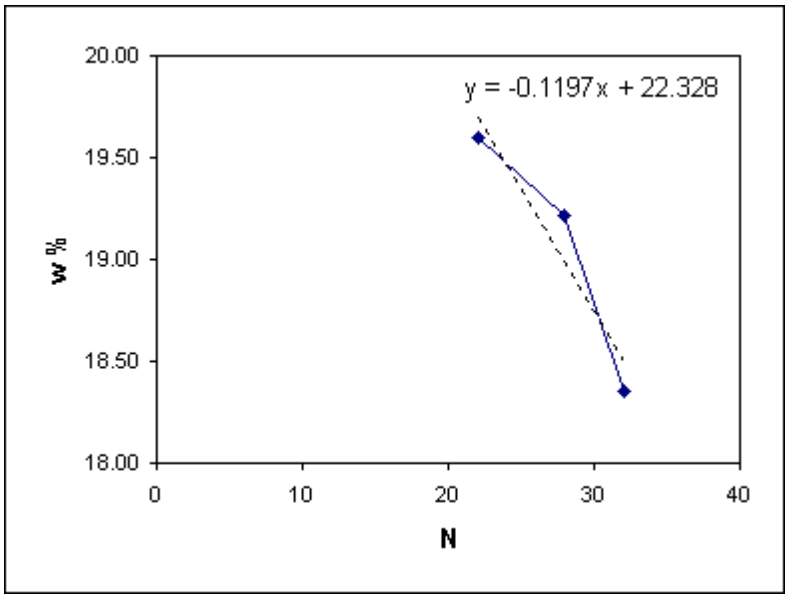

Boring B-1 Sample ST
Natural Moisture Content = 14.80 %

Unconfined Compression Test	
Initial Height, in	6.31
Initial Diameter, in	2.80
Mass, g	1476.68
Initial w%	14.80
Final w%	12.80
Strain Rate, %/min	1.00

Unconfined Compressive Strength, q_u = 4386.13 lb/ft^2

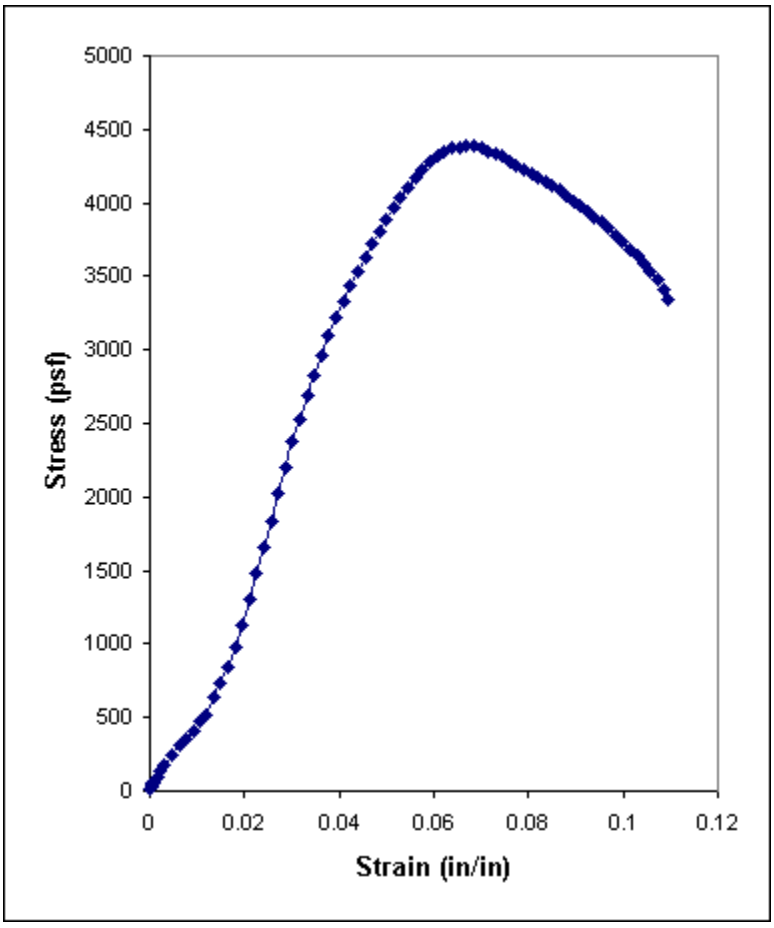

Boring B-2 Sample ST
Natural Moisture Content = 17.42 %

Liquid Limit Test			
Test No.	1	2	3
W1	38.70	38.31	38.87
W2	66.54	63.10	76.90
W3	60.98	58.55	69.92
w%	24.96	22.48	22.48
N	16	28	30

Liquid Limit % =	23.24

Plastic Limit Test			
Test No.	1	2	3
W1	38.62	38.26	
W2	40.93	40.94	
W3	40.61	40.60	
w%	16.08	14.53	

Plastic Limit % =	15.31

Plasticity Index, PI =	7.94

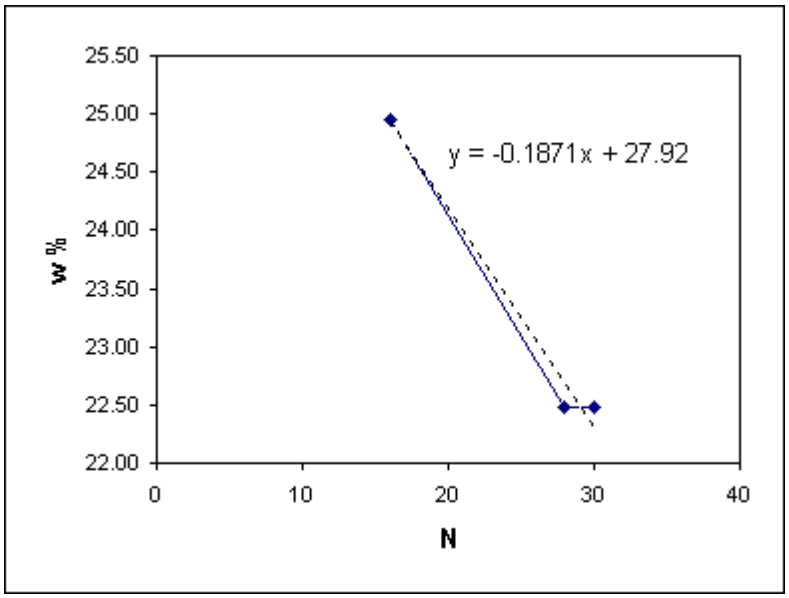

Boring B-2 Sample ST
Natural Moisture Content = 17.42 %

Unconfined Compression Test	
Initial Height, in	6.13
Initial Diameter, in	2.80
Mass, g	1414.34
Initial w%	17.42
Final w%	14.54
Strain Rate, %/min	1.00

Unconfined Compressive Strength, q_u = 4187.81 lb/ft^2

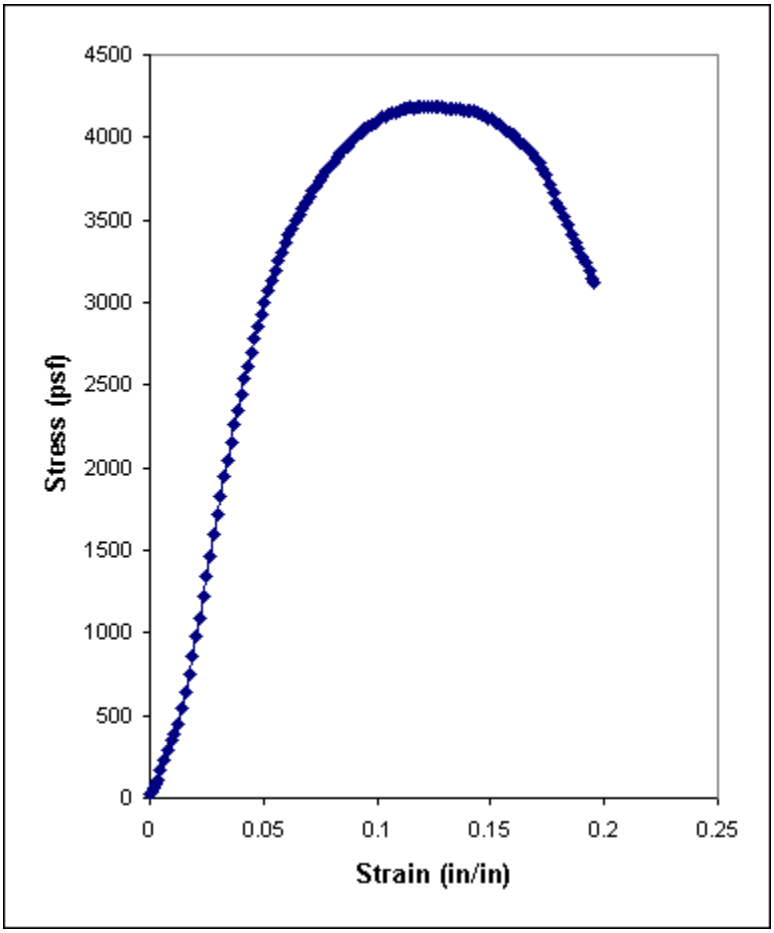

Boring B-1 Sample S-7				
Sieve Analysis				
Mass of original sample = 116.72 g				
Sieve No.	**Sieve Size (mm)**	**Mass Retained (g)**	**Percent Retained**	**Percent Passing**
4	4.75	0.50	0.43%	99.57%
10	2	2.26	1.94%	97.64%
20	0.85	4.45	3.81%	93.82%
40	0.425	6.59	5.65%	88.18%
60	0.25	7.22	6.19%	81.99%
140	0.106	15.06	12.90%	69.09%
200	0.075	10.49	8.99%	60.10%
	Pan	70.03	60.00%	
	Total	116.60		

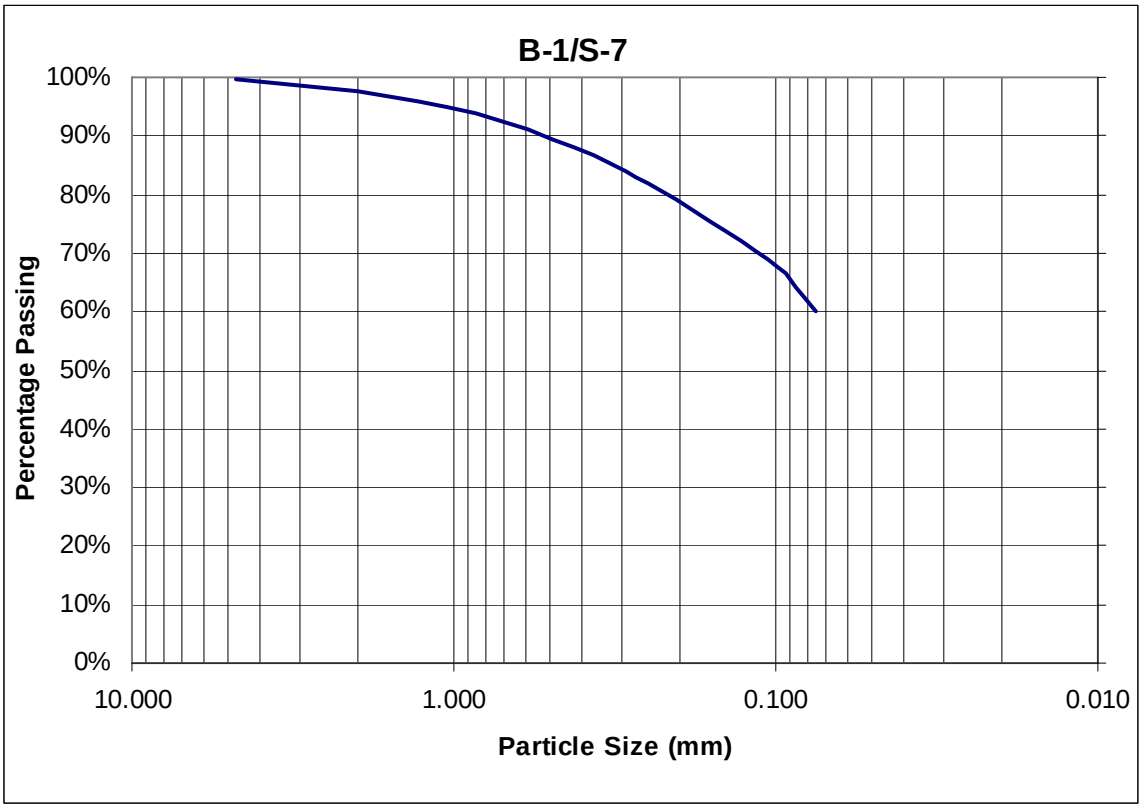

Boring B-1 Sample S-10				
Sieve Analysis				
Mass of original sample = 101.12 g				
Sieve No.	**Sieve Size (mm)**	**Mass Retained (g)**	**Percent Retained**	**Percent Passing**
4	4.75	2.31	2.28%	97.72%
10	2	7.87	7.78%	89.93%
20	0.85	15.02	14.85%	75.08%
40	0.425	24.21	23.94%	51.14%
60	0.25	26.75	26.45%	24.68%
140	0.106	19.18	18.97%	5.72%
200	0.075	1.77	1.75%	3.97%
	Pan	4.03	3.99%	
	Total	101.14		

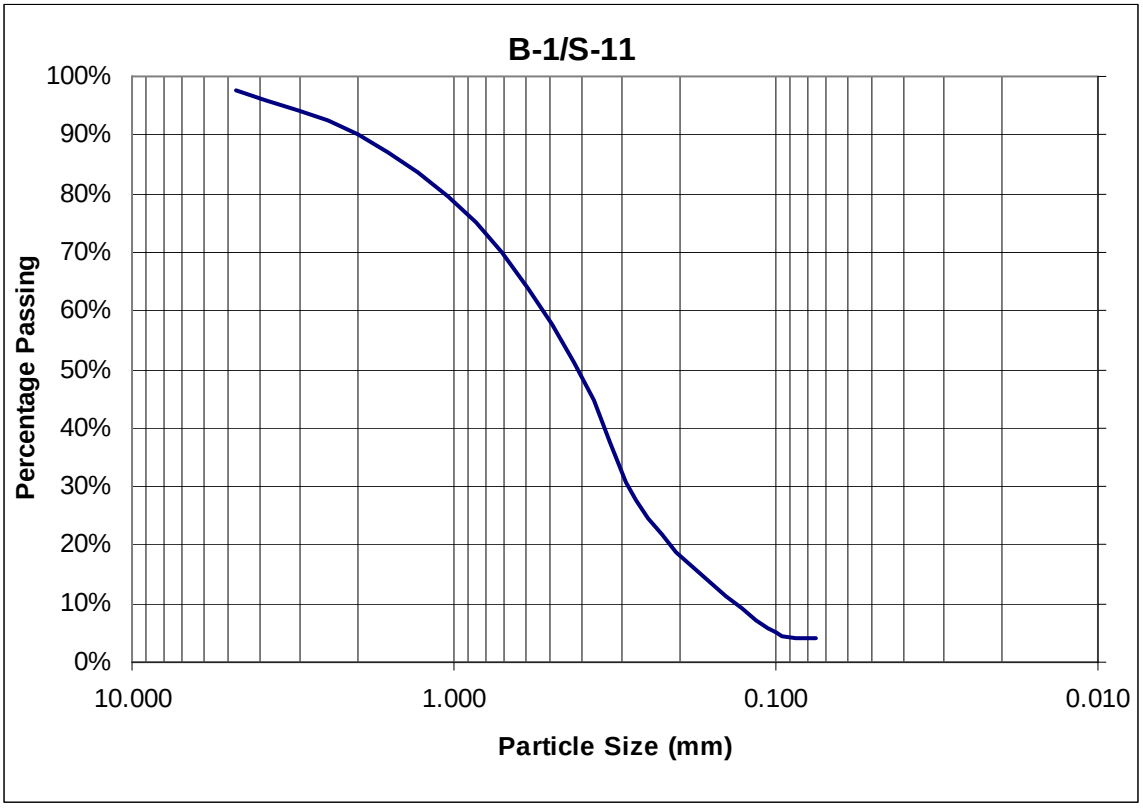

Boring B-2 Sample S-1				
Sieve Analysis				
Mass of original sample = 157.75 g				
Sieve No.	**Sieve Size (mm)**	**Mass Retained (g)**	**Percent Retained**	**Percent Passing**
4	4.75	2.86	1.81%	98.19%
10	2	8.30	5.26%	92.93%
20	0.85	15.04	9.53%	83.39%
40	0.425	24.07	15.26%	68.13%
60	0.25	29.13	18.47%	49.67%
140	0.106	44.84	28.42%	21.24%
200	0.075	12.35	7.83%	13.41%
	Pan	21.04	13.34%	
	Total	157.63		

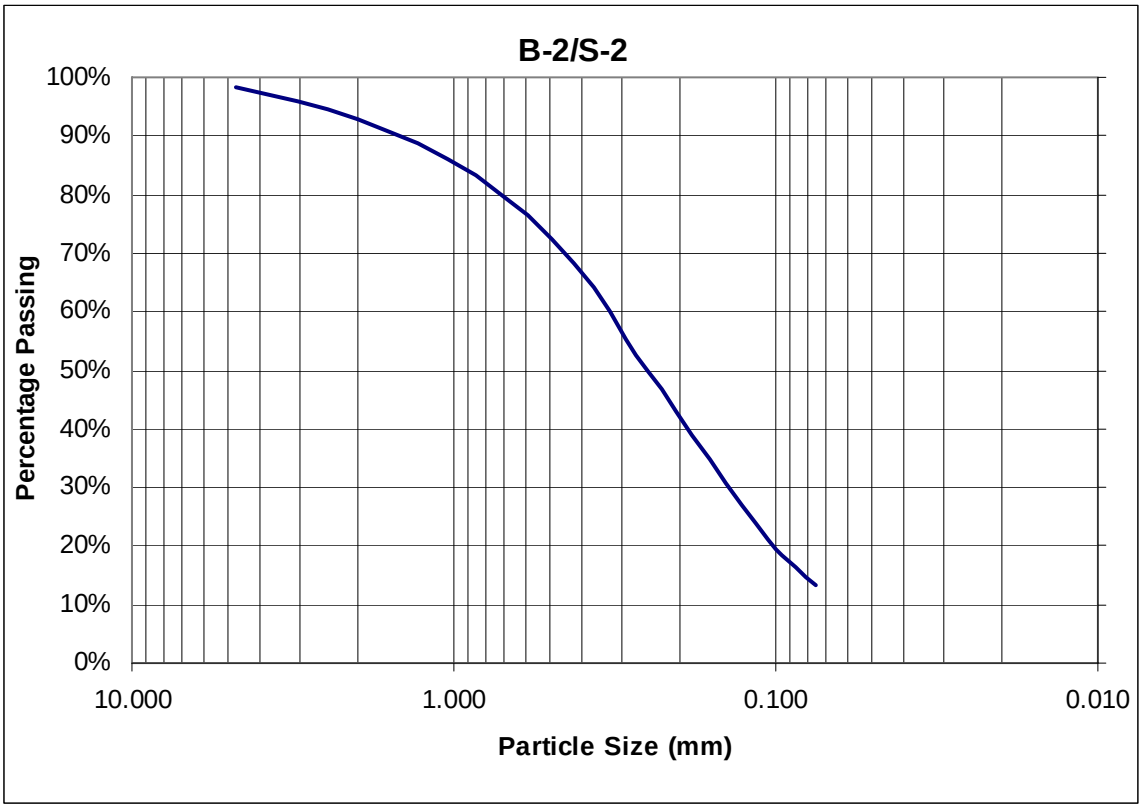

Boring B-2 Sample S-10				
Sieve Analysis				
Mass of original sample = 153.13 g				
Sieve No.	**Sieve Size (mm)**	**Mass Retained (g)**	**Percent Retained**	**Percent Passing**
3/8 in	9.5	49.20	32.13%	67.87%
4	4.75	19.69	12.86%	55.01%
10	2	18.64	12.17%	42.84%
20	0.85	17.19	11.23%	31.61%
40	0.425	2.34	1.53%	30.09%
60	0.25	15.79	10.31%	19.77%
140	0.106	10.62	6.94%	12.84%
200	0.075	3.90	2.55%	10.29%
	Pan	13.87	9.06%	
	Total	151.24		

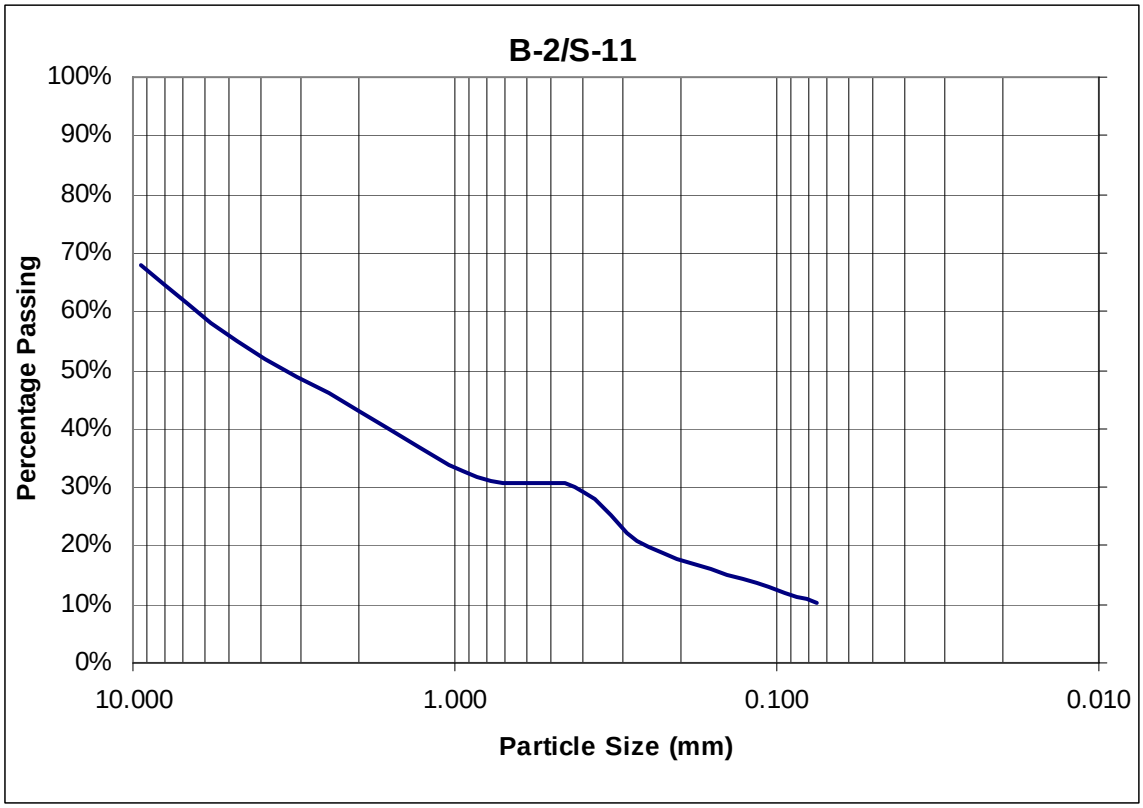

Wisconsin Highway Research Program
University of Wisconsin-Madison
1415 Engineering Drive
Madison, WI 53706
608/262-2013
www.whrp.org